ANALYSES OF SOLID OXIDE FUEL CELL AND GAS TURBINE HYBRID POWER PLANTS ACCOUNTING FOR LONG-TERM DEGRADATION EFFECTS

ANALYSES OF SOLID OXIDE FUEL CELL AND GAS TURBINE HYBRID POWER PLANTS ACCOUNTING FOR LONG-TERM DEGRADATION EFFECTS

By Haoxiang Lai, B.Eng., M.A.Sc.

A Thesis Submitted to the School of Graduate Studies in Partial Fulfilment of the Requirements for the Degree Doctor of Philosophy

McMaster University DOCTOR OF PHILOSOPHY (2023) Hamilton, Ontario (Chemical Engineering)

TITLE: Analyses of Solid Oxide Fuel Cell and Gas Turbine Hybrid Power Plants Accounting for Long-term Degradation Effects

AUTHOR: Haoxiang Lai, B.Eng., M.A.Sc. (McMaster University)

SUPERVISOR: Dr. Thomas A. Adams II

NUMBER OF PAGES: xx, 163

Abstract

Electricity generation from fossil fuels such as coal and natural gas (NG) contributes more than half of the global electricity production and is anticipated to still account for a major share in the medium term till 2050. To reduce the environmental impacts such as global warming potential of global electricity generation, it is vital to improve the current conventional power production technology that utilizes fossil fuels. Solid oxide fuel cells (SOFC) are a promising alternative power generation technology to conventional fossil fuel-based power production due to their higher efficiency and lower greenhouse gas emissions. However, the large-scale commercialization of SOFCs is limited due to their fast degradation under constant power operation which results in a short lifetime. In a SOFC and gas turbine (GT) hybrid design, the SOFC can be operated in constant voltage mode with decreasing power output over time such that the stack lifetime can be largely extended due to much slower degradation. This constant voltage mode of SOFC operation results in increasing heating value of the exhaust stream over time which can be utilized by the GT for power production, allowing this hybrid plant to keep an overall baseload power production.

This thesis focuses on the designs, eco-technoeconomic analyses, and life cycle analyses of coal-based and NG-based SOFC/GT hybrid plants (with and without a steam cycle) accounting for long-term degradation effects, in comparison with standalone SOFC plants (with and without a steam cycle). A pseudo-steady-state model simulation approach was employed to integrate real-time dynamic 1D SOFC models with steady-state balance-of-plant models, in order to capture dynamic behaviours caused by degradation. Model simulations, eco-technoeconomic analyses, and life cycle

analyses were conducted over a 30-year plant lifetime using Matlab Simulink, Aspen Plus, Python, and SimaPro.

The results reveal that the main factors affecting the eco-technoeconomic and life cycle environmental results are the plant efficiency and total SOFC manufacturing over the plant's lifetime, which are both strongly connected to SOFC long-term degradation effects. Compared to a standalone SOFC plant with a steam cycle, the design of SOFC/GT hybrid plant with a steam cycle sacrifices the plant efficiency (4.1 percentage point in coal-based cases and 12 percentage point in NG-based cases), but greatly increase the SOFC stack lifetime (around 16 times longer) which results in much lower cost (reduces levelized cost of electricity by 68% in coal-based cases and 82% in NG-based cases) and lower life cycle environmental impacts (reduces around 6% ReCiPe endpoint).

Research Contributions and Highlights

- Designs and model simulations of standalone solid oxide fuel cell (SOFC) plants and SOFC/gas turbine (GT) hybrid plants accounting for long-term degradation effects that utilize fossil fuels for power production.

- Model integration and simulation by taking a pseudo-steady-state approach to integrate dynamic models and steady-state models.

- Eco-technoeconomic analyses (eTEA) of standalone SOFC plants and SOFC/GT hybrid plants accounting for long-term degradation effects, utilizing coal and natural gas as the fuel sources.

- Cradle-to-product life cycle analyses (LCA) for standalone SOFC plants and SOFC/GT hybrid plants accounting for long-term degradation effects.

Acknowledgments

First and foremost, I would like to thank my supervisor, Dr. Thomas Adams II. Back in the summer of my third-year undergraduate study, I was strongly attracted by Dr. Adams' summer research project. From then on, he has been inspiring me in research and modeling which I really enjoyed. I really appreciate his support, encouragement, guidance, and positive attitude during these years.

I would also like to thank my committee members, Dr. Swartz, Dr. Narimani and Dr. Cotton, for their insightful suggestions and supportive ideas along my research progress.

Thanks to the Hyper team in NETL Morgantown site: David, Farida, Valentina, Nana, and Hao for all the support. Special thanks to David and Farida for the help on system design, model modifications and simulations.

Thanks to NSERC, OGS, and U.S. DOE for the financial support.

A particularly special thanks to the entire Adams group for their support throughout my graduate study: Lingyan, Jake, Jaffer, Leila, Vida, Yaser, Chinedu, Pranav, Ikenna, Nina, Mina, Yurong, Giancarlo, Sarah, James, Tokiso, Amir, Taran, Jamie, Madison, Nagat, Nilou, Sakthi, Fatima, and Avinash.

I would also like to express my appreciation to the Department of Chemical Engineering at McMaster and all my MACC friends for their support during my time here.

Last but not least, I would like to thank my parents, Weichuan and Liling, for their endless love, encouragement, and support in my life.

Contents

3   Eco-technoeconomic Analyses of NG-powered SOFC/GT Hybrid Plants Accounting for Long-term Degradation Effects via Pseudo-steady-state Model Simulations   60

4 Life Cycle Analyses of SOFC/Gas Turbine Hybrid Power Plants Accounting for Long-term Degradation Effects **115**

List of Figures

List of Tables

Nomenclature

AC   Alternating Current

AD   Acidification

BoP   Balance-of-plant

CA   Carcinogenics

CCA   Cost of CO_2 Avoided

CCHP   Combined Chilling, Heating, and Power

DC   Direct Current

EC   Ecotoxicity

EOS   Equation Of State

eTEA   Eco-technoeconomic Analysis

EU   Eutrophication

FD   Fossil fuel Depletion

FEc   Freshwater Ecotoxicity

FEu   Freshwater Eutrophication

FS   Fossil resource Scarcity

FU   Fuel Utilization

GT   Gas Turbine

GW   Global Warming

HCT   Human Carcinogenic Toxicity

HHV   Higher Heating Value

HNCT   Human Non-carcinogenic Toxicity

IR   Ionizing Radiation

LCOE   Levelized Cost of Electricity

LHV	Lower Heating Value
LSM	Lanthanum Strontium Manganite
LU	Land Use
MEc	Marine Ecotoxicity
MEu	Marine Eutrophication
MS	Mineral resource Scarcity
NCA	Non carcinogenics
NG	Natural Gas
OD	Stratospheric Ozone Depletion
OF, HH	Ozone Formation, Human Health
OF, TE	Ozone Formation, Terrestrial Ecosystems
PID	Proportional Integral Derivative (Controller)
PMF	Fine Particulate Matter Formation
RE	Respiratory Effects
SOFC	Solid Oxide Fuel Cell
SM	Smog
ST	Steam cycle (steam turbine)
TA	Terrestrial Acidification
TE	Terrestrial Ecotoxicity
WD	Water consumption (depletion)
WGS	Water-gas-shift reaction
YSZ	Yttria-stabilized Zirconia

Declaration of Academic Achievement

As the author of this thesis, I can confirm I was the first author of all the following articles that are included in this thesis. My contributions to these articles include Conceptualization, Data curation, Formal analysis, Investigation, Methodology, Software, Validation, Visualization, Writing – Original draft preparation.

- Lai, H., Harun, N. F., Tucker, D., and Adams II, T. A., 2021, "Design and eco-technoeconomic analyses of SOFC/GT hybrid systems accounting for long-term degradation effects," Int. J. Hydrogen. Energy, 46(7), pp. 5612–5629.

- Lai, H., and Adams II, T. A., 2022, "Eco-technoeconomic analyses of NG-powered SOFC/GT hybrid plants accounting for long-term degradation effects via pseudo-steady-state model simulations," J. Electrochem. Energy Convers. Storage. (In review, JEECS-22-1137)

- Lai, H., and Adams II, T. A., 2023, "Life cycle analyses of SOFC/gas turbine hybrid power plants accounting for long-term degradation effects," (Submitted, JCLEPRO-D-23-04847)

Besides these articles, I also contributed to the following article as the second author. My contribution to this article includes Conceptualization, Investigation, Methodology, Software, Validation, Writing – Reviewing and Editing. This article is not included in this thesis.

- Naeini, M., Lai, H., Cotton, J. S., and Adams II, T. A., 2021, "A Mathematical Model for Prediction of Long-Term Degradation Effects in Solid Oxide Fuel Cells," Ind. Eng. Chem. Res., 60(3), pp. 1326–1340.

Chapter 1

Introduction

1.1   Background and Motivation

The global electricity demand reached 24,700 TWh (terawatt-hours) in 2021, which was equivalent to a 33% increase from 2010, and is anticipated to climb to 30,621 TWh in 2030 in the Stated Policies Scenario (STEPS) [1]. Although the global electricity supply is projected to shift away from fossil fuels to renewables, electricity production from unabated fossil fuels is anticipated to still account for a major share of 47% and 41% in STEPS and the Announced Pledges Scenario (APS), respectively, in 2030 (Figure 1.1) [1]. The unabated fossil fuels mainly include coal and natural gas (NG), with around 26% and 20% shares, respectively, in the global electricity supply anticipated in 2030 in STEPS. Looking at the longer term in STEPS, the global electricity supplies from coal and NG in 2050 are anticipated to shrink by 35% and 3% from those in 2030, respectively [1]. With the increases in global electricity demand and public awareness of global warming, reliable and sustainable electricity generation has become desirable. Despite the anticipated shift of power supply to renewables, it is vital to improve the efficiencies and emissions of the current fossil-fuel-based power systems due to their remaining large share. For the medium to long term, one potential solution is to find an alternative to conventional electricity generation utilizing fossil fuels, with improvements in eco-technoeconomic aspects.
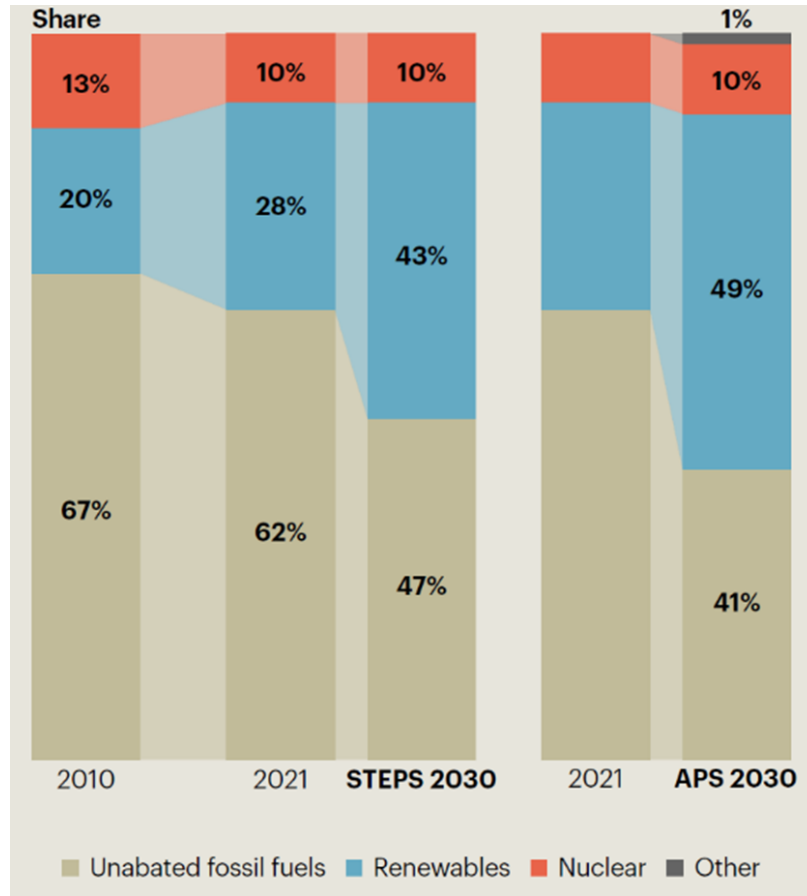
Figure 1.1: Global electricity generation share by source and scenario from 2010 to 2030. Reproduced from [1].

1.1.1 Solid Oxide Fuel Cell

Solid oxide fuel cells (SOFC) are a promising technology for reliable power production through electrochemical reactions which allow more efficient electricity generation than conventional combustion-based power production technologies such as pulverized coal power plants, integrated gasification combined cycle plants (IGCC), and natural gas combined cycle plants (NGCC) [2]. SOFCs can utilize a variety of fuel gas such as hydrogen gas, carbon monoxide, methane (NG), and methanol, as well as syngas generated from coal, NG, diesel, and biomass [2-6]. Figure 1.2 shows a simple schematic of a SOFC cell that uses syngas (mainly CO and H_2) in the anode with air

supplied in the cathode for electricity generation through electrochemical reactions [7]. A SOFC stack, which consists of several SOFCs in series and/or parallel connection, is usually operated at high temperatures (usually above 700°C) [2]. The consequent high-temperature exhaust stream allows integration with other systems for heating purposes or additional electricity production. When the SOFCs are equipped with seals, the anode stream can be maintained separated from the cathode stream, and thus the anode exhaust consists of mainly H_2O and CO_2. This enables efficient CO_2 capture with low cost due to easy H_2O/CO_2 separation [2].
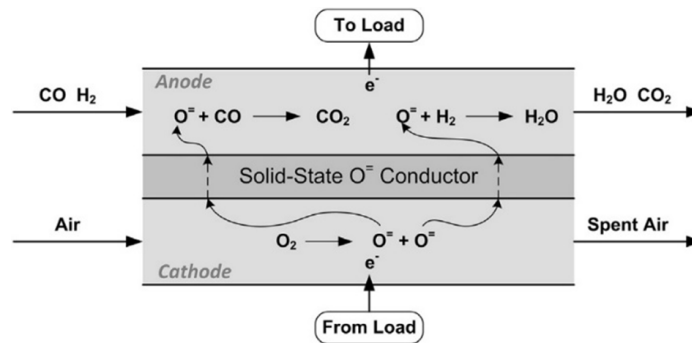
Figure 1.2: Simple schematic of a SOFC utilizing syngas as the fuel source. Reprinted from [7].

Although SOFCs have many advantages compared to conventional power production technologies from fossil fuel, they experience degradation which limits their lifetime [8, 9]. SOFC degradation involves various mechanisms affected by the material and interior structure of the anode, cathode, electrolyte, and interconnects. Conventional SOFCs, consisting of Nickel Yttria-stabilized Zirconia (Ni-YSZ) anodes, $La_{1-x}Sr_xMnO_3$ (LSM) cathodes, and YSZ electrolytes, experience degradation mechanisms including but not limited to Ni coarsening, Ni oxidation, sulfur poisoning, changes in anode pore size, and changes in material conductivity [10-12]. Looking at the stack level, the overall degradation rate is affected by operating conditions such as current density (the major

factor), fuel utilization (FU) and temperature. In a constant power operating mode, which is also known as baseload power production, the current density must increase over time to maintain a constant power output due to degradation. Furthermore, the degradation rate increases over time due to the increase in current density, resulting in a short stack lifetime [8].

Despite developing new materials that degrade more slowly, another approach to overcome the degradation effects is to change the operating conditions and strategies. By changing the operating mode from constant power to constant voltage, the current density and FU decrease over time such that the degradation rate can be significantly reduced and the stack lifetime can be increased up to more than 10 times [8, 13]. However, in this constant voltage mode, the power output of the SOFC stack decreases as the current density decreases. Although the stack lifetime is greatly extended in this mode, it is not useful for baseload power production.

1.1.2   Solid Oxide Fuel Cell and Gas Turbine Hybrid System

As mentioned in the previous section, a SOFC stack can be integrated with other energy systems that utilize the high-temperature exhaust stream from the stack for either heating purposes or secondary power generation. In the constant voltage mode, the exhaust stream from the stack not only has a high temperature but also has increasing heat value over time due to the decrease of FU, and can be used by a gas turbine (GT) to produce power that increases over time. A GT is a suitable secondary power generation unit for the SOFC stack since GTs are widely used in industry for baseload and peaking power production (changing power output according to the power demand) from NG or syngas [2, 8]. The resulting integrated system is also

known as SOFC/GT hybrid system and a simple example system utilizing coal-based syngas is shown in Figure 1.3. In this hybrid system, the SOFC stack is operated in constant voltage mode such that the stack produces less and less power over time and the stack lifetime is largely extended due to slow degradation. The GT utilizes the increasing heating value of the exhaust stream from the stack and produces more and more power over time, resulting in an overall baseload power production system.
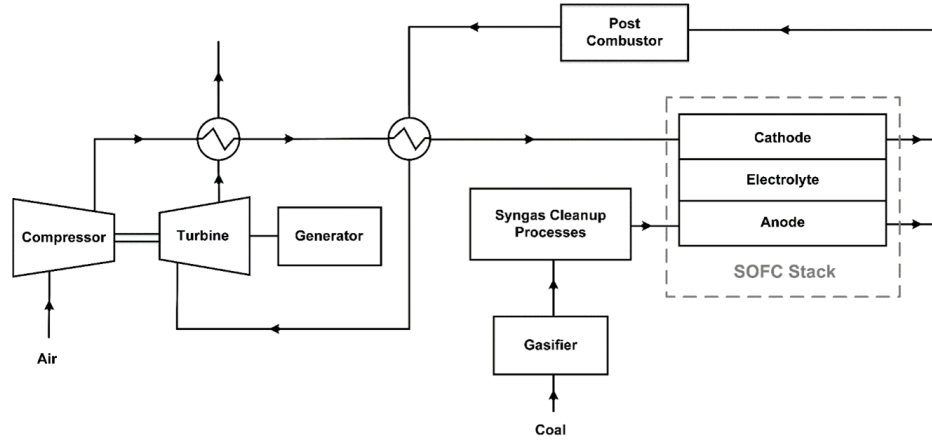
Figure 1.3: Process flow diagram of a simple coal-based SOFC/GT hybrid system.

1.1.3   Eco-technoeconomic and Life Cycle Analyses

To this end, a standalone SOFC plant with a SOFC stack operated in constant power mode is a promising alternative to conventional baseload power production plants utilizing fossil fuels. By changing the operating strategy of the stack from constant power to constant voltage accounting for degradation effects and integrating with a GT, a SOFC/GT hybrid plant sacrifices the efficiency of electricity production (since GTs are less efficient than SOFCs) but increases the SOFC stack lifetime [2, 8]. However, the economic and environmental comparisons between standalone SOFC plants and SOFC/GT hybrid plants accounting for long-term degradation effects

remain unclear. For example, the SOFC/GT hybrid plant with lower efficiency and longer stack lifetime is expected to have higher operating costs (e.g., fuel cost) but lower capital cost due to less stack replacement over the plant's lifetime. In the aspect of cradle-to-product life cycle environmental impacts, lower efficiency might result in higher emissions from plant operation, and a longer stack lifetime is associated with lower life cycle environmental impacts from SOFC manufacturing. Therefore, it is vital to conduct eco-technoeconomic analyses (eTEA) and life cycle analyses (LCA) of standalone SOFC plants and SOFC/GT hybrid plants accounting for long-term degradation effects to further compare their economic performances and environmental impacts.

1.2   Research Outline

This thesis presents eco-technoeconomic analyses and cradle-to-product life cycle analyses of standalone SOFC plants and SOFC/GT hybrid plants utilizing fossil fuels via pseudo-steady-state model simulations which account for long-term SOFC degradation effects. This overall objective is divided into three objectives as presented in the following chapters:

Chapter 2 presents the first peer-reviewed publication in International Journal of Hydrogen Energy. It examines the designs, model simulations, and eTEAs of coal-based standalone SOFC plants and SOFC/GT hybrid plants accounting for long-term degradation effects. Four base cases are designed and studied: (1) standalone SOFC plant, (2) standalone SOFC plant with a steam cycle, (3) SOFC/GT hybrid plant, and (4) SOFC/GT hybrid plant with a steam cycle. A pseudo-steady-state approach is taken to integrate dynamic SOFC models (with dynamic degradation calculation accounted)

with steady-state balance-of-plant models for model simulations. Simulations and eTEAs are conducted using Matlab Simulink, Aspen Plus, and Python. Sensitivity analyses are performed to examine the economic performances of the base cases under assumptions such as SOFC unit prices and the frequency of SOFC stack replacement in the hybrid cases.

Full citation:

Lai, H., Harun, N. F., Tucker, D., and Adams II, T. A., 2021, "Design and eco-technoeconomic analyses of SOFC/GT hybrid systems accounting for long-term degradation effects," Int. J. Hydrogen. Energy, 46(7), pp. 5612–5629.

Chapter 3 presents the manuscript of the second sub-project submitted to Journal of Electrochemical Energy Conversion and Storage. Instead of using coal as the fuel source in the previous chapter, this chapter presents the designs, model simulations, and eTEAs of NG-based standalone SOFC plants and SOFC/GT hybrid plants accounting for long-term degradation effects. Model simulations and eTEAs for four similar designs of base cases are performed following similar procedures as Chapter 2 using Matlab Simulink, Aspen Plus, and Python. Despite of different upstream designs and operating conditions due to changing the fuel source from coal to NG, the model simulation is improved by including a model-based controller. Besides SOFC unit prices and the frequency of SOFC stack replacement in the hybrid cases that are assessed in the sensitivity analyses in Chapter 2, NG prices and non-fuel costs are also investigated in the sensitivity analyses in this chapter. To this end, the eTEAs of both coal-based and NG-based standalone SOFC plants and SOFC/GT hybrid plants are conducted, which mostly cover fossil fuels used as fuel sources for power production.

Full citation:

Lai, H., and Adams II, T. A., 2022, "Eco-technoeconomic analyses of NG-powered SOFC/GT hybrid plants accounting for long-term degradation effects via pseudo-steady-state model simulations," J. Electrochem. Energy Convers. Storage. (In review, JEECS-22-1137)

Chapter 4 presents the manuscript of the third sub-project which has been submitted. Based on the simulation results of the four coal-based cases and four NG-based cases in the previous chapters, cradle-to-product life cycle analyses are performed for all these base cases as well as their corresponding boundary-expanded cases. The LCAs include not only the plant operation in each case, but also the cradle-to-gate SOFC manufacturing, balance-of-plant manufacturing, and plant maintenance. The life cycle environmental impact results are computed using ReCiPe and TRACI methods in SimaPro. To this end, the three sub-projects (or three chapters) present the complete eTEAs and LCAs for fossil-fuel-based (coal- and NG-based) standalone SOFC plants and SOFC/GT hybrid plants (both with or without a steam cycle) accounting for long-term degradation effects.

Full citation:

Lai, H., and Adams II, T. A., 2023, "Life cycle analyses of SOFC/gas turbine hybrid power plants accounting for long-term degradation effects," (Submitted, JCLEPRO-D-23-04847)

1.3   Possible Overlap in the Chapters

Possible overlap might be found in Chapter 2 to 4, mainly as background descriptions and motivations (literature reviews) and descriptions of similar methodologies between studies. No actual results of analyses are repeated in these chapters.

1.4   Author's Contributions to Articles

As the author of this thesis, I can confirm I was the primary performer of all research and the first author of all the articles in the preceding chapters.

References

[1] "World Energy Outlook 2022 – Analysis," IEA. https://www.iea.org/reports/world-energy-outlook-2022 (accessed Dec. 08, 2022).

[2] T. A. Adams II, J. Nease, D. Tucker, and P. I. Barton, "Energy conversion with solid oxide fuel cell systems: A review of concepts and outlooks for the short-and long-term," Ind. Eng. Chem. Res., vol. 52, no. 9, pp. 3089–3111, 2013.

[3] M. C. Williams, J. P. Strakey, and W. A. Surdoval, "US Department of Energy's solid oxide fuel cells: Technical advances," Int. J. Appl. Ceram. Technol., vol. 2, no. 4, pp. 295–300, 2005.

[4] T. A. Trabold, J. S. Lylak, M. R. Walluk, J. F. Lin, and D. R. Troiani, "Measurement and analysis of carbon formation during diesel reforming for solid oxide fuel cells," Int. J. Hydrog. Energy, vol. 37, no. 6, pp. 5190–5201, 2012.

[5] N. Minh, "Coal based solid oxide fuel cell technology development," ECS Trans., vol. 7, no. 1, p. 45, 2007.

[6] F. P. Nagel, T. J. Schildhauer, and S. M. Biollaz, "Biomass-integrated gasification fuel cell systems–Part 1: Definition of systems and technical analysis," Int. J. Hydrog. Energy, vol. 34, no. 16, pp. 6809–6825, 2009.

[7] J. Nease and T. A. Adams II, "Coal-fuelled systems for peaking power with 100% CO2 capture through integration of solid oxide fuel cells with compressed air energy storage," J. Power Sources, vol. 251, pp. 92–107, 2014.

[8] D. Tucker, M. Abreu-Sepulveda, and N. F. Harun, "SOFC lifetime assessment in gas turbine hybrid power systems," J. Fuel Cell Sci. Technol., vol. 11, no. 5, 2014.

[9] A. Hagen, R. Barfod, P. V. Hendriksen, Y.-L. Liu, and S. Ramousse, "Degradation of anode supported SOFCs as a function of temperature and current load," J. Electrochem. Soc., vol. 153, no. 6, pp. A1165–A1171, 2006.

[10] A. Nakajo, Z. Wuillemin, and D. Favrat, "Simulation of thermal stresses in anode-supported solid oxide fuel cell stacks. Part I: probability of failure of the cells," J. Power Sources, vol. 193, no. 1, pp. 203–215, 2009.

[11] T. Yoshizumi, S. Taniguchi, Y. Shiratori, and K. Sasaki, "Sulfur poisoning of

SOFCs: voltage oscillation and Ni oxidation," J. Electrochem. Soc., vol. 159, no. 11, p. F693, 2012.

[12] M. Naeini, H. Lai, J. S. Cotton, and T. A. Adams II, "A Mathematical Model for Prediction of Long-Term Degradation Effects in Solid Oxide Fuel Cells," Ind. Eng. Chem. Res., vol. 60, no. 3, pp. 1326–1340, Jan. 2021, doi: 10.1021/acs.iecr.0c05302.

[13] M. A. Abreu-Sepulveda, N. F. Harun, G. Hackett, A. Hagen, and D. Tucker, "Accelerated Degradation for Hardware in the Loop Simulation of Fuel Cell-Gas Turbine Hybrid System," J. Fuel Cell Sci. Technol., vol. 12, no. 2, 2015.

Chapter 2

Design and Eco-technoeconomic Analyses of SOFC/GT Hybrid Systems Accounting for Long-term Degradation Effects

Design and Eco-techno-economic Analyses of SOFC/ GT Hybrid Systems Accounting for Long-term Degradation Effects

Haoxiang Lai[a], Nor Farida Harun[b,c], David Tucker[c], and Thomas A. Adams II[a*]

a McMaster University, Department of Chemical Engineering, Hamilton, ON, Canada

b Leidos Research Support Team, Leidos, Morgantown, WV, USA

c US Department of Energy, National Energy Technology Laboratory, Morgantown, WV, USA

* Corresponding Author. tadams@mcmaster.ca

Highlights

- Standalone solid oxide fuel cells compared against fuel cell/gas turbine hybrids.

- Considers long term degradation impacts on system for up to 6 year period.

- Eco-technoeconomic and CO_2 emissions analyses performed.

- Hybrid systems have lower electricity costs and lower CO_2 emissions.

Abstract

This study compares two SOFC/GT (solid oxide fuel cell with gas turbine) hybrid systems to that of two standalone SOFC systems via eco-techno-economic analyses that account for long-term degradation effects. Four cases were examined: 1) standalone SOFC plant without a steam bottoming cycle; 2) standalone SOFC plant with a steam bottoming cycle; 3) SOFC/GT hybrid plant without a steam bottoming cycle; and 4) SOFC/GT with a steam bottoming cycle. This study employed a real-time 1D SOFC model with an empirical degradation calculation integrated with steady-state

balance-of-plant models. Simulations used Matlab Simulink R2017a, Aspen Plus V10, and Python 3.7.4 with a pseudo-steady-state approach. The results showed that, with some trade-offs, the SOFC/GT hybrid plant with the steam bottoming cycle is the best option, with an overall efficiency of 44.6% LHV , an LCOE (levelized cost of electricity) of \$US 77/MWh, and a CCA (cost of CO_2 avoided) of -\$US 69.2/tonneCO$_2$e. The sensitivity analysis also indicated that SOFC/GT hybrid plants were less sensitive to SOFC price compared to standalone SOFC plants. The sensitivity analysis indicated that using a larger gas turbine and replacing the SOFC stack less frequently was the better design choice for the SOFC/GT hybrid plant. This is the first such study to determine the value of SOFC/GT systems compared to standalone SOFC through rigorous system analysis while considering SOFC degradation on a dynamic basis throughout the life of the cells.

Keywords: Solid oxide fuel cell, SOFC/GT hybrid, eco-technoeconomic analysis, degradation

2.1   Introduction

A solid oxide fuel cell (SOFC) is a high-efficiency power-production technology that produces low levels of greenhouse gas emissions. SOFCs generally use fuel gases such as CO, H_2, natural gas, or syngas to generate electricity via electrochemical reactions. SOFCs offer a promising alternative to conventional coal power plants, as they can be run using coal-based syngas (a mixture primarily consisting of CO and H_2) while still providing high electrical efficiency and low greenhouse gas emissions [1]. Figure 2.1 shows a simple schematic of a SOFC cell that uses CO and H_2 as a fuel source [2].

Despite these advantages, SOFCs are prone to degradation, which can reduce their lifetime to as little as 1.5 years when constant power output is maintained (baseload power production mode). In this constant power mode, the SOFC's fuel flow rate and current density must be increased over time in order to counteract degradation effects and provide a constant power output. However, increases in the fuel flow rate and current density over time also increase the degradation rate, thus shortening the cell's lifetime [3, 4].
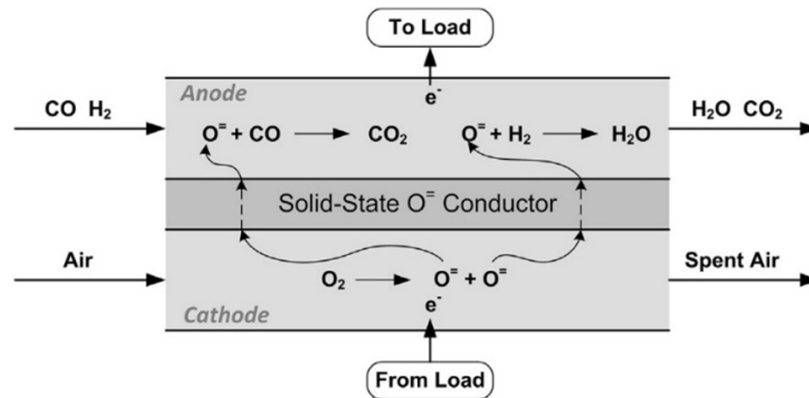
Figure 2.1: Simple schematic of a SOFC utilizing syngas as the fuel source. Reprinted from [2]. This figure was published in J. Power Sources, vol. 251, J. Nease and T. A. Adams II, "Coal-fuelled systems for peaking power with 100% CO_2 capture through integration of solid oxide fuel cells with compressed air energy storage," pp. 92–107, Copyright Elsevier (2014).

2.1.1   SOFC/GT Hybrid System

SOFC degradation is affected by the material and interior structure of the anode, cathode, electrolyte, and interconnects. For example, a recent review suggests that one of the best ways to overcome degradation issues is to develop new materials that do not degrade as quickly [5]. Although researchers have investigated the use of various materials and interior structures in SOFC cells, other findings have shown that different

operating conditions can influence an SOFC's lifetime [3]. For example, when SOFCs are operated in constant voltage mode instead of constant power mode, power output and fuel utilization (percentage of fuel utilized in the anode) decline as the fuel cells degrade over time. This means that it may be possible to overcome the degradation problem using existing materials by changing the SOFC operating conditions, as well as including other balance of plant components chosen for this purpose. This is the one key premise of the SOFC/GT hybrid concept.

The decline in fuel utilization causes an increase in the amount of unused fuel in the anode exhaust, which can be potentially be used in a secondary power source to help compensate for the decrease in SOFC power production. Despite this decrease in power production over time, it is possible to extend the lifetime of the SOFC stack to 13 or 14 years compared to operating in constant power mode [3]. For this reason, the results in the literature suggest that operating in constant voltage mode (rather than constant power mode) may be significantly better from a systems perspective if a GT was used to capture the energy from the anode exhaust, which gradually increases over time as the system decays and power drops. The benefit of the significantly longer SOFC lifetimes plus the use of the GT to recoup some of the lost power over time could outweigh the losses associated with gradual SOFC power declines and the extra complexity and capital costs of the system. However, this is the first study to address those tradeoffs via a rigorous analysis that factors in the decay and how this decay is influenced by key system operating parameters.

To this end, an SOFC/GT (gas turbine) hybrid system has been studied as a baseload power-production design that utilizes this operating strategy [6]. In this hybrid system, the GT uses the gradually increasing heating value of anode exhaust to produce additional power, thus compensating for the gradually decreasing power production from the SOFC stack. Significantly, the GT is designed to reach its full power-production

capacity at the end of the SOFC stack's lifetime, which means that the efficiency of the GT is low at the beginning and increases over time due to the increasing heating value of the anode exhaust. The net outcome is a system that produces power nearly constantly, with an SOFC that degrades much more slowly than in a standalone SOFC system.

Although prior studies have explored various aspects of SOFC/GT hybrid systems, including modeling and control [7, 8], exergy analysis [9, 10], thermo-economic analysis [11], and system optimization [12-14], none have examined long-term degradation effects in SOFCs. Some of the most recently studied SOFC/GT conceptual process designs augment SOFC/GT hybrids with additional integrated balance-of-plant components, especially in a combined-chilling-heat-and-power context (CCHP). For example, Zhao et al. presents a SOFC/GT hybrid system for CCHP which incorporates humidified air for the cathode using steam generated from waste heat for efficiency improvements [15]. Kumar et al. [16], You et al. [17], and Karimi et al. [18] each incorporate organic Rankine cycles for CCHP into SOFC/GT hybrid systems, with various other components such as ammonia-based chillers [16], desalination [17, 19], or domestic hot water [18]. Behzadi et al. utilize the waste heat from SOFC/GT systems to power double effect absorption chillers (instead of a bottoming cycle) and use the produced electricity to power an RO desalination system [20]. Gholamian et al. use the electricity from an SOFC/GT system to power electrolyzers for hydrogen production as an alternative method for producing hydrogen (from gasified biomass) [21]. However, very few of these consider degradation and it is unclear how these complex systems—especially the tertiary components such as cooling cycles, organic Rankine cycles, humidification, or desalination—would function in the context of long-term degradation.

Degradation plays an important role in the system's dynamics, as it impacts the

SOFC's performance with respect to power output and anode exhaust heating value, which in turn affects the performance of the GT. Previous studies have utilized a GT model consisting of a simple empirical equation that estimates power output and efficiency based on the anode exhaust's heating value [3]. In contrast, this work adopts a more realistic reduced model that predicts the GT's power-output efficiency based on changes in the anode exhaust's heating value caused by the degradation effects in the SOFC. The long-term performance of the SOFC/GT hybrid system, with degradation effects, can then be assessed via model simulations.

2.1.2   Long-term SOFC Degradation

To date, researchers have studied various mechanisms that may be responsible for SOFC degradation, as well as how degradation is impacted by the SOFC operating conditions; however, a general long-term degradation model that accounts for every degradation mechanism has yet to be developed. Different models have been developed to account for mechanisms such as Ni coarsening and Ni oxidation[22, 23], and sulfur poisoning [24, 25], while degradation studies have examined specific SOFC components such as the anode [22, 24], cathode [27, 28], electrolyte [29], and interconnects [30, 31]. Unfortunately, most of the developed models mainly focus on degradation analysis at a microstructure level, or a few specific degradation mechanisms, or a specific SOFC component. Thus, the development of a model that is able to account for the overall degradation effects in an SOFC is highly desirable, as such a model would enable the long-term performance of a standalone SOFC system or an SOFC/GT hybrid system to be studied effectively. However, developing a model that accounts for all degradation mechanisms would be very time consuming, and is therefore beyond the

scope of this work. Indeed, not only would it potentially be extremely time consuming to develop a model that integrates every mechanism and its corresponding data, but it is also not necessary for a long-term assessment of the overall degradation effects in an SOFC system. In this work, we only require a model that can predict the overall degradation effects with respect to time or operating conditions.

Therefore, in this work, we used a model that was developed in a prior work from experimental stack data. The model used regression analysis based on to develop an algebraic expression that relates the degradation rate of an SOFC stack to its operating conditions [32]. Despite not accounting for every degradation mechanism in the SOFC stack or its different components, this expression is able to predict the stack's overall degradation rate at a system level based on its operating current density, temperature, and fuel utilization. Furthermore, while this expression does not provide a detailed account of the system's various degradation mechanisms, it is nevertheless sufficient for use in analyzing the system.

2.1.3   System Analysis of SOFC/GT Hybrid System Accounting for Long-term Degradation

To the best of our knowledge, there exists no detailed long-term performance analyses of SOFC/GT hybrid systems that also consider degradation effects, and this is the first such study of its kind. Eco-techno-economic analyses (eTEA) are one potentially useful approach for such long-term analyses, as they possess the ability to bridge the gap between lab-scale SOFC studies and the large-scale commercialization of SOFC power production processes. For example, a recent study by Al-Khori et al. used eTEAs to quantify the efficiency, cost, and environmental benefits achieved through

tight integration of SOFCs with other system components [33]. Therefore, this work presents an eTEA of SOFC/GT hybrid systems with respect to system efficiency, levelized cost of electricity (LCOE), and cost of CO_2 avoided (CCA), and compares the results to those obtained for standalone SOFC systems using models that account for long-term degradation. This is important because degradation has a major impact on system design, health, efficiency, cost, environmental, and other metrics of quality and performance. Since degradation has not yet been considered in SOFC/GT systems level analyses of this type, it means that previous eTEAs that neglect degradation likely are too conservative by underestimating costs and overestimating performance. Similarly, this work is also the first to find optimal SOFC replacement times for SOFC/GT systems that incorporate degradation models into a rigorous system level simulation.

One of the key challenges in the design and analysis of this system is that the post-combustion exhaust temperatures of the fuel cell exhaust change as the system decays. Depending on how the cell is operated, the energy conversion that takes place in the fuel cell decreases over time, leaving more of the original energy of the fuel in the exhaust. This means that the heating value of the exhaust and the subsequent postcombustion exhaust temperatures increase over time as the cells decay, such that downstream units such as the gas turbine and steam power cycle (if it exists) must be designed to handle gradual change over the course of its life. In this work, we present four designs variants that can handle this gradual change and consider this in the design and subsequent analysis. This appears to be the first work that considers this effect in a steam bottoming cycle for an SOFC/GT with long term decay.

In a previous publication [34], we performed a system analyses on a standalone SOFC system and a SOFC/GT hybrid system with a focus on system efficiency, cost estimation, and CO_2 emissions. The results of these analyses revealed that the exhaust

from both systems contained a large amount of waste heat, especially in the case of the standalone SOFC system. Therefore, this work includes two additional base cases in which steam bottoming cycles are added to the original two cases in an attempt to capture and further utilize this excess exhaust heat. In addition, the SOFC models used in this work have been updated with more stable temperature controllers, and cost of CO_2 avoided (CCA) has been added to the eTEA evaluation matrix. Furthermore, sensitivity analyses were conducted to study the impact of the frequency of SOFC stack replacement in the SOFC/GT hybrid cases and how SOFC price affects overall performance over the system's lifetime.

2.2 Process Modeling

2.2.1 Process Overview

To compare the long-term system performances of the SOFC/GT hybrid and standalone SOFC systems, four designs were selected as base cases:

(1) Standalone SOFC plant (constant SOFC power)

(2) Standalone SOFC plant with steam bottoming cycle

(3) SOFC/GT hybrid plant (constant SOFC voltage)

(4) SOFC/GT hybrid plant with steam bottoming cycle (also referred to as SOFC with combined cycle plant)

The proposed standalone SOFC system (Base Case 1) consisted of two main components: an SOFC stack with a post combustor, and an upstream syngas production

and clean-up process (Figure 2.2(a)). The upstream syngas process is made up of: a coal gasifier that produces syngas from coal; an air separation unit, which provides the gasifier with oxygen; a scrubber, which removes HCl from the syngas; a water-gas shift reactor to convert CO and H_2O to CO_2 and H_2, and COS and H_2O to CO_2 and H_2S; a Selexol process, which is a solvent-based H_2S removal process; and a multi-stage turbine to bring the pressure down to 1 bar before fed to the SOFC anode. The purpose of the upstream syngas process is to produce clean syngas, which serves as the SOFC anode's fuel source. The SOFC stack is operated at near atmospheric pressure, with cathode air being supplied through a blower and preheated by the post-combustion gas exhaust. As can be seen in the process flow diagram in Figure 2.2(b), Base Case 2 is identical to Base Case 1, with the exception of an added steam bottoming cycle to capture the waste heat from the exhaust gas. The steam bottoming cycle contains a water tank, a pump, a steam generator (or heat exchanger between the flue gas and water), a multi-stage steam turbine, and a condenser.

Base Case 3 (SOFC/GT hybrid system) consists of three main components: an SOFC stack equipped with a post combustor; an upstream syngas production and clean-up process; and a gas turbine, including a compressor and a recuperator (Figure 2.2(c)). The SOFC stack section and the upstream syngas process are the same as in Base Case 1 (standalone SOFC system), but the SOFC stack in Base Case 3 is operated at 4 bar. The hybrid system is also equipped with cold air bypass streams to control the cathode inlet temperature and the gas turbine inlet temperature. Base Case 4 (Figure 2.2(d)) shares the same design as Base Case 3, with the exception of the addition of a steam bottoming cycle to the end of the process.
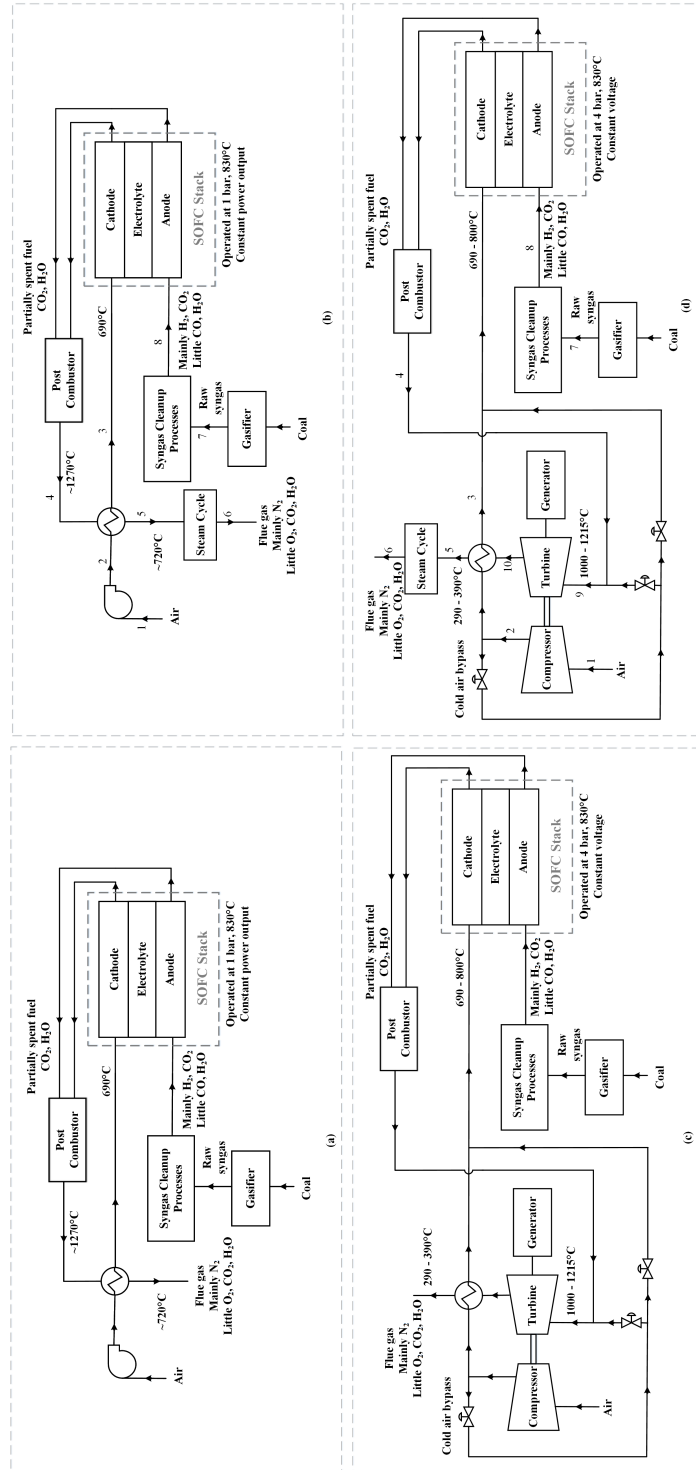
Figure 2.2: Process flow diagrams of the four base cases. Subfigures a through d represent Base Case 1 − 4, respectively. Sample stream conditions for Cases 2 and 4 are given in the Appendix.

2.2.2   Plant Models

The plant model of each base case contains two parts: a dynamic SOFC model and a steady-state balance-of-plant model. The dynamic SOFC model includes the SOFC stack and the post combustor, and it accounts for thermal and electrochemical changes in the SOFC as well as degradation in real time. The steady-state balance-of-plant model of each case includes the rest of the units except the SOFC stack and the post-combustor on Figure 2.2. Specifically, for Base Case 1, the balance-of-plant model contains the gasifier, the syngas cleanup processes (details can be found in previous section), the air blower, and the heat exchanger.

2.2.2.1   Dynamic SOFC Model

This work used a one-dimensional real-time model of a co-flow, planar anode-supported SOFC consisting of an Ni-doped yttria-stabilized zirconia (YSZ) anode, a YSZ-lanthanum strontium magnetite cathode, and a YSZ electrolyte [35]. The model takes a mixed approach, using the finite difference and finite volume methods to obtain real-time thermal (heat transfer) and electrochemical calculations, respectively. The cell is discretized in 20 nodes (20 control volumes) lengthwise in the direction of the gas flow. This number of nodes was found to be optimal in prior work through a grid size sensitivity study, and used consistently for a variety of studies over the past decade. Increasing the node count was found to cause the computational time to increase exponentially, but with negligible increase in solution accuracy as compared to experimental data. Below 20 nodes, the solution became inaccurate at millisecond timescales [36-38].

In addition, characteristic variables such as current density, Nernst potential, temperature, and fuel composition are calculated for each control volume at each sampling time. For more details on the model, including model equations, the experimental data used in developing the model, and validation, please see [32, 39].

$$r_d = \frac{0.59FU + 0.74}{1 + \exp\frac{T-1087}{22.92}}(e^{2.64i} - 1) \qquad (1)$$

The degradation effect in the model is described by Eq.(1), where r_d, FU, T, and i represent degradation rate, fuel utilization, temperature, and current density, respectively. This expression was formed via regression analysis and extrapolation using prior experimental data. This process is described in greater detail in [32, 39]. The degradation rate is calculated in terms of percent of voltage drop per thousand hours, and is further used to calculate the effect of degradation on ohmic resistance and cell voltage. The model was implemented in Matlab Simulink R2017a, and then modified and augmented with upgraded controllers.

The control strategy for Base Case 1 includes three feedback controllers. They are the SOFC power output controller, the SOFC fuel utilization controller, and the SOFC average cell temperature controller, which controls each of those variables by manipulating the SOFC load (current), the anode inlet fuel flow rate, and the cathode inlet air flow rate, respectively. We note that although fuel flow rate is allowed to vary, it changes slowly over the cell life, and within a small range. Although recent research shows that large and sudden fuel composition switches can be problematic for the balance-of-plant [40], the present designs use only very slow changes in flow rate and no changes in fuel composition.

For Base Case 3, however, a different control strategy was implemented which includes a feedback net power controller by manipulating the anode inlet fuel flow rate, a feedback voltage controller by manipulating the SOFC load, and a feedforward SOFC average cell temperature controller by manipulating the cold air bypass valve (to adjust the cathode inlet air temperature). As the SOFC ages, the heating value of the anode exhaust gradually increases, thus increasing the combustor exhaust temperature which if not controlled will cause both the gas turbine inlet and exhaust temperatures to increase. In turn, since the turbine exhaust preheats the cathode inlet air, the cathode air would also increase over time to unacceptable levels. By drawing a cold bypass stream, the controller can ensure that both the gas turbine inlet temperature and the cathode air inlet temperature do not become too large as the SOFC decays.

For the net power controller in Base Case 3, as the anode inlet fuel flow rate changed, the power produced by the SOFC and the heating value of the post combustor exhaust would also change. The heating value of the post combustor exhaust was used to predict the gas turbine power production accounting for off-design efficiency change. A gas turbine characteristic curve, which correlates efficiency with power production for off-design operations, was used to predict the gas turbine power production in different operating conditions (heating value of the gas turbine inlet). This curve was generated with proprietary data from a turbine manufacturer (Siemens), and cannot be released for intellectual property reasons. Base Case 2 and Base Case 4 used the same control strategies in Base Case 1 and Base Case 3, respectively. All controllers used in this work were proportional-integral-derivative controllers. Manual tuning techniques were used to determine the tuning parameters.

2.2.2.2   Steady-state Balance-of-plant Model

The dynamic SOFC model represents the SOFC stack and the post combustor in all of the base cases, with the balance-of-plant for each case being modeled with Aspen Plus V10. Steady-state modeling in Aspen Plus was chosen for its ability to reduce modeling complexity while still providing good representations of the systems and equipment sizes, which can then be used to perform the e-TEA. In Aspen Plus, the Peng-Robinson equation of state (EOS) was used along with the Boston-Mathias modification, with a few exceptions: the NBC/NRC steam tables were used for pure water streams; the Electrolyte-NRTL method with Henry coefficients and electrolyte chemistry specification obtained from the AP065 databank was used for streams mainly consisting of CO_2 and H_2O near the critical point; and the Redlich-Kwong-Soave EOS with predictive Holderbraum mixing rules was used for streams mostly consisting of CO_2 and H_2O below the critical point. A detailed discussion regarding the selection of the thermodynamic method and assumptions is available in [2, 41].

The upstream model units (upstream to the SOFC in Figure 2.2) in the steady-state Aspen model of Base Case 1 including the gasifier, the air separation unit, the scrubber, the water-gas shift reactor, and the Selexol process were modelled using the parameters given in [2]. A multi-stage turbine was added to the end of the upstream process (contained within the Syngas Cleanup Processes box in Figure 2.2) to bring the syngas pressure down to 1 bar which is the operating pressure of the SOFC. The isentropic efficiency of the multistage turbine was assumed constant of 88%. This multi-stage turbine produced around 9% of the gross power production of the plant (the total power production of the plant without subtracting any power consumption in the plant). Therefore, a turbine characteristic curve (which correlates efficiency

with power production) was not considered because it would only change within the range of around 0.6% of the gross power production when it was considered. The air blower was modelled by assuming a constant isentropic efficiency of 90%. An efficiency characteristic curve was not considered for this unit since it consumed negligible amount of electricity. The net power of the air separation unit, the air blower, and the multi-stage turbine in the upstream process was considered as the parasitic load to the plant, and it was around 0.3% of the net power production of the plant. The heat exchanger was designed by assuming 10°C of minimum temperature approach.

The upstream part of the balance-of-plant model for Base Case 2 is the same as Base Case 1. A steam bottoming cycle was added to the downstream in Base Case 2, which contains a water pump, heat exchanger (a steam generator using the heat of the flue gas), a multi-stage steam turbine, a cooler, and a water tank. The steam cycle was set up with the multi-stage steam turbine inlet conditions as 550°C and 100 bar. The multi-stage turbine was modeled with hot bypasses between the stages to ensure 100% vapor fraction within the entire unit. Pump efficiency of 90%, 10°C minimum temperature approach for the heat exchanger, and 89% isentropic efficiency of steam turbines were assumed. The outlet pressure as well as the hot bypass ratio of each stage in the multi-stage turbine was determined by using the optimization tool in Aspen Plus. The objective of the optimization is to produce maximum power with the constraints of 100% vapor fraction between the stages and at least 95% vapor fraction in the outlet. By using the optimization tool, the optimal outlet pressure of the three stages were found to be 24.7 bar, 4.7 bar, and 1.1 bar, with bypassing 7.7% of the total steam to the medium pressure turbine.

For Base Case 3, the upstream process in the balance-of-plant model is almost

the same as Base Case 1 except that the multi-stage turbine outlet was set to 4 bar for the pressurized SOFC operating condition in Base Case 3. The net power and electrical efficiency of the turbine and the compressor was computed by using the gas turbine characteristic curve mentioned earlier. The recuperator was modeled as a heat exchanger by assuming 10°C of minimum temperature approach.

Base Case 4 has the same upstream process and GT section as Base Case 3, and the additional steam bottoming cycle was set up similarly to Base Case 2. However, Base Case 4 cannot have the same operating conditions as Base Case 2, since the heating value of the flue gas in Base Case 4 is much lower than that in Base Case 2. In Base Case 4, the inlet conditions to the multi-stage steam turbine was set to 254°C and 25 bar. Following the same optimization procedure as in Base Case 2, the optimal outlet pressure of the three stages of the steam turbine in Base Case 4 were found to be 5.3, 3.3, and 1.1 bar, with bypassing 71.2% of the total steam to the medium pressure turbine. Further optimization of this steam cycle with different designs, configurations, operating conditions might be considered in future work.

2.2.3   Pseudo Steady-State Model Simulation
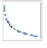
The four base cases were designed using a power scale of 550 MW net electricity produced (combined AC and DC) and a plant lifetime of 30 years. Table 2.1 shows the common conditions applied to all base cases, while Table 2.2 lists the simulation variables for the SOFC models in Matlab Simulink for Base Cases 1 and 3. To simulate these systems that have dynamic model parts and steady-state model parts, a pseudo steady-state simulation approach was taken. A time step of one week for the pseudo

steady-state simulation was chosen, because the SOFC degradation rate did not change much (change within 0.5% relatively) within a week. By taking this pseudo steady-state time step, we assumed that the dynamic behaviors of the dynamic models within a week can be treated as steady-state at the starting point of the week. The dynamic models were simulated in Matlab Simulink with input variables shown in Table 2.2, either with their constant values or their initial values, and predicted variables. Data were recorded with a sampling time of 0.08 hours, and the weekly data were retrieved from this recorded data set and used for the pseudo steady-state simulations with steady-state Aspen Plus models. The details of the simulation processes are given in the following subsections.

Table 2.1: Conditions for all four base cases.

Net Power	550 MW
Plant lifetime	30 years
Initial FU (fuel utilization)	80%
Initial current density	0.5 A/cm^2
SOFC T$_{avg}$	830°C

Table 2.2: Variables used in the SOFC Simulink models for Base Cases 1 and 3. The sparklines represent the trends during simulation, and $\rightarrow$ indicates constant value or variable controlled at a constant setpoint.

		Trend Base Case 1: Standalone SOFC	Base Case 3: SOFC/GT Hybrid	Note
Operating variables	Stack power	$\rightarrow$	⬂	Controlled or being affected by other operating variables
	Voltage	⬂	$\rightarrow$	
	Current density	⬈	⬂	
	Fuel utilization	⬂	$\rightarrow$	
	Average cell temperature	$\rightarrow$	$\rightarrow$	
	Turbine power and efficiency	N/A	⬈	Predicted by reduced model To be matched by ouputs from Aspen Plus model
Inlet variables	Fuel flow	⬈	⬈	The outputs of Aspen Plus simulations should match the values of these variables at each time step. Fuel flow and air flow in Base Case 1, and fuel flow and air temperature in Base Case 3 were manipulated by controllers. The others were constant.
	Fuel temperature	$\rightarrow$	$\rightarrow$	
	Fuel pressure	$\rightarrow$	$\rightarrow$	
	Fuel composition	$\rightarrow$	$\rightarrow$	
	Air flow	⬈	$\rightarrow$	
	Air temperature	$\rightarrow$	⬈	
	Air pressure	$\rightarrow$	$\rightarrow$	
Outlet variables	Combusted gas flow	⬈	⬈	Provided as inputs to Aspen Plus model
	Combusted gas temperature	⬈	⬈	
	Combusted gas pressure	$\rightarrow$	$\rightarrow$	
	Combusted gas composition	$\rightarrow$	$\rightarrow$	

2.2.3.1   Control Strategy in Dynamic Model accounting for Balance-of-plant Model

For Base Case 1, controllers embedded in the model were used to maintain a constant net power output (550 MW, SOFC power subtracted by the parasitic load), a constant FU, and a constant T (average cell temperature) throughout the simulation. A reduced correlation was used in the dynamic model to predict the parasitic load which should be computed by the Aspen Plus steady state model. The reduced correlation was built by using data from the simulations of the dynamic model and the steady-state model with the pseudo steady-state approach for a large number of time steps. This reduced correlation predicted the parasitic load at each sampling time for the net power controller. In Base Case 2, the FU and T were also kept at a constant level, but the SOFC power production set point was decreased over time. This is because the power produced by the steam bottoming cycle increases over time, as did the heating value of the flue gas which increases as the fuel cells degrade (fuel flow increased by the controller but FU stayed the same). Lowering the power set point can lower the degradation rate and keep the net power production at 550 MW. For the hybrid systems (Base Cases 3 and 4), the voltage and T were maintained at a constant setpoint by the controllers. The SOFC stack's power production was controlled (decreasing setpoint) by estimating the parasitic load and the GT's power production (based on the heating value of the anode exhaust and the efficiency characteristic curves as stated in previous section). This allowed for a constant net power production of 550 MW in Base Case 3. For Base Case 4, it was somewhat more complicated to incorporate increasing power production from the steam bottoming cycle in estimations for the SOFC power controller since it was not easy to develop

a reduced correlation between the steam power and the heating value of the flue gas. As such, we used the same simulation results that were used in Base Case 3, and we allowed the steam cycle produce to produce as much power as possible; we then scaled down the entire plant to maintain an average net power of 550 MW. We admitted this is not an effective way of modeling simulation, but it achieved the objective of computing the e-TEA results with negligible errors. Future study can focus on an model predictive controller that controls the setpoint of the SOFC power by model-predicting the GT power, steam power, and parasitic load to maintain a constant net power production of 550 MW.

2.2.3.2 Simulation Methodology

The simulation strategy involved a combination of Aspen Plus V10 simulations and Matlab/Simulink simulations. In short, Matlab/Simulink was used to perform dynamic simulations of the SOFC and post-combustor and Aspen Plus was used to perform pseudo-steady state simulations of the balance of plant, in order to simulate slow dynamics over long time periods (many years). A pseudo-steady-state assumption is made such that the system is at steady state at the end of each timestep. Within a given timestep, the Aspen Plus and Matlab/Simulink simulations are used for different unit operations within the same process, including recycle. Therefore, within a time step, an iterative solution is required to converge the flowsheet, analogous to the tear-stream approach commonly found in sequential modular simulation solvers. The dynamic portions of the model occur in Matlab/Simulink during a timestep, where a new steady state is reached well before each one week timestep has elapsed. The solution process was automated through Matlab scripts which kept track of information, made function calls to Simulink or Aspen Plus, and handled the

iterative flow sheet convergence algorithm. Because of the difficulty in interfacing with Aspen Plus via Matlab, Python 3.7.4 was used as an intermediary between Aspen Plus and Matlab, using a script that forwarded commands from Matlab to Aspen Plus, and then returned the results from Aspen Plus back to the Matlab script in the form of text files containing the necessary data. A more detailed description follows.

The flow of information during a simulation is shown in Figure 2.3 as an example. At the beginning of each pseudo steady-state time step, the GT power, GT efficiency, parasitic load, and inlet coal flow rate were guessed (as described later). The dynamic simulation was run in Matlab Simulink using these guesses as well as the results of certain variables of the previous Aspen Plus simulation as inputs to the Simulink model, and assuming that they were held constant throughout the entire weeklong timestep. These were the SOFC anode inlet fuel temperature, pressure, and composition as well as the cathode inlet air flow rate and pressure. The fuel flow rate and cathode feed air temperature were also taken from the Aspen Plus simulation as an input to the Simulink model, but these were only used as initial conditions at the beginning of the weeklong timestep. The dynamic model was then run using a timestep size of 0.08 hours for a total run time of one week. During the dynamic simulation, the GT power, GT efficiency, and the parasitic load were determined by the Simulink model. The fuel flow rate and air temperature were manipulated by the controllers as the simulation continued.

At the end of each weeklong time step, these variables were recorded (shown in in Figure 2.3 as A1, B1, and C1). The values of key variables at the end of the weeklong dynamic simulation (specifically the combusted gas flow, temperature, pressure, and composition) and the guessed inlet coal flow rate were used as inputs for the
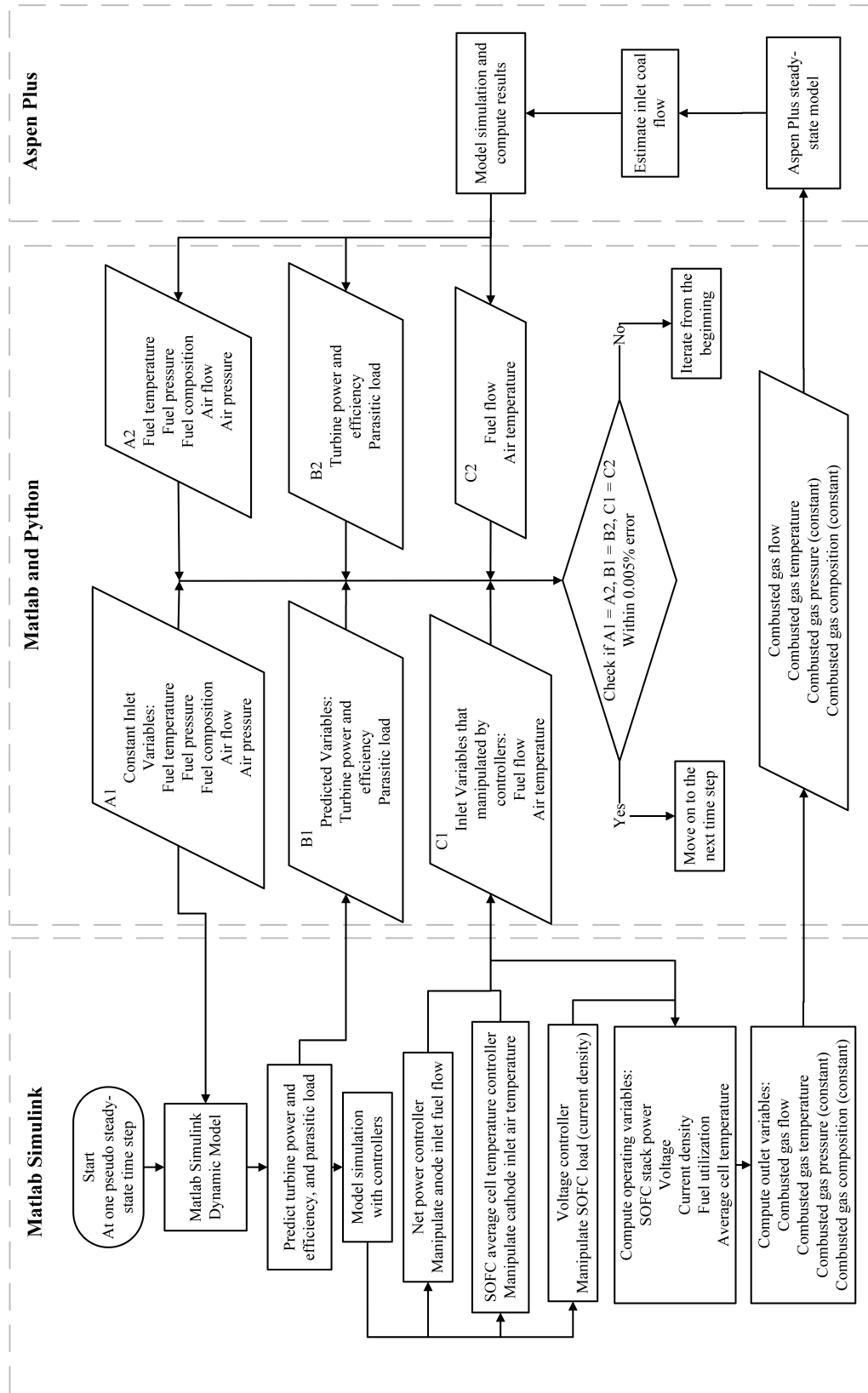
Figure 2.3: Illustration of information flow within one pseudo steady-state time step for Base Case 3.

Aspen Plus steady-state model, which was then simulated. The steady-state model simulation results (A2, B2, and C2) were recorded and compared to the recorded data (A1, B1, and C1) from the end of the weeklong dynamic model simulation. If there is less than 0.005% relative error between the values of variable sets A2, B2, and C2 determined by Aspen Plus and the variable sets A1, B1, and C1 determined by Simulink, the weeklong timestep was accepted, and the next weeklong timestep begun. If the error was too great, the timestep was rejected. Instead, new guesses for the GT power, GT efficiency, parasitic load, and inlet coal flow rate were made, and the dynamic simulations began anew. For brevity, the strategy used to generate guesses is not detailed here. However, it involved the use of reduced models generated from a large number of pre-runs which characterized the relationships between GT power, GT efficiency, coal input flow rates, and other key variables. These reduced models were quite effective such that only one or two iterations were necessary per weeklong timestep.

2.2.4   Eco-technoeconomic Analysis

The eTEAs were conducted using the standard cost and performance baselines reported by the U.S. Department of Energy [42]. The price of the SOFC stack was assumed to be $US 2,000/kW, while the cost of the Siemens SGT6-9000 gas turbine used in Base Cases 3 and 4 was estimated based on the values reported in [43, 44] (additional details are shown in the Appendix). All dollars shown in this work are 2018 U.S. dollars. The costs of steam cycles were estimated by scaling the costs of similar cases in the baseline report with an assumed capacity factor of 0.6 [42]. The cost of the heat exchangers was estimated based on a study conducted by Woods [44], and assumed a shell-and-tube configuration made of 304 stainless steel [45]. The

upstream process, coal (as fuel), and operating costs were estimated based on the values in the baseline report [42]. The Chemical Engineering Plant Cost Index was used to convert all costs to U.S. dollars in 2018, which served as the reference point for the baseline report. The levelized cost of electricity (LCOE) and cost of CO_2 avoided (CCA) were calculated using Eq.(2) and Eq.(3), and the net present value (NPV) was calculated assuming a 5% inflation rate and a time-value-of-money interest rate of 10% [42]. All references to CO_2 emissions in this work refers only to the direct CO_2 emissions.

When computing LCOE and CCA, we used the following definitions. First, we consider the James et al. baseline Case B4A integrated gasification combined cycle (IGCC) coal power plant without CO_2 capture as our reference point for comparison, which has CO_2 emissions of CO_2 Emission$_{base}$=751 kg CO_2e/MWh of electricity and an LCOE of LCOE$_{base}$ = \$US 97.5/MWh [42]. Thus the LCOE and CCA was computed for the four SOFC-based plants in this study as follows:

$$LCOE_{plant} = \frac{NPV_{plant}\ over\ the\ lifetime}{total\ power\ production\ over\ the\ lifetime} \tag{2}$$

$$CCA_{plant} = \frac{LCOE_{plant}\ -\ LCOE_{base}}{CO_2\ Emission_{base}\ -\ CO_2\ Emission_{plant}} \tag{3}$$

Where the "plant" subscripts indicate one of the four plants considered in this work. Note that this CCA definition implies that the assumed status quo is to construct IGCC coal power plant with no carbon capture, and that by CO_2 emissions would be avoided by constructing one of the four power plants considered in this study instead of an IGCC coal power plant. The reader is referred to [46] for an extensive discussion on why this formulation is the most appropriate choice for CCA in this context.

In this work, the SOFC stack efficiency is defined as the stack DC power output divided by the LHV of the syngas fuel it consumed. The overall system efficiency (net efficiency) is defined as the DC power output of the SOFC stack plus the AC power output of all gas and steam turbines minus the parasitic loads, divided by the LHV of the coal entering the system.

2.3   Results and Discussion

Figure 2.4 shows the simulation results for the dynamic SOFC Simulink models, and Figure 2.5 shows the simulation results for the entire plants, including the balance-of-the-plant. Subplots a-d represent Base Cases 1-4.

As can be seen in Base Case 1, power production and fuel utilization were kept as 550 MW and 80%, respectively. The voltage dropped from the initial condition of approximately 0.8 V, and the current density increased from 0.5 A/cm^2. The average temperature of the SOFC stack was maintained at around 830°C. Under these operating conditions, the standalone SOFC was predicted to have a lifetime of around 3132 hours (or around 19 weeks) before catastrophic breakage would occur. Figure 2.5(a) shows the replacement of the SOFC stack every 19 weeks throughout the plant's 30-year lifetime. The stack efficiency dropped as the SOFC degraded because the stack progressively required more fuel to produce the same amount of power, while low plant efficiency was attributable to the high heating value of waste gas leaving the system (flue gas stream in Figure 2.2(a)) that was not utilized.

In Figure 2.4(b), the power output in Base Case 2 (the standalone SOFC with a
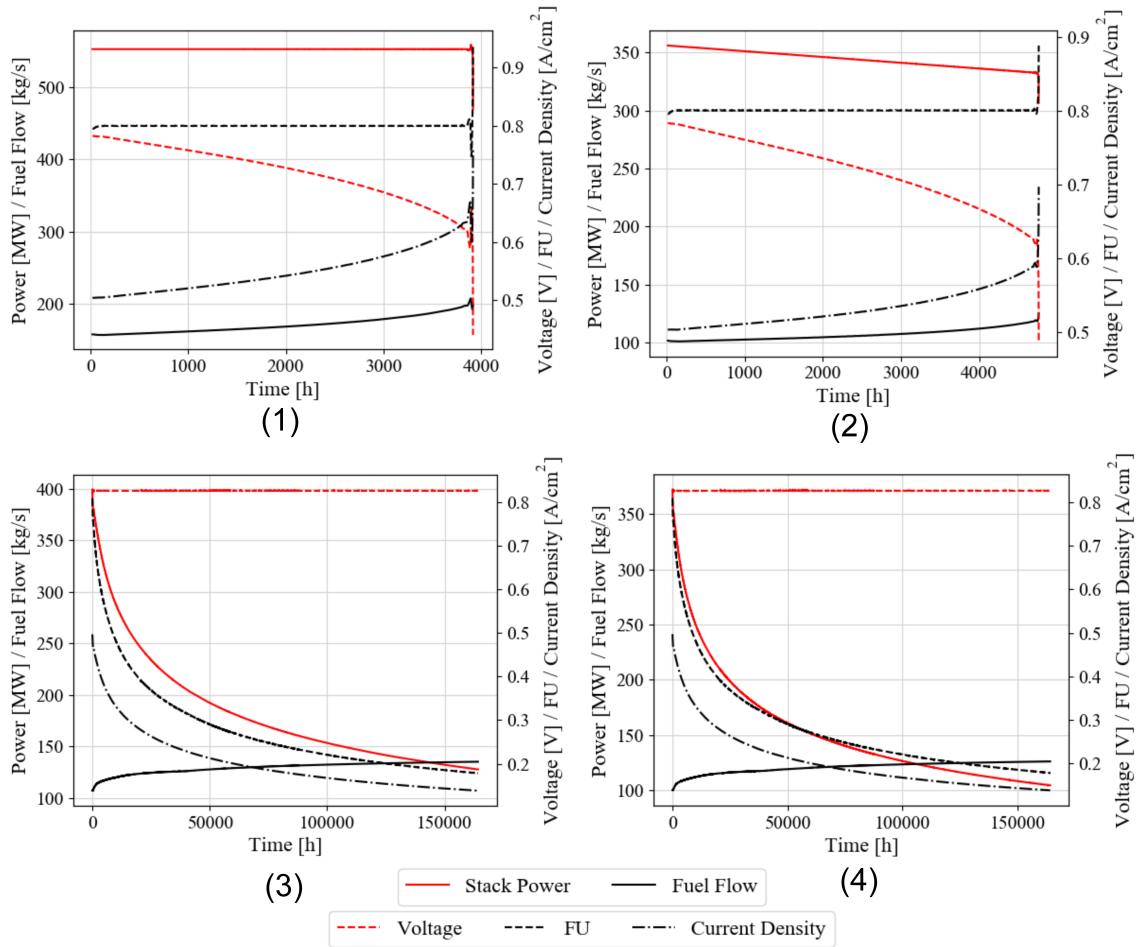
Figure 2.4: SOFC performance curves for Base Cases (1) – (4) in subfigures a through d. Power and fuel flow can be read from the primary y-axis. Voltage, FU, and current density can be read from the secondary y-axis.

steam cycle) slightly decreased over the system's lifetime as controlled. However, incorporating the power produced by the steam cycle made it possible to maintain a net power of nearly 550 MW. This alteration increased the SOFC stack's lifetime to 23 weeks, as the slight decrease in power output slowed the increase in current density, which in turn slowed the degradation rate. Furthermore, plant efficiency increased compared to Base Case 1, as the waste heat in the anode exhaust was reused by the steam cycle.
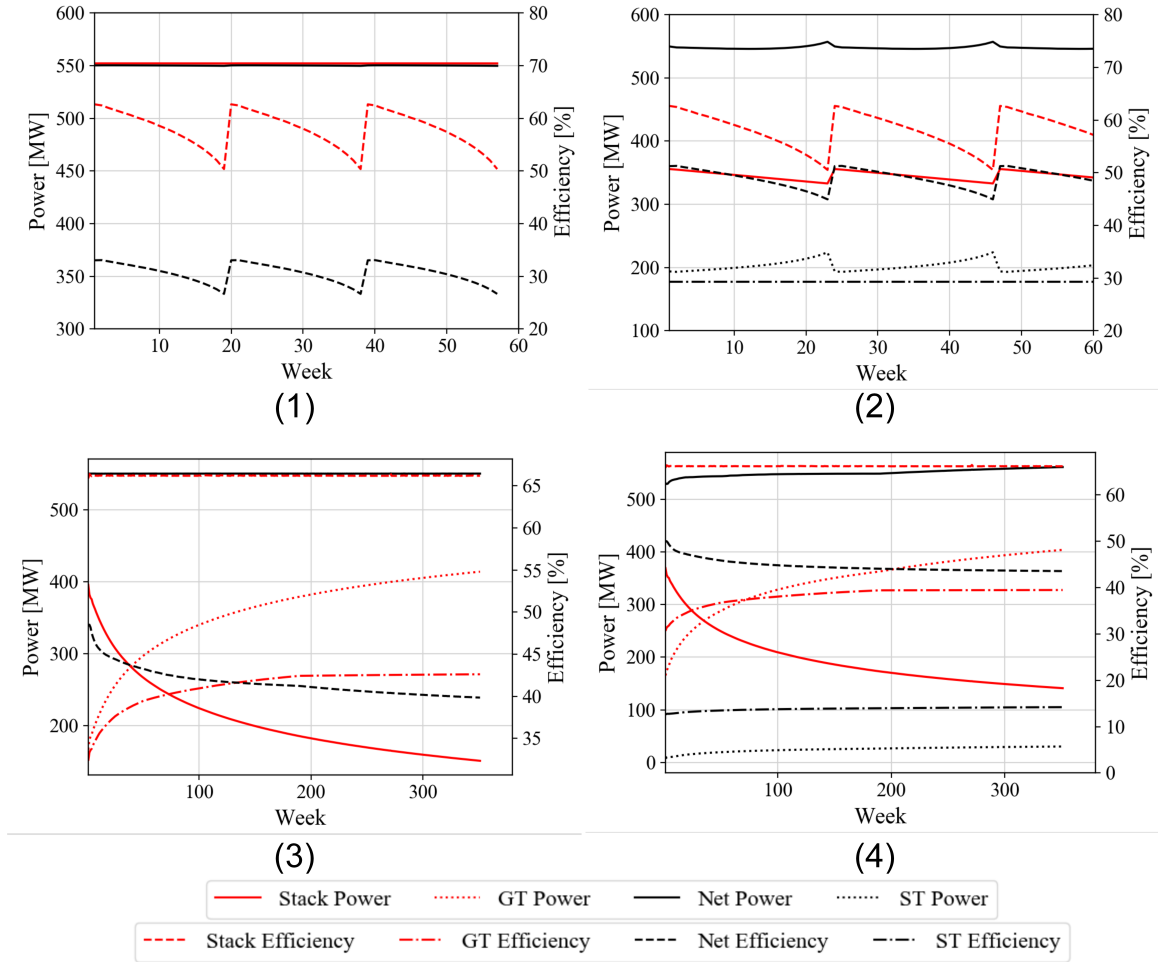
Figure 2.5: Plant performance curves of Base Cases (1) – (4) in subfigures a through d. Power and efficiency can be read from the primary y-axis and secondary y-axis, respectively.

The SOFC stack in Base Case 3 (SOFC/GT hybrid plant) was operated in constant voltage mode to increase the lifetime of the SOFC. Although the simulation predicted that the SOFC could be used for about 14 years before catastrophic breakdown would occur, a practical regular replacement time of 351 weeks (6.7 years or about 59,000 hours) was selected because the fuel utilization dropped to 25% at this point compared to 80% at the beginning of life. Additionally, the SOFC stack's power output decreased to around 150 MW at 25% fuel utilization, which is around 37.5%

of its initial capacity (400 MW). Accordingly, the current density dropped from 0.5 A/cm^2 to approximately 0.19 A/cm^2. The average temperature of the stack was regulated at 830°C. Figure 2.5(c) shows the power load shifting from the SOFC stack to the GT as the SOFC progressively degrades, which enables net power to be maintained at 550 MW. The GT was designed to achieve maximum power capacity at the end of the 351 week life cycle, gradually increasing in efficiency until it hits 42.6% (as designed [43]) at peak design performance. The net efficiency of the entire system gradually decreased over time due to the power load shifting from the more efficient SOFC stack to the less efficient GT. As shown in Figure 2.5, the steam cycle produced much less power in Base Case 4 than in Base Case 2 due to the lower exhaust-gas heating value in the former case (can also be seen in Figure 2.2).

Table 2.3 summarizes the key parameters used in the eco-techno-economic comparison of the four base cases. SOFC stacks were purchased and replaced every 19 weeks for standalone SOFC plant (Base Case 1), and every 351 weeks for the SOFC/GT hybrid plant (Base Cases 3 and 4) over each respective plant's 30-year-lifetime. The standalone SOFC plant (Base Case 1) had higher first year capital costs than the SOFC/GT hybrid plant (Base Case 3), as it required three 550 MW SOFC stacks compared to only one 400 MW stack for the hybrid plant (Figure 2.6). Moreover, the SOFC/GT hybrid plant (Base Case 3) had higher efficiency, lower costs, and lower greenhouse gas emissions than the SOFC standalone plant (Base Case 1) over their respective 30-year lifetimes. The SOFC/GT plant had a levelized cost of electricity (LCOE) of $82/MWh, which is around 80% lower than that of the SOFC standalone plant. Furthermore, the hybrid plant had a CO_2 emissions rate of 493 kg/MWh, which is around 27% lower than that of the standalone plant. Comparing between Base Case 1 and Base Case 2, it is evident that the addition of a steam bottoming cycle resulted

in increased plant efficiency, which in turn led to a lower LCOE and CCA. This result can also be observed in the data for Base Case 3 and Base Case 4, as the addition of the steam bottoming cycle again increased efficiency and lowered the plant's LCOE and CCA. This implies that it would be worthwhile to add a steam bottoming cycle to a SOFC/GT hybrid plant. As can also be seen, the CCA for Base Cases 3 and 4 had negative CCAs, while Base Cases 1 and 3 had positive CCAs. This result indicates that not only are SOFC/GT hybrid plants preferable to standalone SOFC plants from an economic-environmental point of view, but the SOFC/GT hybrid plants are both more profitable and less environmentally damaging than conventional coal power plants. Similarly, even though the standalone SOFC with steam cycle plant is the most energetically efficient and has the least CO_2 emissions, it is not worth the high replacement costs associated with frequent SOFC replacement.

Figure 2.6 shows the number of times the SOFC stacks in Base Cases 1 and 3 need to be replaced each year over the system's lifetime. As can be seen, the SOFC stack in the SOFC/GT plant has a relatively long lifetime, only needing to be replaced every 6-7 years, while the stack in the standalone SOFC plant must be replaced 2-3 times per year. Accounting for the number of stacks purchased every year instead of the aggregate number required over the plant's lifetime can reduce the capital investment, especially for the SOFC standalone plant, because we considered net present value.

Table 2.3: Results of key parameters of eTEA for all base cases.

	BC 1 SOFC Standalone	BC 2 SOFC with steam cycle	BC 3 SOFC/GT Hybrid	BC 4 SOFC/GT with steam cycle
SOFC Stack Efficiency (LHV)	57.9%	57.7%	66.2%	66.2%
Overall Plant Efficiency (LHV)	30.7%	48.7%	41.6%	44.6%
First year Capital Cost ($ Million)	$7,210	$5,077	$4,130	$3,942
Average Annual SOFC Replacement Cost ($ Million)	$3,037	$1,601	$113	$105
Annual Material, Operating and Maintenance Cost ($ Million)	$501	$313	$367	$342
LCOE ($/MWh)	$430	$241	$82	$77
CO_2 Emission (kg/MWh)	674	422	493	460
CCA ($/tonne$CO_2$e)	$4,312	$436	-$59.1	-$69.2
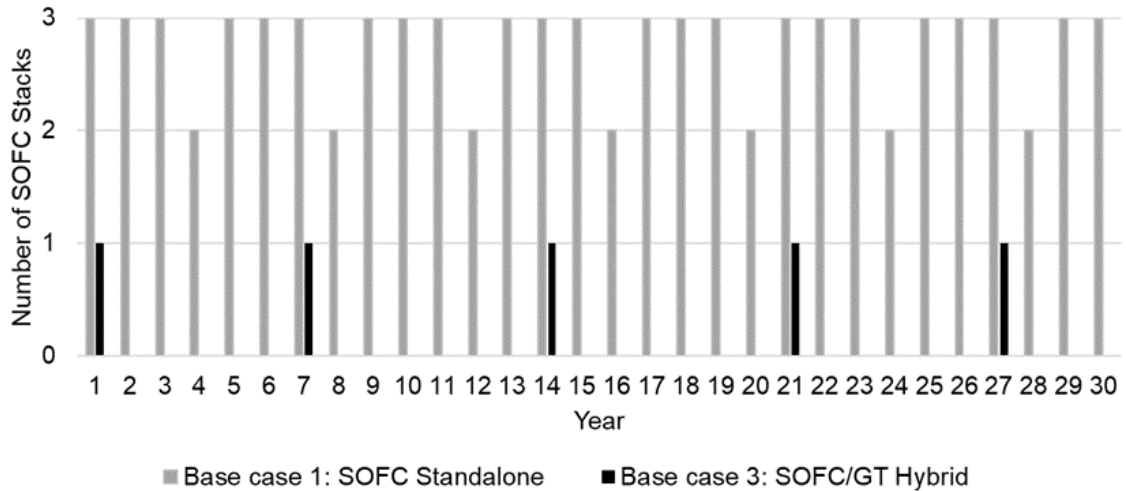
Figure 2.6: SOFC stack replacement frequency for Base Cases 1 and 3 over a 30 year plant lifetime.

2.4 Sensitivity Analysis

The first sensitivity analysis examined SOFC lifetime in the SOFC/GT hybrid plants (Base Case 3 and 4). As noted earlier, the lifetime of the SOFC in the hybrid plants was chosen based on engineering judgement, with the stack replacement occurring when FU dropped to 25%. The sensitivity analysis was performed to assess the impact of changing the SOFC when FU dropped to 20% and 30%. This analysis requires each system in each case to be redesigned, since the GT is designed to reach peak power capacity and efficiency at the end of the SOFC's lifetime; thus, replacing the SOFC at 20% FU necessitated a larger GT, while replacing it at 30% FU necessitated a smaller one. The base case GT was a Siemens SGT6-9000HL, which has a power capacity of 405 MW and a maximum efficiency of $42.6\%_{LHV}$ [43]. A SGT5-8000H GT with a power output of 450 MW and an efficiency of $42.6\%_{LHV}$ was selected for the case wherein the SOFC was replaced at 20% FU. Conversely, two SGT5-2000E GTs, each featuring a power output of 187 MW and an efficiency of $36.5\%_{LHV}$, were selected

for the 30% FU case. The model simulations were then re-run, the results of which are presented in Figure 2.7. The circles in the figure represent the results obtained for the above-discussed GTs. As can be seen, the 30% FU condition for Base Case 3 resulted in the lowest plant efficiency, and therefore the highest LCOE and CCA. This is because we could not find a real GT with the desired power production at the replacement cut-off of 30% FU, which forced us to use two smaller, less efficient GTs instead. Base Case 4 was minimally affected by the low efficiency GTs, as the steam bottoming cycle was able to capture some of the waste heat not captured by the GTs. Scaling simulations were also run using the assumption that the base case GT can be scaled up and down for different power capacity while still retaining a maximum efficiency of $42.6\%_{LHV}$.

The results of these simulations are shown as triangle markers in the Figure 2.7. Clear trends can be seen when the SOFC stack was replaced earlier (at 30% FU), with greater plant efficiency resulting from the greater power load produced from the more efficient SOFC over the plant's lifetime. However, replacing the SOFC stack earlier also resulted in worse LCOE and CCA values, which suggests that it is better to use a larger GT and replace SOFC stack less frequently in SOFC/GT hybrid plants.

The second sensitivity analysis examined the effects of varying the SOFC price from $US 1,000/kW to $US 8,000/kW (as the market price in North America [47]), with a base case price of $US 2,000/kW. The results of this analysis are shown in Figure 2.8. The standalone SOFC plant (Base Case 1) was strongly affected by SOFC price, while the hybrid plants were less affected. The results also showed that it is not worthwhile to switch from conventional coal power plants to SOFC power plants (even SOFC/GT with steam cycle plant) when the SOFC price is $US 8,000/kW. The next step in this

(a)

(b)

(c)
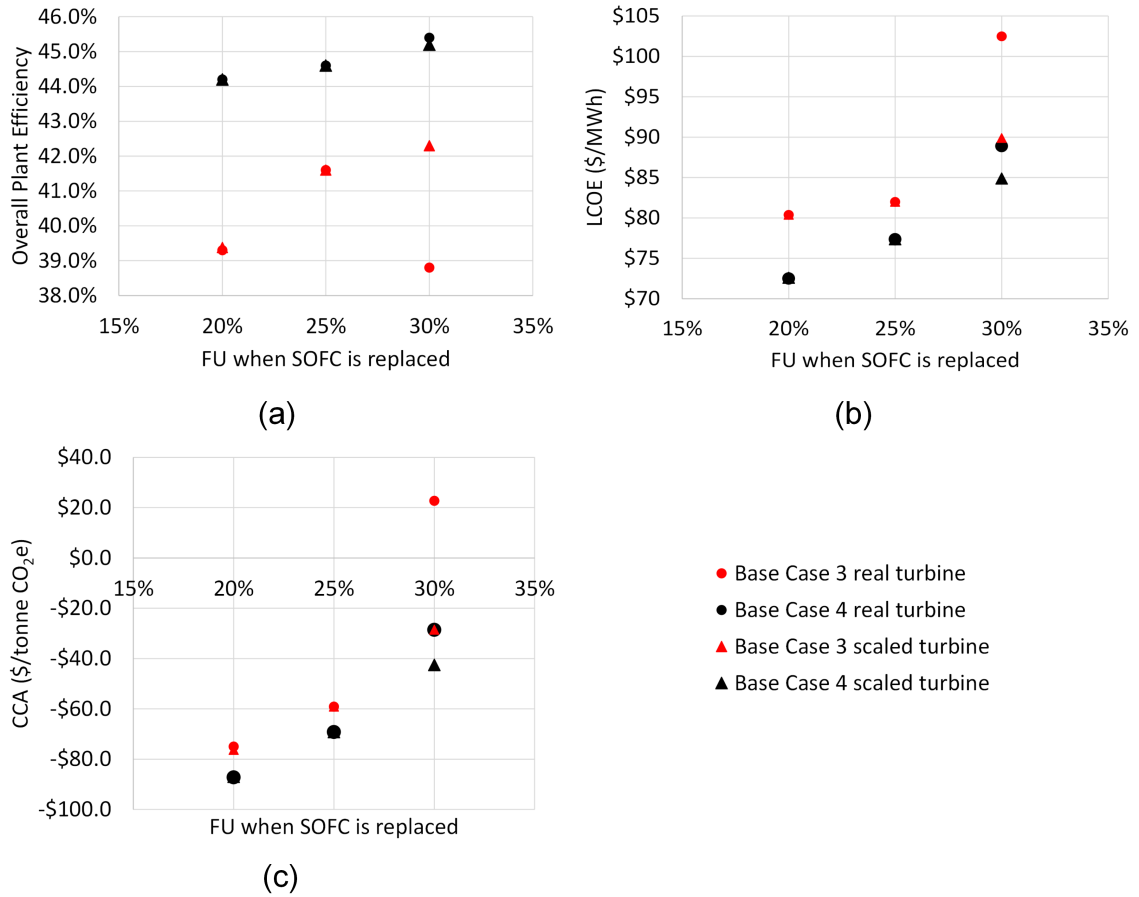
Figure 2.7: Sensitivity analysis results of various lifetime of SOFC stack for Base Cases 3 and 4.

work was to identify the SOFC price that results in a CCA of zero for Base Cases 3 and 4.
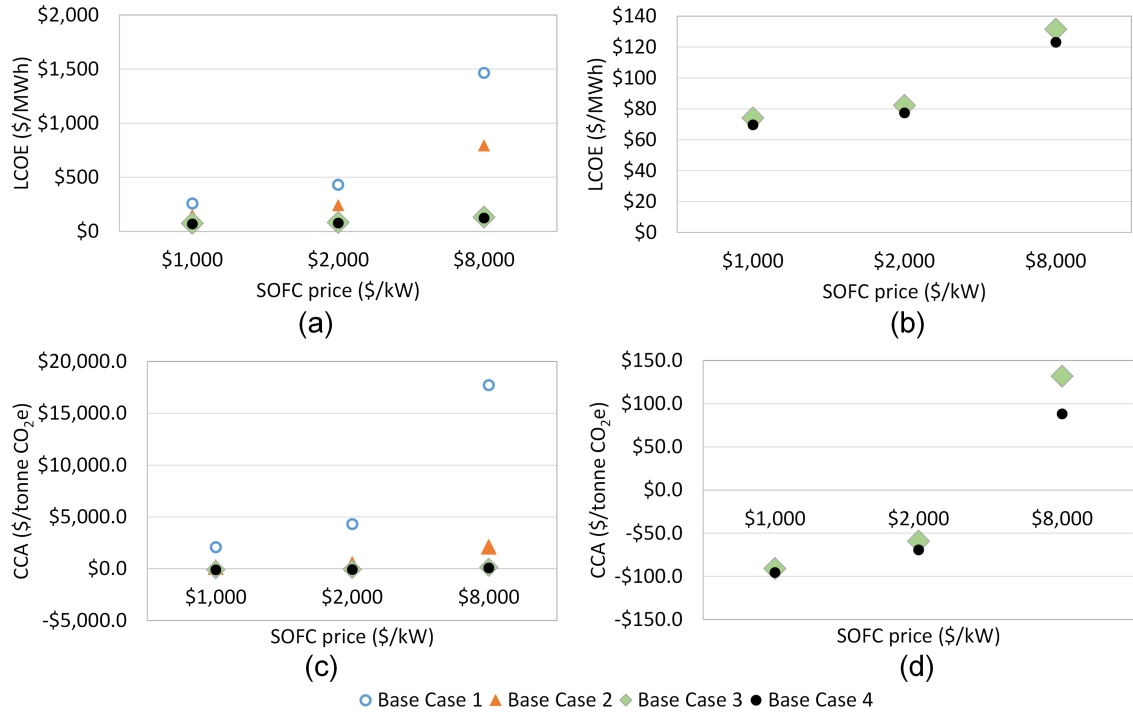
Figure 2.8: Sensitivity analysis results of various SOFC prices for all four base cases. Subplots (b) and (d) are the same plots of (a and c), respectively, without showing Base Cases 1 and 2 for clarity.

2.5   Conclusion and Future work

By studying the eTEA of the four proposed base cases, Base Case 4 (SOFC/GT hybrid plant with steam bottoming cycle) was identified as the best design among the four base cases. Base Case 4 had the lowest LCOE ($US 77/MWh) and lowest CCA (-$US 69.2/tonneCO$_2$e), indicating that Base Case 4 was the least costly to build and the most environmentally friendly among the four base cases. The main reason is that the SOFC lifetime in the hybrid cases (Base Case 3 and 4) was much longer (351 weeks) than those (19 weeks and 23 weeks) in the standalone cases (Base Case 1 and 2) due to the operation of constant voltage mode which had much slower degradation. The much longer lifetime of SOFC resulted in much lower cost (SOFC stack replaced

less frequently) over the lifetime. Moreover, the design with steam bottoming cycle in Base Case 4 increased the overall plant efficiency when compared to Base Case 3. It was interesting that Base Case 2 had the highest overall plant efficiency as $48.7\%_{LHV}$. This is because the SOFC stack (the most efficient unit in the plant) in Base Case 2 contributed the most amount of power to the total power production over the 30-year-lifetime when compared to the hybrid cases (Base Case 3 and 4), although the stack efficiency itself ($57.7\%_{LHV}$) was lower than that in the hybrid cases ($66.2\%_{LHV}$). When compared to Base Case 1 (power production solely from the SOFC stack), Base Case 2 had a steam bottoming cycle to capture the large amount of the waste heat in the flue gas, which boosted the overall plant efficiency. However, Base Case 2 had high values of LCOE ($US 241/MWh) and CCA ($US 436/tonneCO$_2$e), which means that it was not economically or environmentally feasible. Therefore, among the four base cases, the design of Base Case 4 was recommended for large-scale power production with SOFC from an eco-techno-economic perspective.

The results of sensitivity analysis showed that using a larger GT and replacing the SOFC stack less frequently would result in lower LCOE and CCA values for the hybrid cases (Base Case 3 and 4) due to lower costs over the plant lifetime. However, this sacrificed the overall plant efficiency as more power load was shifted from the more efficient SOFC to the less efficient GT. Further optimization of finding the optimal SOFC lifetime (or the replacement time) in the hybrid cases would be interesting to explore in future work. The sensitivity analysis also showed that the SOFC price had a greater impact on the standalone cases (Base Case 1 and 2) than the hybrid cases (Base Case 3 and 4). Based on the sensitivity analysis results, the design of Base Case 4 was still recommended.

This work illustrated the eTEA of SOFC/GT hybrid plants in comparison to SOFC standalone plants accounting for long-term degradation. However, the degradation was predicted solely on one model during simulations. This prevents us noticing whether the eTEA results were too optimistic or pessimistic since no other references of eTEA with degradation were available for comparison. Obviously performing eTEA with no degradation considered would be too optimistic since the lifetime of SOFC stacks would greatly increase and the costs would be much lower. Future eTEA studies with different degradation models or different degradation rates would be desired.

Because this work is the first to examine how SOFC/GT systems perform better in the face of long-term degradation, traditional steady-state power generation was considered as the most suitable scope for the analysis. Future work could examine enhanced and more complex systems in the long-term degradation context by considering additional features presented recently such as organic Rankine cycles, chillers for cold production, integrated wind and solar systems [48], or energy storage features such as compressed air energy storage [49] and batteries [50] for use in a load-following application. It is not yet known how well these systems might perform or how they may need to be modified when long-term degradation is considered.

Simulation Files

Models and codes related to this work have been released to the public in LAPSE (http://PSEcommunity.org/LAPSE:2020.0904).

Acknowledgements

Nomenclature

AC	Alternating Current
CCA	Cost of CO_2 Avoided
CCHP	Combined Chilling, Heating, and Power
DC	Direct Current
EOS	Equation Of State
eTEA	Eco-technoeconomic Analysis
FU	Fuel Utilization
GT	Gas Turbine
LCOE	Levelized Cost of Electricity
LHV	Lower Heating Value
SOFC	Solid Oxide Fuel Cell
YSZ	Yttria-stabilized Zirconia

References

[1] T. A. Adams II, J. Nease, D. Tucker, and P. I. Barton, "Energy conversion with solid oxide fuel cell systems: A review of concepts and outlooks for the short-and long-term," Ind. Eng. Chem. Res., vol. 52, no. 9, pp. 3089–3111, 2013.

[2] J. Nease and T. A. Adams II, "Coal-fuelled systems for peaking power with 100% CO_2 capture through integration of solid oxide fuel cells with compressed air energy storage," J. Power Sources, vol. 251, pp. 92–107, 2014.

[3] D. Tucker, M. Abreu-Sepulveda, and N. F. Harun, "SOFC lifetime assessment in gas turbine hybrid power systems," J. Fuel Cell Sci. Technol., vol. 11, no. 5, 2014.

[4] A. Hagen, R. Barfod, P. V. Hendriksen, Y.L. Liu, and S. Ramousse, "Degradation of Anode Supported SOFCs as a Function of Temperature and Current Load," J. Electrochem. Soc., vol. 153, no. 6, p. A1165, 2006.

[5] F.S. da Silva, T. de Souza, "New materials for solid oxide fuel cell technologies: A literature review," Int. J. Hydrogen Energy, vol 42, pp26020-26036, 2017.

[6] D. Tucker et al., "Evaluation of methods for thermal management in a coal-based SOFC turbine hybrid through numerical simulation," J. Fuel Cell Sci. Technol., vol. 9, no. 4, 2012.

[7] R. Kandepu, L. Imsland, B. A. Foss, C. Stiller, B. Thorud, and O. Bolland, "Modeling and control of a SOFC-GT-based autonomous power system," Energy, vol. 32, no. 4, pp. 406–417, 2007.

[8] R. Toonssen, S. Sollai, P. V. Aravind, N. Woudstra, and A. H. M. Verkooijen, "Alternative system designs of biomass gasification SOFC/GT hybrid systems," Int. J. Hydrogen Energy, vol. 36, no. 16, pp. 10414–10425, 2011.

[9] F. Calise, A. Palombo, and L. Vanoli, "Design and partial load exergy analysis of hybrid SOFC–GT power plant," J. Power Sources, vol. 158, no. 1, pp. 225–244, 2006.

[10] A. V. Akkaya, B. Sahin, and H. H. Erdem, "An analysis of SOFC/GT CHP system based on exergetic performance criteria," Int. J. Hydrogen Energy, vol. 33, no. 10, pp. 2566–2577, 2008.

[11] M. Santin, A. Traverso, L. Magistri, and A. Massardo, "Thermoeconomic

analysis of SOFC-GT hybrid systems fed by liquid fuels," Energy, vol. 35, no. 2, pp. 1077–1083, 2010.

[12] F. Calise, M. D. d'Accadia, L. Vanoli, and M. R. Von Spakovsky, "Single-level optimization of a hybrid SOFC–GT power plant," J. Power Sources, vol. 159, no. 2, pp. 1169–1185, 2006.

[13] F. Calise, M. D. d'Accadia, L. Vanoli, and M. R. von Spakovsky, "Full load synthesis/design optimization of a hybrid SOFC–GT power plant," Energy, vol. 32, no. 4, pp. 446–458, 2007.

[14] B. Fredriksson Möller, J. Arriagada, M. Assadi, and I. Potts, "Optimisation of an SOFC/GT system with CO_2-capture," J. Power Sources, vol. 131, no. 1, pp. 320–326, 2004.

[15] H. Zhao and Q. Hou, "Thermodynamic performance study of the MR SOFC-HAT-CCHP system," Int. J. Hydrogen Energy, vol. 44, p. 4332-4329, 2019.

[16] P. Kumar and O. Singh, "Thermoeconomic analysis of SOFC-GT-VARS-ORC combined power and cooling system," Int. J. Hydrogen Energy, vol. 44, p. 27575-27586, 2019.

[17] H. You, J. Han, and Y. Liu, "Conventional and advanced exergoeconomic assessments of a CCHP and MED system based on solid oxide fuel cell and micro gas turbine," Int. J. Hydrogen Energy, vol. 45, p. 12143-12160, 2020.

[18] M. H. Karimi, N. Chitgar, M. A. Emadi, P. Ahmadi, and M. A. Rosen, "Performance assessment and optimization of a biomass-based solid oxide fuel cell and micro gas turbine system integrated with an organic Rankine cycle," Int. J. Hydrogen Energy, vol. 45, p. 6262-6277, 2020.

[19]. V. Eveloy, P. Rodgers, "Techno-economic-environmental optimization of a solid oxide fuel cell-gas turbine hybrid coupled with small-scale membrane desalination," Int. J. Hydrogen Energy, vol 42, pp15828-15850, 2017.

[20] A. Behzadi, A. Habibollahzade, V. Zare, M. Ashjaee, "Multi-objective optimization of a hybrid biomass-based SOFC/GT/double effect absorption chiller/RO desalination system with CO_2 recycle," Energy Conversion Manage., vol 181, pp302-318, 2019.

[21] E. Gholamian, P. Hanafizadeh, A. Habibollahzade, P. Ahmadi, "Evolutionary based multi-criteria optimization of an integrated energy system with SOFC, gas

turbine, and hydrogen production via electrolysis," Int. J. Hydrogen Energy, vol 43, pp16201-16214, 2018.

[22] T. Parhizkar and R. Roshandel, "Long term performance degradation analysis and optimization of anode supported solid oxide fuel cell stacks," Energy Convers. Manag., vol. 133, pp. 20–30, 2017.

[23] A. Nakajo, F. Mueller, J. Brouwer, and D. Favrat, "Progressive activation of degradation processes in solid oxide fuel cell stacks: Part II: Spatial distribution of the degradation," J. Power Sources, vol. 216, pp. 434–448, 2012.

[24] E. M. Ryan, W. Xu, X. Sun, and M. A. Khaleel, "A damage model for degradation in the electrodes of solid oxide fuel cells: Modeling the effects of sulfur and antimony in the anode," J. Power Sources, vol. 210, pp. 233–242, 2012.

[25] J. B. Hansen, "Correlating sulfur poisoning of SOFC nickel anodes by a Temkin isotherm," Electrochem. Solid State Lett., vol. 11, no. 10, p. B178, 2008.

[26] F. N. Cayan, S. R. Pakalapati, I. Celik, C. Xu, and J. Zondlo, "A degradation model for solid oxide fuel cell anodes due to impurities in coal syngas: Part I theory and validation," Fuel Cells, vol. 12, no. 3, pp. 464–473, 2012.

[27] J. I. Gazzarri and O. Kesler, "Short-stack modeling of degradation in solid oxide fuel cells: Part I. Contact degradation," J. Power Sources, vol. 176, no. 1, pp. 138–154, 2008.

[28] Z. Yang, M. Guo, N. Wang, C. Ma, J. Wang, M. Han, "A short review of cathode poisoning and corrosion in solid oxide fuel cell," Int. J. Hydrogen Energy, vol 42, pp. 24948-24959, 2017.

[29] A. V. Virkar, "A model for solid oxide fuel cell (SOFC) stack degradation," J. Power Sources, vol. 172, no. 2, pp. 713–724, 2007.

[30] D. Larrain and D. Favrat, "Simulation of SOFC stack and repeat elements including interconnect degradation and anode reoxidation risk," J. Power Sources, vol. 161, no. 1, pp. 392–403, 2006.

[31] M. Bianco, J.P. Ouweltjes, and J. Van herle, "Degradation analysis of commercial interconnect materials for solid oxide fuel cells in stacks operated up to 18000 hours," Int. J. Hydrogen Energy, vol. 44, p. 31406-31422, 2019.

[32] M. A. Abreu-Sepulveda, N. F. Harun, G. Hackett, A. Hagen, and D. Tucker,

"Accelerated Degradation for Hardware in the Loop Simulation of Fuel Cell-Gas Turbine Hybrid System," J. Fuel Cell Sci. Technol., vol. 12, no. 2, 2015.

[33] K. Al-Khori, Y. Bicer, S. Boulfrad, and M. Koç, "Techno-economic and environmental assessment of integrating SOFC with a conventional steam and power system in a natural gas processing plant," Int. J. Hydrogen Energy, vol. 44, p. 29604-29617, 2019.

[34] H. Lai H, N. F. Harun, D. Tucker, and T.A. Adams II. Design and eco-techno-economic analyses of SOFC/gas turbine hybrid systems accounting for long-term degradation. Comput. Aided Chem. Eng., 48:415-420 (2020).

[35] D. Hughes, W. J. Wepfer, K. Davies, J. C. Ford, C. Haynes, and D. Tucker, "A Real-Time Spatial SOFC Model for Hardware-Based Simulation of Hybrid Systems," Proceedings of the ASME 2011 9th International Conference on Fuel Cell Science, Engineering and Technology collocated with ASME 2011 5th International Conference on Energy Sustainability. ASME 2011 9th International Conference on Fuel Cell Science, Engineering and Technology, Washington, DC, USA. August 7–10, 2011. pp. 409-428

[36] N. F. Harun, D. Tucker, and T. A. Adams II, "Impact of fuel composition transients on SOFC performance in gas turbine hybrid systems," Applied Energy, vol 164, p446-461, 2016.

[37] D.O. Hughes, "A hardware-based transient characterization of electrochemical start-up in an SOFC/gas turbine hybrid environment using a 1-D real time SOFC model," Atlanta, Georgia: Georgia Institute of Technology; 2011.

[38] D.F. Cheddie, N. D. H. Munroe, "A dynamic 1D model of a solid oxide fuel cell for real time simulation", J. Power Sources, vol 171, pp634–643, 2007.

[39] V. Zaccaria, D. Tucker, and A. Traverso, "A distributed real-time model of degradation in a solid oxide fuel cell, part I: Model characterization," J. Power Sources, vol. 311, pp. 175–181, 2016.

[40] A. Amiri, S. Tang, R. Steinberger-Wilckens, M.O. Tadé, "Evaluation of fuel diversity in Solid Oxide Fuel Cell system," Int. J. Hydrogen Energy, vol 43, pp23475-23487, 2018.

[41] T. A. Adams II and P. I. Barton, "High-efficiency power production from coal with carbon capture," AIChE J., vol. 56, no. 12, pp. 3120–3136, 2010, doi: 10.1002/aic.12230.

[42] R. E. James, D. Kearins, M. Turner, M. Woods, N. Kuehn, and A. Zoelle, "Cost and Performance Baseline for Fossil Energy Plants Volume 1: Bituminous Coal and Natural Gas to Electricity," NETL, NETL-PUB-22638, Sep. 2019. doi: 10.2172/1569246.

[43] "SGT6-9000HL (405 MW) heavy-duty gas turbine," siemens.com Global Website. https://new.siemens.com/global/en/products/energy/power-generation/gas-turbines/sgt6-9000hl.html (accessed Feb. 23, 2020).

[44] "Siemens SGT5-2000/3000/4000 Series | PowerWeb." http://www.fi-powerweb.com/Engine/Industrial/Siemens-SGT5-2000-3000-4000.html (accessed Feb. 23, 2020).

[45] D. R. Woods, Cost Estimation for the Process Industries. McMaster University, 1983.

[46] T. A. Adams II, L. Hoseinzade, P. B. Madabhushi, and I. J. Okeke, "Comparison of CO_2 capture approaches for fossil-based power generation: review and meta-study," Processes, vol. 5, no. 3, p. 44, 2017.

[47] "Solid Oxide Fuel Cell Market 2019 Global Analysis, Opportunities and Forecast to 2028," MarketWatch. https://www.marketwatch.com/press-release/solid-oxide-fuel-cell-market-2019-global-analysis-opportunities-and-forecast-to-2028-2019-04-08 (accessed Feb. 24, 2020).

[48] R.A. Evrin and I. Dincer, "Thermodynamic analysis and assessment of an integrated hydrogen fuel cell system for ships," Int. J. Hydrogen Energy, vol. 44, p. 6919-6928, 2019.

[49] P. Jienkulsawad, D. Saebea, Y. Patcharavorachot, and A. Arpornwichanop, "Performance assessment of a hybrid solid oxide and molten carbonate fuel cell system with compressed air energy storage under different power demands," Int. J. Hydrogen Energy, vol. 45, p. 835-848, 2020.

[50] Y.-W. Xu, X.-L. Wu, X. Zhong, D. Zhao, J. Fu, J. Jiang, Z. Deng, X. Fu, and X. Li, "Development of solid oxide fuel cell and battery hybrid power generation system," Int. J. Hydrogen Energy, vol. 45, p. 8899-8914, 2020.

Appendix

The following cost assumptions were used in this analysis, beyond those discussed in the main text. Standard power law relationships were used to model capital costs as follows, with basis years noted. CEPCI values were used for upscaling costs to 2018 (CEPCI for 2018=603.1, 2016=541.7, 1970=123). See main text for discussion and references.

- Gas turbine system (turbine + compressor + recuperator): exponent of 0.6 and basis of 73 million $US2016 for a 268 MW turbine

- Steam turbine system (turbine + boilers + pump): exponent of 0.6, basis of 340$US2017/kW

- Blower: 5120$US1970 for 30 kW system, 0.55 exponent

- Primary heat exchangers: 8000$US1970 for 100 m^2 surface area, 0.71 exponent

- Coal gasification system (coal handling, gasification, treatment, cleaning, and syngas preparation for anode feed): about 2.7 billion $US2018 for feed rate of about 135 tonne coal per hour, 0.6 exponent

- Fixed operating costs (complete system): about 116 million $US2018 for feed rate of about 135 tonne coal per hour, 1.0 exponent

- Variable operating costs (complete system): about 81 million $US2018 for feed rate of about 135 tonne coal per hour, 1.0 exponent

- Fuel costs (coal): 71.9$US2018 per tonne (as received)

Sample stream conditions for Case 2 and Case 4 are given in Tables 2.A.1 and 2.A.2, respectively. The reader can find more detailed stream information for additional substreams and cases at the LAPSE link provided in the Simulation Files section.

Table 2.A.1. Sample stream conditions of Case 2 near the end of the cell life (about 22 weeks), with stream numbers corresponding to Figure 2.2.

Stream	1	2	3	4	5	6	7	8
Temp (°C)	15	16	690	1204	677	170	210	586
P (bar)	1.0	1.0	1.0	1.0	1.0	1.0	55.0	1.0
F (kmol/s)	43.71	43.71	43.71	47.95	47.95	47.95	6.47	6.13
H_2O	-	-	-	0.074	0.074	0.074	0.320688	0.024649
O_2	0.210	0.210	0.210	0.152	0.152	0.152	trace	trace
N_2	0.790	0.790	0.790	0.721	0.721	0.721	0.0070	0.0065
AR	-	-	-	-	-	-	0.0063	0.0067
CO	-	-	-	-	-	-	0.270	0.012
CO_2	-	-	-	0.053	0.053	0.053	0.120	0.393
H_2	-	-	-	-	-	-	0.268	0.557
NH_3	-	-	-	-	-	-	40 ppm	-
COS	-	-	-	-	-	-	227 ppm	-
H_2S	-	-	-	-	-	-	5661 ppm	24 ppm
HCL	-	-	-	-	-	-	623 ppm	-
CH_4	-	-	-	-	-	-	682 ppm	720 ppm

Table 2.A.2. Sample stream conditions of Case 4 near the beginning of the cell life (about 2 weeks), with stream numbers corresponding to Figure 2.2.

Stream	1	2	3	4	5	6	7	8	9	10
Temp (°C)	15	182	690	957	274	220	210	641	957	705
P (bar)	1.0	4.1	4.1	4.1	1.0	0.9	55.0	4.0	4.1	1.0
F (kmol/s)	34.66	34.66	34.66	38.55	38.55	38.55	5.76	5.45	38.55	38.55
H_2O	-	-	-	0.082	0.082	0.082	0.321	0.025	0.082	0.082
O_2	0.210	0.210	0.210	0.148	0.148	0.148	trace	trace	0.148	0.148
N_2	0.790	0.790	0.790	0.711	0.711	0.711	0.007	0.007	0.711	0.711
AR	-	-	-	-	-	-	0.006	0.007	-	-
CO	-	-	-	-	-	-	0.270	0.012	-	-
CO_2	-	-	-	0.059	0.059	0.059	0.120	0.393	0.059	0.059
H_2	-	-	-	-	-	-	0.268	0.557	-	-
NH_3	-	-	-	-	-	-	40 ppm	-	-	-
COS	-	-	-	-	-	-	0.000	-	-	-
H_2S	-	-	-	-	-	-	0.006	24 ppm	-	-
CL_2	-	-	-	-	-	-	trace	trace	-	-
HCL	-	-	-	-	-	-	0.001	-	-	-
CH_4	-	-	-	-	-	-	0.001	0.001	-	-

Chapter 3

Eco-technoeconomic Analyses of NG-powered SOFC/GT Hybrid Plants Accounting for Long-term Degradation Effects via Pseudo-steady-state Model Simulations

Eco-technoeconomic Analyses of NG-powered SOFC/ GT Hybrid Plants Accounting for Long-term Degradation Effects via Pseudo-steady-state Model Simulations

Haoxiang Lai[a] and Thomas A. Adams II[a*]

a McMaster University, Department of Chemical Engineering, Hamilton, ON, Canada

* Corresponding Author. tadams@mcmaster.ca

Highlights

- Solid oxide fuel cell and gas turbine hybrid systems compared against standalone solid oxide fuel cell

- Considers long-term degradation effects

- Natural gas powered systems

- Eco-technoeconomic analyses

- Hybrid systems have lower costs and lower CO_2 emissions

Abstract

In this study, four solid oxide fuel cell (SOFC) power plants, with natural gas (NG) as the fuel source, that account for long-term degradation were designed and simulated. The four candidate SOFC plants included a standalone SOFC plant, a standalone SOFC plant with a steam bottoming cycle, an SOFC/GT (gas turbine) hybrid plant, and an SOFC/GT hybrid plant with a steam bottoming cycle. To capture dynamic

behaviors caused by long-term SOFC degradation, this study employed a pseudo-stead-state approach that integrated real-time dynamic 1D SOFC models (degradation calculation embedded) with steady-state balance-of-plant models. Model simulations and eco-technoeconomic analyses were performed over a 30-year plant lifetime using Matlab Simulink R2017a, Aspen Plus V12.1, and Python 3.7.4. The results revealed that, while the standalone SOFC plant with a steam bottoming cycle provided the highest overall plant efficiency ($65.0\%_{LHV}$), it also had high SOFC replacement costs due to fast degradation. Instead, the SOFC/GT hybrid plant with a steam bottoming cycle was determined to be the best option, as it had the lowest levelized cost of electricity (\$US 35.1/MWh) and the lowest cost of CO_2 avoided (-\$US100/tonneCO_2e).

Keywords: Solid oxide fuel cell, SOFC/GT hybrid, eco-technoeconomic analysis, long-term degradation

3.1   Introduction

Solid oxide fuel cells (SOFCs) produce electricity through electrochemical reactions by utilizing fuel gasses including, but not limited to, hydrogen gas, syngas, and natural gas. SOFCs are considered a next-generation power production technology that can provide greater efficiency and lower green house gas emissions compared to conventional power plants [1]. However, the large-scale commercialization of SOFCs is limited, as their lifetime is constrained due to degradation. In constant power output operation mode—also known as baseload power production—SOFC degradation occurs quickly as a result of the increasing current density (to maintain a constant power output) [2,3]. One approach to overcoming these degradation issues is to slow

the degradation rate by developing new materials that degrade more slowly [4], while another option is to keep the existing materials, but change the operating strategies or conditions [2].

Previous findings have shown that operating an SOFC in constant voltage mode instead of constant power mode can slow its degradation and significantly increase its lifetime. The strategy behind using constant voltage mode is to allow the current density to decrease over time, thereby slowing degradation [2]. However, as the current density decreases, the power output also decreases, which is not useful for baseload power production. In addition, fuel utilization also decreases over time in constant voltage mode, which causes the heating value of the anode exhaust gas stream from the SOFC to increase. SOFC/GT hybrid systems are predicated on using a gas turbine (GT) to capture this growing output of surplus chemical energy and using it to produce power. Integrating a GT into the SOFC system is advantageous, as it allows the SOFC stack to be operated in constant voltage mode, which slows SOFC degradation, and provides a means of harnessing the unspent fuel from the SOFC exhaust to compensate for the decline in power output as the SOFC ages. Thus, the net outcome is a (near) baseload power system wherein the power load gradually shifts from the SOFC to the GT [5]. Furthermore, the lifetime of the SOFC stack in a hybrid system in constant voltage mode can be more than ten times longer than the lifetime of an SOFC stack in a standalone system operated in constant power mode [6]. The SOFC/GT hybrid concept has been the focal point of various types of studies, including modeling and control [7–9], efficiency and exergy analysis [10–12], system optimization [13–17], and techno-economic analysis [18–21]. However, very few of these studies have accounted for long-term degradation in their model simulations.

Researchers have developed different SOFC degradation models for various degradation mechanisms including Ni coarsening and oxidation [22–25] and sulfur poisoning [3,26,27]. On the other hand, researchers have also conducted a number of degradation studies focusing on different SOFC components, such as the anode [22,26,28–30], cathode [31,32], electrolyte [33,34], and interconnects [35]. Recently, Naeini et al. developed a degradation model that integrates existing models of most degradation mechanisms in the literature, including Ni coarsening and oxidation, sulfur poisoning, and changes in anode pore size, conductivity, and electrolyte conductivity [36]. Instead of focusing on the degradation mechanisms, Abreu-Sepulveda et al. examined how operating conditions such as current density and fuel utilization in real-time operation impact the overall SOFC degradation rate [37]. Subsequently, Zaccaria et al. upgraded Abreu-Sepulveda et al.'s model to account for temperature effects as well as local behaviours [38]. For this work, we have selected the degradation model developed by Zaccaria et al. [38], which is an empirical model derived from experimental data for SOFC standalone and SOFC/GT systems. Thus it is most suitable for our application. A comparison of the degradation models in the literature is outside the scope of this work.

In our previous work, we designed and conducted eco-technoeconomic analyses (eTEAs) of coal-powered SOFC/GT hybrid plants and standalone SOFC plants accounting for long-term degradation effects [6]. With the exception of our prior work using coal, we are unaware of any eTEAs of SOFC/GT hybrid plants that consider long-term degradation effects over the plant's lifetime. Systems that incorporate the SOFC/GT concept have been studied with respect to one or more of the following topics: economy, energy, exergy, thermal management, and environment [21, 39–43]. However, all of these works assumed the use of a steady-state system and did not consider long-term degradation. We believe that long-term degradation plays an

important role in the eTEA of SOFC/GT hybrid systems, as it strongly affects the performance and the lifetime of the SOFC, especially when a long period of time is considered (e.g., a 30-year plant lifetime). Moreover, when considering long-term SOFC degradation, it is important to consider that the GT's power production increases over time; as such, the GT should be designed to reach its maximal efficiency and power capacity at the end of the SOFC's lifetime. To this end, a GT characteristic curve should be used, as the GT's power and efficiency change with load. The dynamic behaviors of the SOFC and the GT in a hybrid system affect the eTEA results and cannot be captured by steady-state simulations. In our previous study, we utilized a pseudo-steady-state approach—which integrated both dynamic models and steady-state models—to capture the dynamic behaviors of SOFC/GT plants and to conduct an eTEA of coal-powered SOFC/GT plants and standalone SOFC plants [6]. In the present study, we build on our previous eTEA by examining large-scale SOFC/GT hybrid plants and standalone SOFC plants that use natural gas (NG) rather than coal as the fuel source, while also considering the effects of long-term degradation. To conduct our analysis, we designed several different NG-powered standalone SOFC plants and SOFC/GT plants and subjected them to simulations. In the dynamic simulations, controllers were upgraded from the previous work to increase system stability. The modeling process is detailed in the next section.

3.2   Process Modeling

3.2.1   Process Overview

Four base cases were selected for the long-term e-TEA studies: Base Case 1—standalone SOFC plant; Base Case 2—standalone SOFC plant with a steam bottoming cycle; Base Case 3—SOFC/GT hybrid plant; and Base Case 4—SOFC/GT hybrid plant with a steam bottoming cycle. The process flow diagrams for the four base cases are shown in Figure 3.1.

As shown in Figure 3.1(a), Base Case 1 has two main components: an SOFC stack with a post-combustor, and an upstream syngas production process. The upstream syngas process produces raw syngas by reforming natural gas from the natural gas pipeline. Table 3.1 shows the conditions of the natural gas received from the pipeline [44]. Once the raw syngas has been produced, it is converted to hydrogen-rich syngas (around 60 mol% H_2) using water-gas shift reactors. Although SOFCs can directly take CH_4 as a fuel source, findings have shown that degradation can be slowed by using fuel gas with lower concentrations of CH_4 and higher concentrations of H_2. Since the SOFC stack is operated at near atmospheric pressure, a multi-stage turbine is employed to reduce the anode upstream pressure and to produce extra power. The exhaust gas from the post-combustion provides heat for the inter-heater in between the turbines, as well as for the cathode inlet air stream. Base Case 2 (Figure 3.1(b)) is identical to Base Case 1, except a steam bottoming cycle has also been added to capture the waste heat from the exhaust gas to produce extra power. The steam bottoming cycle consists of a water tank, a pump, a steam generator (heat exchanger between the flue gas and water), a multi-stage steam turbine, and a condenser.

66

Table 3.1: Assumed conditions of natural gas obtained from the pipeline [44]

Pressure	3 MPa
Temperature	27°C
Composition (molar)	
CH_4	0.931
C_2H_6	0.032
C_3H_8	0.007
C_4H_{10}	0.004
CO_2	0.010
N_2	0.016

The SOFC/GT hybrid plant (Base Case 3, Figure 3.1(c)) consists of three main components: an SOFC stack with a post combustor, an upstream syngas production process, and a gas turbine equipped with a compressor and recuperator. The SOFC portion and the upstream syngas process are almost identical to those in Base Case 1; however, the hybrid plant in Base Case 3 requires a single-stage in the upstream, as the SOFC stack is operated at 4 bar. Cold air bypass streams are designed to control the cathode inlet temperature and the gas turbine inlet temperature. Base Case 4 (Figure 3.1(d)) utilizes the same design as Base Case 3, only it also features the addition of a steam bottoming cycle.
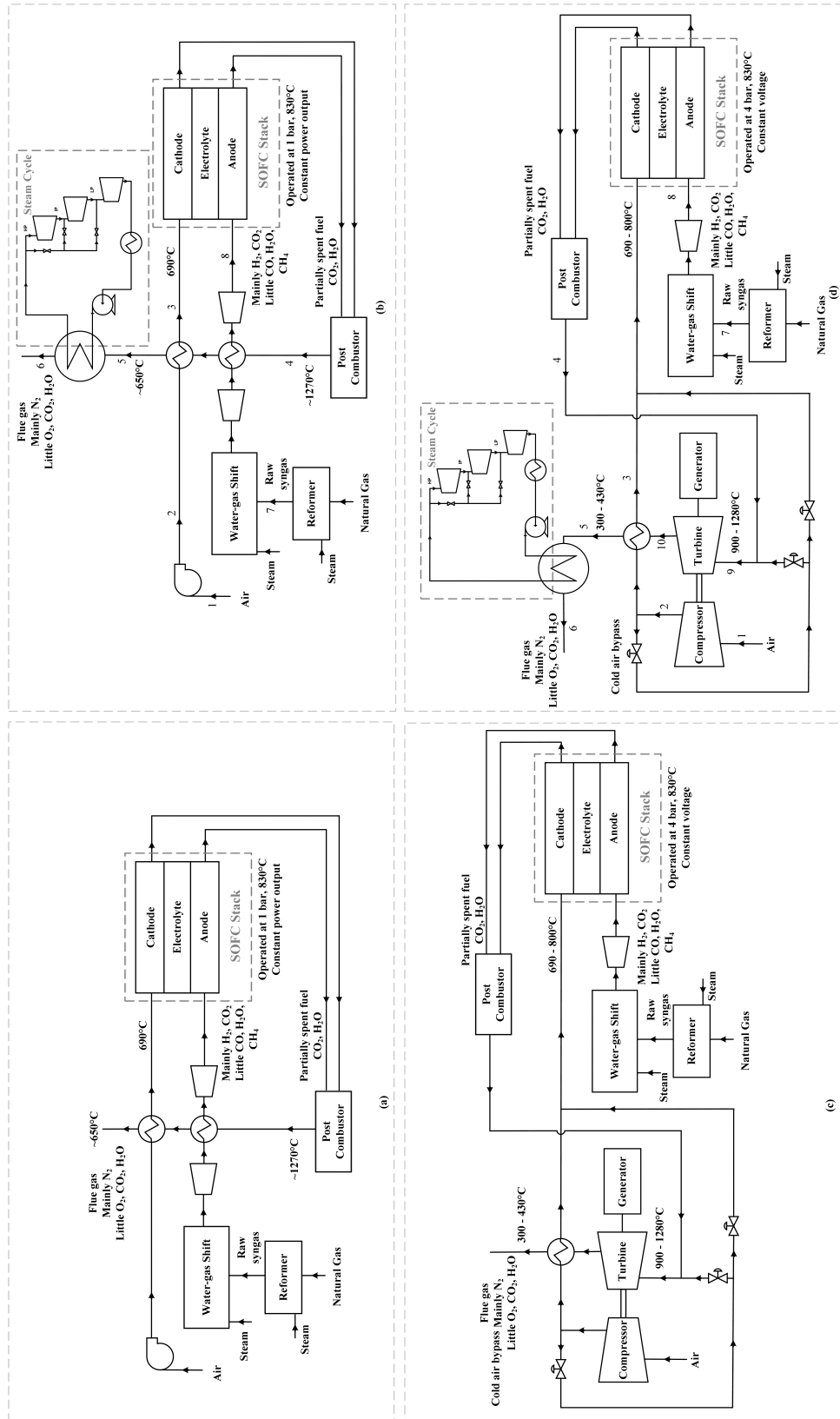
Figure 3.1: Process flow diagrams of the four base cases. Subfigures (a) through (d) represent Base Cases 1-4, respectively. Only major units and streams are shown in the diagrams for brevity.

3.2.2   Plant Models

A dynamic SOFC model and a steady-state balance-of-plant model were developed for each base case. The reason for choosing this hybrid modeling approach rather than completely dynamic modeling or completely steady-state modeling was that the dynamic behaviors of the SOFC (due to degradation) is vital for the eTEA while the dynamic behaviors of the balance-of-plant have insignificant impacts. Developing dynamic models for the balance-of-plant is out of the scope of this study. Instead, we took a pseudo-steady-state approach to integrate and simulate the dynamic SOFC model and the steady-state balance-of-plant model, which will be described in later section. The dynamic SOFC models contained the SOFC stack and the post combustor and provided real time calculations of thermal and electro-chemical changes in the SOFC, as well as degradation. The steady-state balance-of-plant models included everything shown in Figure 3.1, with the exception of the SOFC stack and the post-combustor. For instance, the balance-of-plant model for Base Case 1 included the reformer, water-gas shift process, multi-stage turbine, air blower, and heat exchangers.

3.2.2.1   Dynamic SOFC Model

The dynamic SOFC model used in this work is one-dimensional real-time model of a co-flow, planar anode-supported SOFC with an Ni-doped yttria-stabilized zirconia (YSZ) anode, a YSZ-lanthanum strontium magnetite cathode, and a YSZ electrolyte [38]. This model employs the finite difference and finite volume methods to calculate the SOFC's real-time thermal and electrochemical properties, respectively. The SOFC cell was discretized into 20 nodes (20 control volumes) along the direction of the gas

flow, as a prior sensitivity study determined this to be the optimal number of nodes with regard to the trade-off between numerical complexity and model accuracy. For each node (control volume), characteristic variables such as current density, Nernst potential, temperature, and fuel composition were calculated at each sampling time. Details on the model equations, the experimental data used to develop the model, and model validation are provided in [37,38,45–47].

$$r_d = \frac{0.59FU + 0.74}{1 + \exp \frac{T-1087}{22.92}} (e^{2.64i} - 1) \qquad (1)$$

Equation (1) describes the effect of degradation on the SOFC in the model, where r_d, FU, T, and i represent the degradation rate (in %/(1000h)), fuel utilization (in fraction), temperature (in K), and current density (in A/cm^2), respectively. This equation was derived via regression analysis and extrapolation using prior experimental data. The process used to obtain Eq.1 is described in greater detail in [37,38]. The degradation rate is calculated in terms of percent of voltage drop per thousand hours, and is used to calculate the effect of degradation on ohmic resistance and cell voltage. The model was implemented in Matlab Simulink R2017a and subsequently modified and augmented with upgraded controllers.

The dynamic model of Base Case 1 has three feedback controllers: an SOFC power output controller that manipulates the SOFC load (current); an SOFC fuel utilization controller that manipulates the anode inlet fuel flow rate; and an SOFC average cell temperature controller that manipulates the cathode inlet air flow rate. A different control strategy was implemented in Base Case 3, which included: a feedback net power controller that manipulates the anode inlet fuel flow rate; a feedback voltage

controller that manipulates the SOFC load (current); and a feedforward SOFC average cell temperature controller that manipulates the cold air bypass valves (thus adjusting the cathode inlet air temperature). As the SOFC degrades over time, the amount of unspent fuel in the anode exhaust increases, which results in a corresponding increase in the post-combustor exhaust temperature. This is a concern, as, without proper controls, this can eventually result in the gas turbine inlet temperature rising to unacceptable levels. Thus, the cold air bypass streams manipulated by the controllers help to ensure that the gas turbine inlet temperature and the SOFC average cell temperature remain in acceptable ranges.

In Base Case 3, the net power controller moderated the net power of the system by using the predicted gas turbine power production to determine the adjustment of the anode inlet fuel flow rate (which affects the power production of both the SOFC and the gas turbine). However, as the SOFC degrades, the fuel flow rate and the heating value of the post-combustor exhaust change, which affects the power and efficiency of the gas turbine due to off-design operations. As such, a gas turbine characteristic curve correlating efficiency with power production for off-design operations was employed to predict the GT's power production while also accounting for off-design efficiency changes in different operating conditions (heating value of the gas turbine inlet stream). As this curve was generated using proprietary data from a turbine manufacturer (Siemens), it cannot be released for intellectual property reasons. However, this curve was embedded in the model and grouped with other information for reproduction purposes, which will be explained in section 2.3.1. Base Case 2 and Base Case 4 used the same control strategies as Base Case 1 and Base Case 3, respectively. All controllers used in this work were proportional-integral-derivative controllers, with manual tuning techniques being used to determine the tuning parameters.

71

3.2.2.2   Steady-state Balance-of-plant Model

For each base case, the balance-of-plant, which includes every unit (as shown in Figure 3.1) except the SOFC stack and the post-combustor, was modeled in Aspen Plus V12.1. The advantage of modeling the balance-of-plant in Aspen Plus is that it reduces modeling complexity while still providing representations of the system and equipment sizes that are sufficient for conducting the eTEA. In Aspen Plus, the Peng-Robinson equation of state was used along with the Boston-Mathias modification for most of the units except that the NBC/NRC steam tables were used for pure water streams. A detailed discussion on the selection of the thermodynamic method and the accompanying assumptions is available in [48,49].

The balance-of-plant model for Base Case 1 included the reformer, water-gas shift reactors, upstream multi-stage turbine, air blower, and heat exchangers and pumps responsible for heat management and steam generation (for the water-gas shift). The isentropic efficiency of the multi-stage turbine was assumed to be 88% without considering a turbine characteristic curve. The turbine accounted for around 12% of the plant's gross power production, which refers to the plant's total power production before subtracting any power consumption. A turbine characteristic curve was not implemented in this case because it would increase the model's complexity while only altering the gross power production by around 0.6%. The air blower was assumed to have a constant isentropic efficiency of 90%. Since the blower consumed a negligible amount of electricity, an efficiency characteristic curve was not considered. The heat exchangers were designed by assuming a minimum temperature approach of 10°C. The net power of the balance-of-plant contributed around 9% of the entire plant's net power.

The balance-of-plant model for Base Case 2 included all the same units as the Base Case 1 model, along with a steam bottoming cycle. The steam cycle consisted of a water pump, a heat exchanger (a steam generator that uses heat from the flue gas), a multi-stage steam turbine, a cooler (condenser), and a water tank. The steam cycle was operated with the multi-stage turbine inlet steam conditions set to 550°C and 100 bar, with hot bypasses between the stages to ensure 100% vapor fraction within the entire turbine unit. It was assumed that the pump had 90% efficiency, the heat exchanger (the steam generator) had a minimum temperature approach of 10°C, the condenser had 5°C of subcooling, and the steam turbines had 89% isentropic efficiency. The outlet pressure and hot bypass ratio of each stage in the multi-stage turbine were determined using the optimization tool in Aspen Plus in an attempt to maximize power production while still achieving 100% vapor fraction between the stages and at least 95% vapor fraction in the outlet stream. The optimal outlet pressures of the three stages were determined to be 24.7 bar, 4.7 bar, and 1.1 bar, with bypass ratios of 8% and 2% of the total steam to the medium- and low-pressure turbines, respectively. Similar to the upstream turbines, a characteristic curve was not implemented in steam turbines because it would increase the model's complexity while only altering the gross power production by around 1.3%.

The upstream process in the Base Case 3 balance-of-plant model was almost identical to Base Case 1, except the Base Case 3 model only used a single-stage turbine, as the SOFC stack was operated at a pressure of 4 bar instead of 1 bar. The net power and electrical efficiency of the gas turbine (including the compressor) was determined using the aforementioned gas turbine characteristic curve. In addition, a heat exchanger model was used to represent the recuperator by assuming a minimum temperature

approach of 10°C.

The balance-of-plant model for Base Case 4 was largely the same as the Base Case 3 model, except it also included a steam bottoming cycle with a similar set up to the one used in Base Case 2. Since the heating value of the flue gas in Base Case 4 was much lower than that of Base Case 2, the inlet steam conditions to the multi-stage steam turbine were set to 294°C and 25 bar. Additionally, the same optimization approach that was used for Base Case 2 was applied in Base Case 4, which yielded optimal outlet pressures of 5.3, 3.3, and 1.1 bar for the three steam turbine stages, with a bypass ratio of 35% of the total steam to the medium pressure turbine.

3.2.3   Pseudo Steady-state Model Simulation
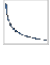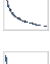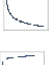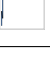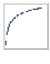
To perform model simulations for the eTEA, the conditions for the four base cases are summarized in Table 3.2, which are the same for all four cases. The four base cases were designed with a net electricity production of 550 MW (combined AC and DC) and a plant lifetime of 30 years. The SOFC average cell temperature for each case was regulated at 830°C by the controllers described in Section 2.2.1. The dynamic models were simulated using input variables (either their constant values or their initial values) and predicted variables, which are presented in Table 3.3. Base Case 1 utilized an SOFC stack operated in constant power mode; however, the stack power allowed for a small and slow drop (around 1.8%) over the cell's lifetime in order to maintain constant net power production for the entire plant. The model simulations were conducted by integrating the dynamic model parts and steady-state model parts with a pseudo steady-state approach. A time step of one week was selected for the

pseudo steady-state simulation, as the SOFC degradation rate did not change much (change within 0.5% relatively) during this time interval. It was assumed that the dynamic behaviors of the dynamic models within a weekly time step could be treated as steady-state at the start of the time step. The simulation data from the dynamic models were recorded with a sampling time of 0.08 h, and the weekly data was then collected and used to run the simulations for the steady-state models. The simulation processes are described in detail in the following subsections.

Table 3.2: Conditions for all four base cases

Net Power	550 MW
Plant lifetime	30 years
Initial FU (fuel utilization)	80%
Initial current density	0.5 A/cm^2
SOFC T$_{avg}$	830°C

Table 3.3: Variables used in the SOFC Simulink models for Base Cases 1 and 3. The sparklines represent the trends of each variable over time during simulation along with their relative change ranges. (for example, the stack power in Base Case 1 decreased by 1.8% over the lifetime of the SOFC) → indicates a constant value or variable controlled at a constant setpoint.

		Trend Base Case 1: Standalone SOFC	Base Case 3: SOFC/GT Hybrid	Note
Operating variables	Stack power	1.8%	71%	Controlled or being affected by other operating variables
	Voltage	20%	→	
	Current density	23%	70%	
	Fuel utilization	→	76%	
	Average cell temperature	→	2.4%	
	Turbine power and efficiency	N/A	67%(power) 31%(efficiency)	Predicted by reduced model To be matched by ouputs from Aspen Plus model
Inlet variables	Fuel flow	22%	25%	The outputs of Aspen Plus simulations should match the values of these variables at each time step. Fuel flow and air flow in Base Case 1, and fuel flow and air temperature in Base Case 3 were manipulated by controllers. The others were constant.
	Fuel temperature	→	→	
	Fuel pressure	→	→	
	Fuel composition	→	→	
	Air flow	28%	→	
	Air temperature	→	17%	
	Air pressure	→	→	
Outlet variables	Combusted gas flow	27%	1.7%	Provided as inputs to Aspen Plus model
	Combusted gas temperature	0.8%	44%	
	Combusted gas pressure	→	→	
	Combusted gas composition	→	→	

76

3.2.3.1   Control Strategy in Dynamic Model Accounting for Balance-of-plant Model

The control strategy in Base Case 1 aimed to maintain a constant net power output (the net power of the SOFC and the balance-of-plant), a constant FU, and a constant T (SOFC average cell temperature). The power controller in the dynamic model adjusted the SOFC power to follow a decreasing trajectory such that the system could achieve constant net power with the addition of the power produced by the balance-of-plant. This outcome is possible due to the fuel flow rate increasing as the SOFC degrades over time, which in turn causes an increase in the power produced by the upstream multi-stage turbine. This decreasing SOFC power trajectory was determined manually through an iterative approach. The trajectory was described using second order polynomial with respect to time. The coefficients of the polynomial were first guessed using information from preliminary simulations, and then iteratively refined by running additional simulations with repeatedly updated coefficients. Only a few iterations were required to reach a final trajectory which achieves essentially constant net system power output (with small variations) as determined by visual inspection.

As can be seen in Table 3.3, the power setpoint trajectory entailed a slow decrease in the SOFC's power over its lifetime, while maintaining the plant's net power at 550 MW. Base Case 2 had the same control strategy as Base Case 1, only it used a different second order polynomial trajectory for the power controller setpoint. In Base Case 2, the steam bottoming cycle also contributed to the balance-of-plant power production by harnessing the increasing heating value of the SOFC's exhaust stream as the SOFC degraded. Following a similar process to Base Case 1, the second

order polynomial trajectory for the power controller in Base Case 2 was determined iteratively as well.

The control strategy used in Base Case 3 entailed maintaining a constant net power, a constant voltage, and a constant T. In this SOFC/GT hybrid plant, the SOFC power decreased as it degraded, but the voltage was kept constant (Table 3.3). On the other hand, the GT harnessed the increasing heating value of the SOFC exhaust stream, allowing it to increase in its power output and efficiency (calculated according to the embedded turbine characteristic curve discussed earlier). In the dynamic model, the net power controller manipulated the anode inlet fuel flow based on information about the power produced by the balance-of-plant (mainly consisting of the power from the GT and upstream turbine) in order to obtain the SOFC power required for achieving a constant net plant power. A model-based controller was used for determining the SOFC power setpoint based on the heating value of the SOFC exhaust to try to achieve 550 MW net power. The model-based controller considered information about the GT characteristic curve, heating value of the SOFC exhaust, upstream turbine power, compressor parasitic loads, and pump parasitic loads. This significantly outperformed a PID controller. Refer to Appendix A in the supplemental material for details. The control strategy used in Base Case 4 was the same as in Base Case 3, except that the balance-of-plant power also included the power produced by the steam bottoming cycle.

3.2.3.2   Simulation Methodology

The model simulation of each base case involved a combination of dynamic model simulation of the SOFC stack and post-combustor in Matlab Simulink and steady-state model simulation of the balance-of-plant in Aspen Plus. To capture the slow dynamics

due to SOFC degradation over a long time period, a pseudo steady-state approach was employed for the combination of dynamic and steady-state model simulations. During the pseudo steady-state simulations, the conditions of certain streams connecting the dynamic SOFC model and the steady-state balance-of-plant model should be consistent. For instance, in Base Case 4, the conditions of streams 3, 4, and 8 (Figure 3.1) computed by the dynamic and steady-state models should be consistent for each time step. Similarly, variables such as the GT power predicted by the dynamic model and the actual GT power computed by the steady-state model should be consistent for each time step. Therefore, an iterative solution is required to converge the combined simulation of the dynamic model and steady-state model for each time step. Solution algorithms were developed as Python (Python 3.7.4) scripts and Matlab scripts to automate the entire simulation for each base case. Specifically, the Matlab script was employed to initiate the dynamic Simulink model simulation, record the resultant data, and save the data as text files that could be read by the Python script. On the other hand, the Python script read the data from Matlab, initiated the steady-state Aspen Plus model simulation, and then recorded and checked whether the simulation results from the dynamic and steady-state models matched within a certain error tolerance. In addition to the pseudo steady-state simulation, the initial conditions of the dynamic model for each case were changed and tested such that the initial current density, initial voltage, and initial fuel utilization were approximately the same for all cases.

Figure 3.2 shows the information flow between the dynamic model and the steady-state model at one pseudo steady-state time step for Base Case 3. As can be seen, some inlet variables (box A1, Figure 3.2) were constant through every time step, including the temperature, pressure, and composition of the inlet fuel stream (stream 8, Figure 3.1), as well as the flow rate and pressure of the inlet air stream (stream 3, Figure

3.1). At one pseudo-steady-state time step (each pseudo-steady-state time step is one week long), the dynamic simulation in Matlab Simulink began the simulation by using the reduced model to estimate the GT's power and efficiency, as well as the total balance-of-plant power. The dynamic simulation ran using a fixed stepsize of 0.08 h with ode4 as the chosen integrator. The controllers manipulated the inlet fuel flow rate, the cathode inlet air temperature, and the SOFC load (current density) to achieve the desired set points for net power, SOFC average cell temperature, and voltage, respectively. During the simulation, operating and outlet variables, including SOFC stack power, voltage, current density, fuel utilization, average cell temperature, combusted gas flow rate, combusted gas temperature, combusted gas pressure, and combusted gas composition, were computed. These outlet variables, as well as the variables shown in boxes A1, B1, and C1 in Figure 3.2, were recorded for every 0.8 h sampling interval within the week-long pseudo steady-state time step. The data for the 5th hour of the pseudo steady-state time step were selected to represent the slow dynamics of the system as a pseudo steady-state, and were used for the balance-of-plant model simulations. These steps were completed by a Matlab script with a function that called Matlab Simulink for the dynamic simulation. The pseudo steady-state data, which were recorded as .csv files by the Matlab script, were then used by a Python script that called Aspen Plus for the balance-of-plant model simulation. The outlet variables from the Simulink model (such as combusted gas flow rate, combusted gas temperature, combusted gas pressure, and combusted gas composition as stream 4 in Figure 3.1) were taken as inlet variables for the Aspen Plus balance-of-plant model. The GT isentropic efficiency in the Aspen model was specified using a reduced model that correlated the GT isentropic efficiency with the GT efficiency predicted in the dynamic model simulation. The inlet natural gas flow rate was also estimated using a reduced model that predicted the natural gas flow
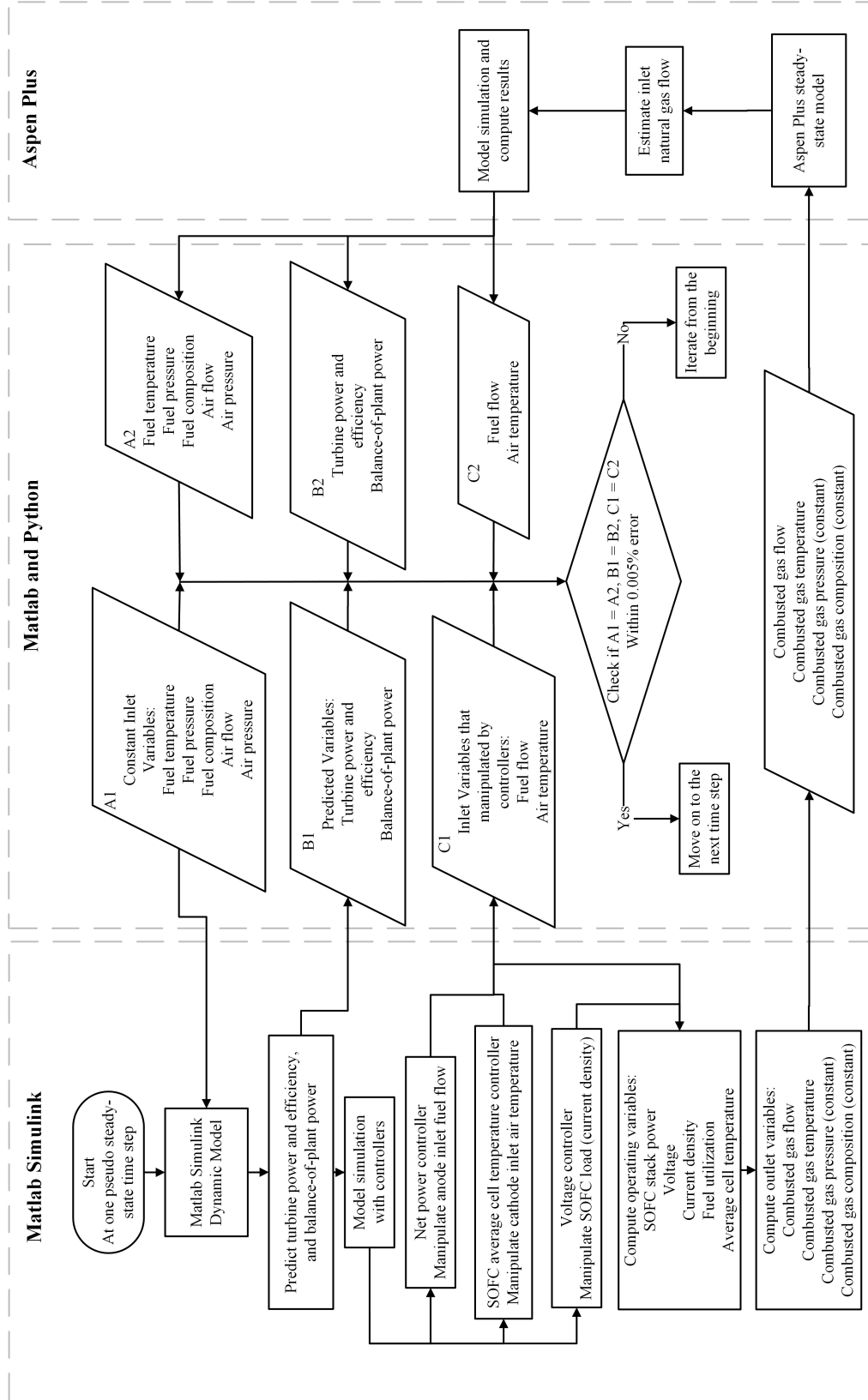
Figure 3.2: Information flow between the dynamic model and steady-state model for one pseudo steady-state time step for Base Case 3

rate based on the SOFC cathode inlet fuel flow rate in the dynamic model. The steady-state simulation of the balance-of-plant model returned results as blocks A2, B2, and C2 (see Figure 3.2), which were compared to blocks A1, B1, and C1 on the dynamic model side, respectively. If the relative error between these variable sets was less than 0.005%, the week-long pseudo steady-state time step was completed. If the error was not acceptable, the algorithm was iterated with new estimated values for certain variables (such as GT efficiency and inlet natural gas flow rate) until the relative error fell within the acceptable range. By using the discussed reduced models to give very good initial guesses, only one or two iterations were required for a pseudo steady-state time step. Pseudo steady-state simulations were performed using the week-long time step over the lifetime of the SOFC stack in each base case (SOFC lifetime varied from case to case), with this cycle being repeated for a plant lifetime of 30 years.

3.2.4   Eco-technoeconomic Analyses

The NGCC (natural gas combined cycle) base case without CO_2 capture presented in [50] was selected as the baseline reference point for the eTEA in this study. The selected reference case had an $LCOE_{base}$ (levelized cost of electricity) of \$US 48.4/MWh and CO_2 Emission$_{base}$ of 373.0 kg CO_2e/MWh (note CO_2e is short for CO_2 equivalents). In the present work, the price of the SOFC was assumed to be \$2,000 per kW of nameplate power capacity, and the cost of the gas turbine used in Base Cases 3 and 4 was estimated based on the data provided in [51,52] (additional details are shown in Appendix B in the supplemental material). All dollar amounts in this work are expressed in 2016 U.S. dollars. The capital cost of the SOFC stacks in

each base case was calculated for each year in the plant's 30-year lifetime based on the number of stacks needed in each year. The capital costs of the upstream NG reformer and the water-gas shift reactor were estimated based on the units used in Case 1-1 (an NG-powered hydrogen production plant equipped with a reformer and water-gas shift reactor) of a baseline report by NETL [53] and adjusted according to the NG flow rate. Details regarding the capital costs of other small units can be found in Appendix B. The operating costs were mainly estimated based on Case B31A of a different baseline report from NETL. This case consisted of an NGCC plant without CO2 capture [44], only with the addition of 21% (estimated based on the portion of capital costs) of the operating cost of Case 1-1 (adjusted with NG flow rate) to account for the reformer and water-gas shift reactor [53]. The NG price we used was \$3.37/GJ (or \$3.55/MMBtu both in HHV), which is the same price as the reference case [50].

The LCOE and CCA (cost of CO_2 avoided) of each case was calculated using Eq. (2) and Eq. (3) as follows:

$$LCOE_{plant} = \frac{Levelized\ cost\ of\ the\ plant\ over\ the\ lifetime}{total\ power\ production\ over\ the\ lifetime} \tag{2}$$

$$CCA_{plant} = \frac{LCOE_{plant}\ -\ LCOE_{base}}{CO_2\ Emission_{base}\ -\ CO_2\ Emission_{plant}} \tag{3}$$

where the "plant" subscripts indicate one of the four base case plants. The levelized cost was calculated by assuming a 5% inflation rate and a time-value-of-money interest rate of 10%. CO_2e Emission refers to direct CO_2e greenhouse gas potential of the plant over the lifetime, which equals the CO_2 emission in all cases since CH_4 was assumed to be completely combusted in the post-combustor and NOx was not considered. The CCA expresses the cost of CO_2e emissions avoided by constructing

and using one of the four base case plants instead of the baseline NGCC plant. An extensive discussion on why this formulation is the most appropriate choice for CCA can be found in [50]. Finally, the SOFC stack efficiency is defined as the stack's DC power output divided by the LHV of the syngas fuel it consumes, and the overall plant efficiency is defined as the SOFC stack's DC power output plus the balance-of-plant AC power output, divided by the LHV of the natural gas entering the plant. Both the efficiencies are calculated over the 30-years plant lifetime.

3.3   Results and Discussion

The dynamic SOFC model simulation results for the four base cases are shown in Figure 3.3, and the corresponding results for the entire plants are shown in Figure 3.4. In Base Case 1 (Figure 3.3(a) and Figure 3.4(a)), the SOFC power output was controlled to follow a declining trajectory (a second order polynomial trajectory) in order to maintain a net plant power (including the balance-of-plant) of 550 MW. The fuel utilization (FU) was also controlled at a constant level of 80%. As the SOFC stack degraded over time, the current density increased from its initial value of 0.5 A/cm^2, while the voltage dropped below 0.8 V. Under these operating conditions, the standalone SOFC stack in Base Case 1 was predicted to have a lifetime of around 20 weeks before catastrophic breakage would occur. Figure 3.4(a) shows the periodic replacement of the SOFC stack every 20 weeks over the plant's 30-year lifetime. Within each replacement cycle, the stack and plant efficiency decreased as the SOFC degraded due to the system requiring greater amounts of fuel to produce the same amount of power.
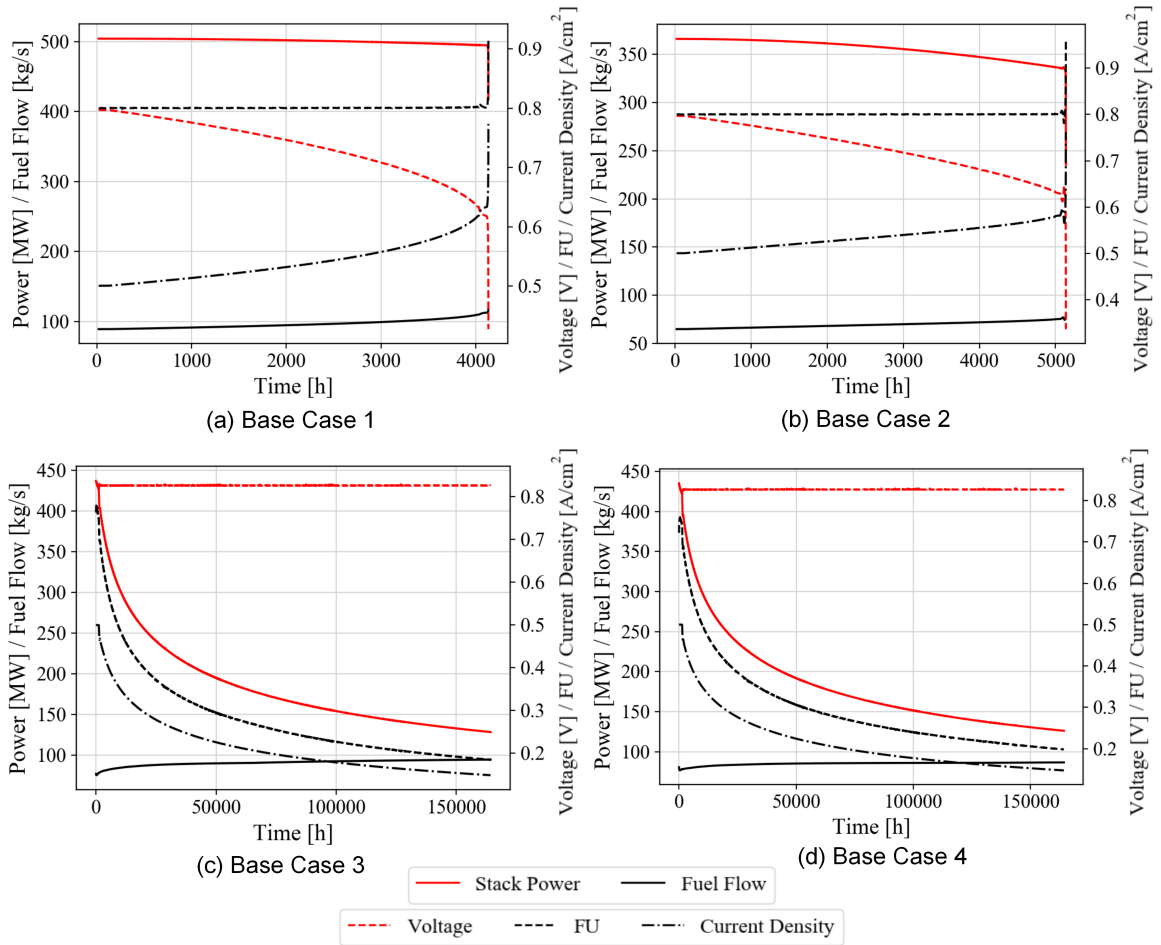
Figure 3.3: SOFC performance curves for Base Cases 1-4. Power and fuel flow can be read from the primary y-axis. Voltage, FU, and current density can be read from the secondary y-axis.

The SOFC performance curves for Base Case 2 followed similar trends to those observed in Base Case 1, except the stack power was allowed to drop further down (also following a second order decreasing trajectory). In Base Case 2, not only did the amount of power produced by the upstream turbine continually increase due to the increase in the fuel flow rate over time, but the power produced by the steam bottoming cycle similarly increased as the heating value of the SOFC anode exhaust stream also increased over time. By offsetting the decreasing stack power with the increase in balance-of-plant power (including the upstream turbine and the steam
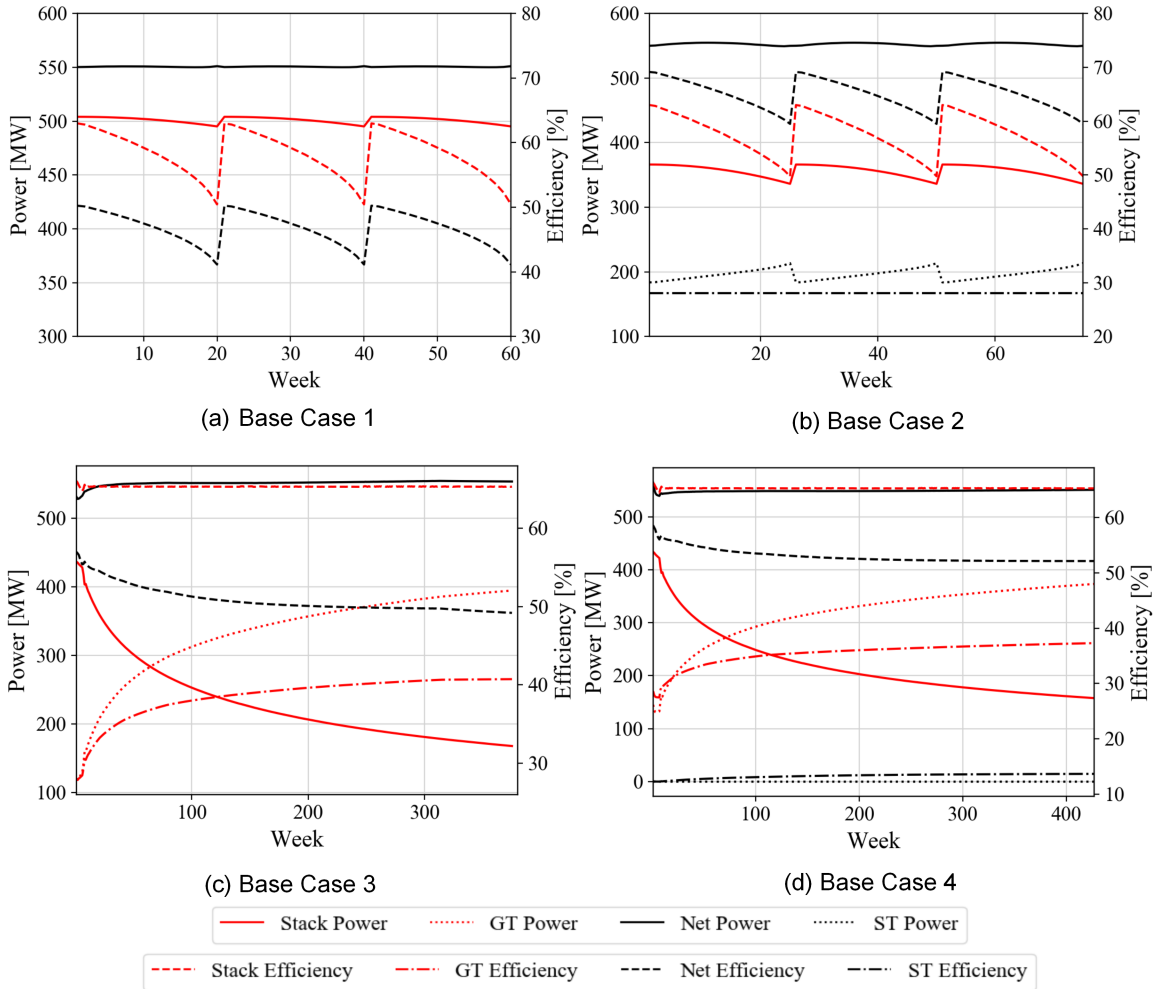
Figure 3.4: Plant performance curves of Base Cases 1-4. Power and efficiency can be read from the primary and secondary y-axes, respectively.

bottoming cycle), the net power was maintained at around 550 MW. Compared to Base Case 1, the decrease in stack power output in Base Case 2 indicated a slower increase in current density, which resulted in a slower degradation rate. Consequently, the lifetime of the SOFC stack in Base Case 2 increased to around 25 weeks. Furthermore, the net plant efficiency in Base Case 2 was also significantly higher compared to Base Case 1, as the steam bottoming cycle was able to capture and reuse the waste heat in the SOFC anode exhaust.

The SOFC stack in Base Case 3 (SOFC/GT hybrid plant) was operated in constant voltage mode with decreasing current density and power output, which can markedly increase the SOFC's lifetime. Although the simulation predicted that the SOFC's lifetime could exceed 14 years, a practical regular replacement lifetime of 375 weeks (around 7.2 years) was chosen, as the FU dropped to 25% at this point. At this replacement point, the SOFC stack's power output decreased to 157.5 MW (about 38.5% of its initial capacity) and its current density dropped from the initial value of 0.5 A/cm^2 to 0.19 A/cm^2. As can be seen in Figure 3.4(c), the plant gradually shifted the power load from the SOFC stack to the GT as the SOFC degraded, thus maintaining a net power output of 550 MW. The GT was designed to operate at its maximum power capacity (405 MW) and maximum efficiency (42.6%) at the end of the 375-week-cycle; as shown in the turbine characteristic curve, the GT's power and efficiency gradually increased throughout each cycle. However, the net plant efficiency decreased throughout each cycle, as the NG fuel flow rate needed to be continually increased to maintain a constant net power output. This decline in net efficiency was also due to the shift in power load from the more efficient SOFC stack to the less efficient GT over the course of each cycle.

The SOFC stack performance curves and plant performance curves in Base Case 4 were very similar to those in Base Case 3, except Base Case 4 also included the addition of curves for the steam bottoming cycle. In Base Case 4, the SOFC stack was operated with constant voltage, along with decreasing current density and power output. Following the same rule as Base Case 3, a lifetime of 427 weeks (around 8.2 years) was selected for the SOFC stack in Base Case 4, as this is the point where the FU dropped to 25%. Compared to Base Case 2, the steam cycle

in Base Case 4 produced much less power due to the much lower heating value of the exhaust stream (can be seen in stream 5, Figure 3.1). However, the addition of the steam cycle resulted in a higher net plant efficiency compared to Base Case 3.

The short stack lifetime in Base Case 1 and 2 indicates that these two SOFC plants might not be applicable in practice under the current operating conditions (80% fuel utilization and 0.5 A/cm^2 initial current density). In fact, running the SOFC with lower fuel utilization or lower current density could reduce the degradation rate and thus increase the stack lifetime [2]. It should be noted that, with lower initial fuel utilization or current density, the degradation rates in Base Case 3 and 4 are expected to be slower too. In this study, the main focus is the comparison between two different operating modes of SOFC: nearly constant power mode (Base Case 1 and 2) and constant voltage mode (Base Case 3 and 4), with all other operating conditions remain the same (such as initial fuel utilization, initial current density, and average cell temperature). The values of these operating conditions were selected according to the experimental conditions which the model was developed based on [37], and changing these operating conditions would be out of the scope of this study.

The results of key parameters of the eTEA for the four base cases are summarized in Table 3.4, including efficiencies, costs, LCOE, and CCA. While the hybrid plants (Base Cases 3 and 4) were generally more efficient than the SOFC standalone plants (Base Cases 1 and 2), Base Case 2 had the highest overall plant efficiency, mainly due to the highly-efficient SOFC power production enabled by the steam bottoming cycle's reuse of waste heat. The hybrid plants sacrificed efficiency by shifting the power load to the less efficient GT as the SOFC replacement cycle progressed in order to prolong the SOFC stack's lifetime. Figure 3.5 shows the number of times the SOFC stacks in

each base case needed to be replaced each year over the plant's 30-year lifetime. For instance, Base Cases 1 and 2 each used three stacks in the first year of the plant's life, as the lifetimes of the stacks in these cases were 20 and 25 weeks, respectively.

Table 3.4: Results of key eTEA parameters for all four base cases over the 30-years plant lifetime

	BC 1 SOFC Standalone	BC 2 SOFC with steam cycle	BC 3 SOFC/GT Hybrid	BC 4 SOFC/GT with steam cycle
SOFC Stack Efficiency (LHV)	58.3%	57.4%	65.3%	65.3%
Overall Plant Efficiency (LHV)	46.8%	65.0%	50.8%	53.0%
First year Capital Cost ($ Million)	$3,558	$2,636	$1,464	$1,445
Average Annual SOFC Replacement Cost ($ Million)	$2,642	$1,515	$120	$90
Annual Material, Operating and Maintenance Cost ($ Million)	$161	$116	$148	$141
LCOE ($/MWh)	$4327	$194	$38.5	$35.1
CO_2 Emission (kg/MWh)	275	198	252	240
CCA ($/tonneCO$_2$e)	$2,833	$831	-$81.4	-$99.9

In contrast, Base Cases 3 and 4 only required one stack each in the first year, as their SOFC stacks had lifetimes of 375 weeks and 427 weeks, respectively. The total number of SOFC stacks required over the 30-year plant lifetime for Base Cases 1-4 were 79, 63, 5, and 4, respectively. As mentioned in the methodology section, the cost of the SOFC stacks was calculated for each year in the plant's 30-year lifetime based on the number of stacks needed in each base case. Predictably, the first-year capital costs for Base Cases 1 and 2 were much higher compared to Base Cases 3 and 4, as Base Cases 1 and

2 each required the use of three stacks in the first year, while Base Cases 3 and 4 only required one. In addition to the SOFC stacks purchased in the first year, this first-year capital costs for each base case accounted for all other units in each plant. The average annual SOFC replacement cost was calculated as the annual average of the sum of the cost of SOFC stacks accounting for time-value-of-money and the inflation rate over the plant's 30-year lifetime. This cost decreased from Base Cases 1-4 because the frequency of SOFC stack replacement correspondingly decreased. Notably, Base Case 2 had the lowest annual material, operating, and maintenance costs, mainly due to having the highest overall plant efficiency. In particular, Base Case 2 achieved significant cost savings on fuel, as it used the least amount of NG out of the four base cases.
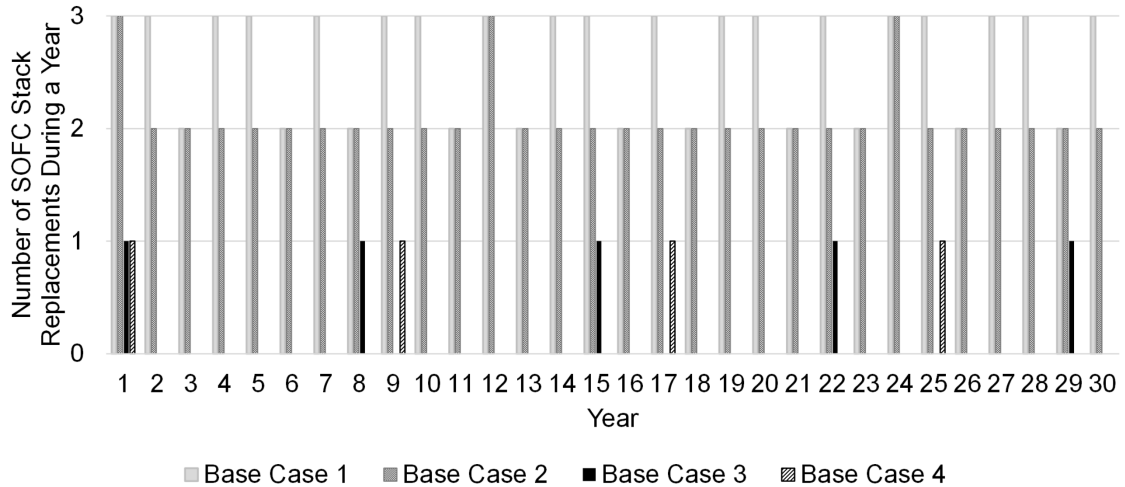
Figure 3.5: SOFC stack replacement frequency for the four base cases over a 30-year plant lifetime

The levelized cost of electricity (LCOE) decreased sequentially from Base Case 1 to Base Case 4 due to the corresponding decrease in the number of SOFC stacks (which contributed the largest portion of the total costs) required over the plant's 30-year lifetime. The findings showed that the hybrid plants (Base Cases 3 and 4) had

lower LCOEs compared to the baseline NGCC plant (baseline = \$48.4/MWh), as determined based on the assumed SOFC price in the four base cases. In addition, all four base cases had lower direct CO_2 emissions compared to the baseline NGCC plant (373.0 kg/MWh), mainly due to their higher efficiency. Predictably, the lowest CO_2 emissions were observed in Base Case 2, as it was the most efficient of the four base cases. However, Base Case 2 had high costs associated with SOFC stack replacement, as the SOFC stack in this case had a fairly short lifetime. As a result, Base Case 2 had a CCA (cost of CO_2 avoided) of \$831/tonneCO$_2$e. This CCA figure indicates that, although Base Case 2 emitted less CO_2 than the baseline NGCC plant, the high cost per tonne of emitted CO_2 undermines its viability. The CCA results for Base Cases 3 and 4 are negative because these cases had both lower costs and lower CO_2 emissions compared to the baseline NGCC plant. The lower LCOEs and negative CCAs recorded for Base Cases 3 and 4 established them as better alternatives than the baseline NGCC plant and Base Cases 1 and 2 from an eco-techno-economic perspective. Ultimately, the eTEA results revealed that Base Case 4 (SOFC/GT hybrid plant with a steam bottoming cycle) had the lowest LCOE (\$35.1/MWh) and lowest CCA (-\$99.1/tonneCO$_2$e) of the four base cases, thus establishing it as the best design.

3.4   Sensitivity Analyses

Since the lifetimes of the SOFC stacks in the SOFC/GT hybrid plants (Base Cases 3 and 4) were chosen arbitrarily, the first sensitivity analysis investigated how the use of different SOFC lifetimes in these plants impacted the eTEA results. Instead of replacing the SOFC stack when FU reached 25%, as we did in the base cases,

we replaced the SOFC stack when FU reached 20% and 30% (henceforth referred to as the "20% FU case" and "30% FU case") in the sensitivity analyses. In Base Cases 3 and 4, the GT was designed to provide peak performance (maximum power output and maximum efficiency) at the end of the SOFC replacement cycle (when FU reached 25%). However, it was necessary to redesign and re-simulate the systems, as changing the replacement point of the SOFC stack also changed the required power capacity of the GT. Compared to the base cases, the 20% FU cases required a larger GT, while the 30% FU cases needed a smaller GT. First, we scaled the GT (model SGT6-9000HL) used in the base cases to the desired power capacities for the 20% FU and 30% FU cases by assuming the scaled GT retained the same maximum efficiency when it was operated at its full power capacity. Second, two real GT models were selected for the 20% FU (model SGT5-8000H) and 30% FU (model SGT5-2000E) cases for comparison with the scaled GTs[51]. Table 3.5 summarizes the GT models, as well as the power capacities and max efficiencies used in all the sensitivity analysis cases. The models of Base Cases 3 and 4 were modified by substituting in the GT models for the 20% FU and 30% FU cases (Table 3.5), generating eight new cases covering the combinations of the plant models in Base Case 3 or 4, along with the 20% FU or 30% FU cases and the scaled GT or real GT.

Table 3.5: List of gas turbine models used in the sensitivity analysis [51]

SOFC stack replaced at	25% FU (base cases)	20% FU		30% FU	
GT model	SGT6-9000HL	Scaled SGT6-9000HL	SGT5-8000H	Scaled SGT6-9000HL	SGT5-2000E×2
Power capacity	405 MW	435 MW	450 MW	350 MW	187 MW×2
Max efficiency	42.6%	42.6%	42.6%	42.6%	36.5%

The eTEA results of the eight cases used in the sensitivity analysis, as well as the results for the base cases, are shown in Figure 3.6. With the exception of the 30% FU cases with real GTs, the results followed the trends observed in the base case studies, namely: longer SOFC stack lifetime (replaced at lower FU) was associated with lower net plant efficiency, lower LCOE, and lower CCA. Replacing the SOFC stack at lower FU further shifted the power load to the less efficient GT, thus resulting in lower net efficiency. On the other hand, as the SOFC stack lifetime increased, the frequency of replacement decreased, thus reducing the costs associated with SOFC stack replacement and, consequently, the LCOE and CCA. The 30% FU cases with real GTs had lower efficiencies, higher LCOEs, and higher CCAs than the 30% FU cases with scaled GTs. This result is due to two small GTs (SGT5-2000E) with lower maximum efficiency being used to satisfy the desired power capacity in the real GT cases. This result implies that replacing the SOFC stack at lower FU (i.e., prolonging the SOFC stack lifetime) in the SOFC/GT hybrid plant design generally results in worse (lower) net efficiency, a better (lower) LCOE, and a better (lower) CCA; however, this approach is also limited by factors such as the availability of practical GT models and SOFC price.

The second sensitivity analysis built upon the first by investigating how SOFC price affected the eTEA of each base case. In addition to the SOFC price used in the base cases ($2,000/kW), we selected a lower price of $1,000/kW and two higher prices of $4,000/kW and $8,000/kW (all figures in 2016 U.S. dollars). The results of the SOFC price sensitivity analysis reveal that Base Case 1 (the standalone SOFC plant) was the most sensitive to SOFC price, as the SOFC stack was replaced most frequently in this case (Figure 3.7). When the base case SOFC price was doubled to $4,000/kW, Base Case 4 (the SOFC/GT hybrid plant with a steam bottoming cycle) remained a potential alternative to the baseline NGCC plant, as its LCOE

(1)

(2)

(3)

- Base Case 3 real turbine
- Base Case 4 real turbine
▲ Base Case 3 scaled turbine
▲ Base Case 4 scaled turbine
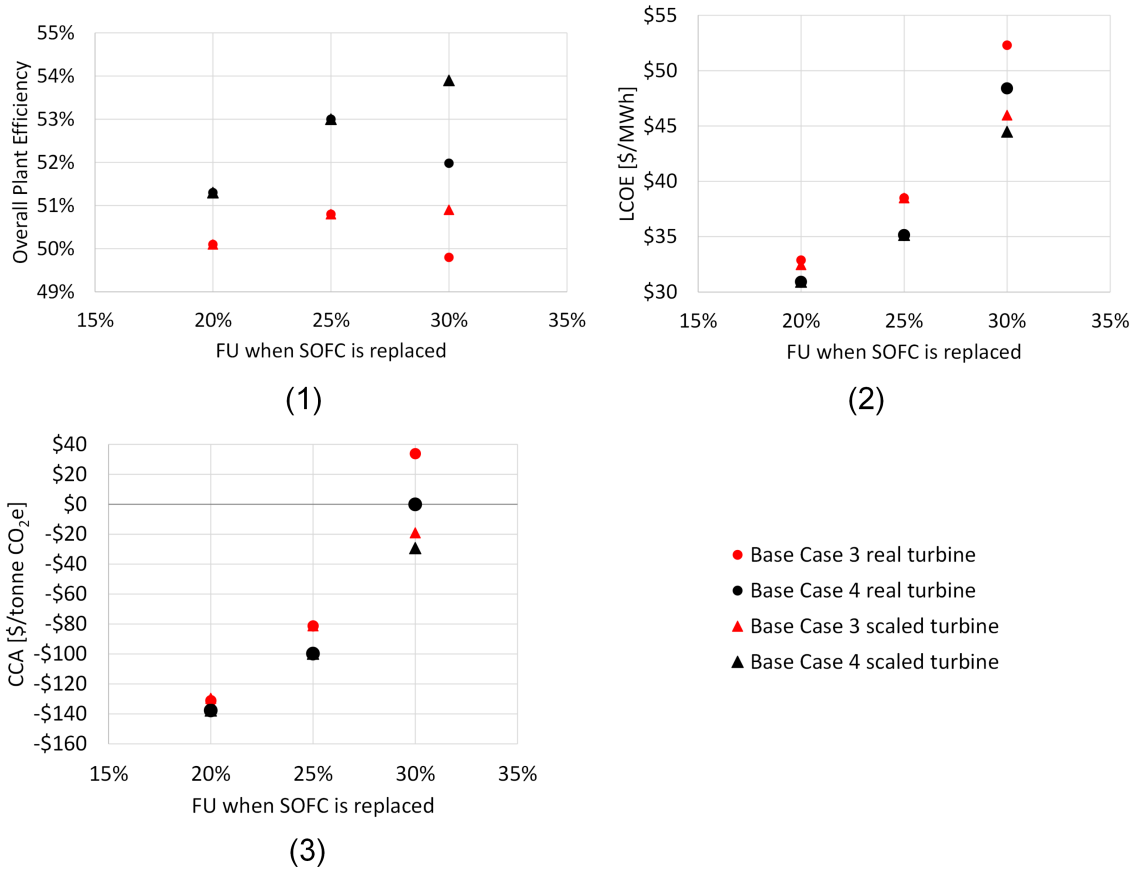
Figure 3.6: Sensitivity analysis results for SOFC/GT hybrid plants in Base Cases 3 and 4 with SOFC stacks replaced at FU of 20%, 25%, and 30%

($50.1/MWh) was close to the baseline and its CCA ($12.7/tonne CO_2e) was close to 0.

Since the NG price has been fluctuating greatly in recent years, we performed a sensitivity analysis to investigate how natural gas prices affect the eTEA results of the four base cases. The LCOE and CCA of the base cases were calculated for a range of NG prices from 30% to 500% of the base price $3.55/MMBtu, as shown in Figure 3.8. We also selected three typical historical prices in June 2020, February 2021, and April 2022 [54] as interesting points of reference as shown in Figure 3.8 (expressed in $US2016 using the consumer price index) [55]. Note that the LCOE of
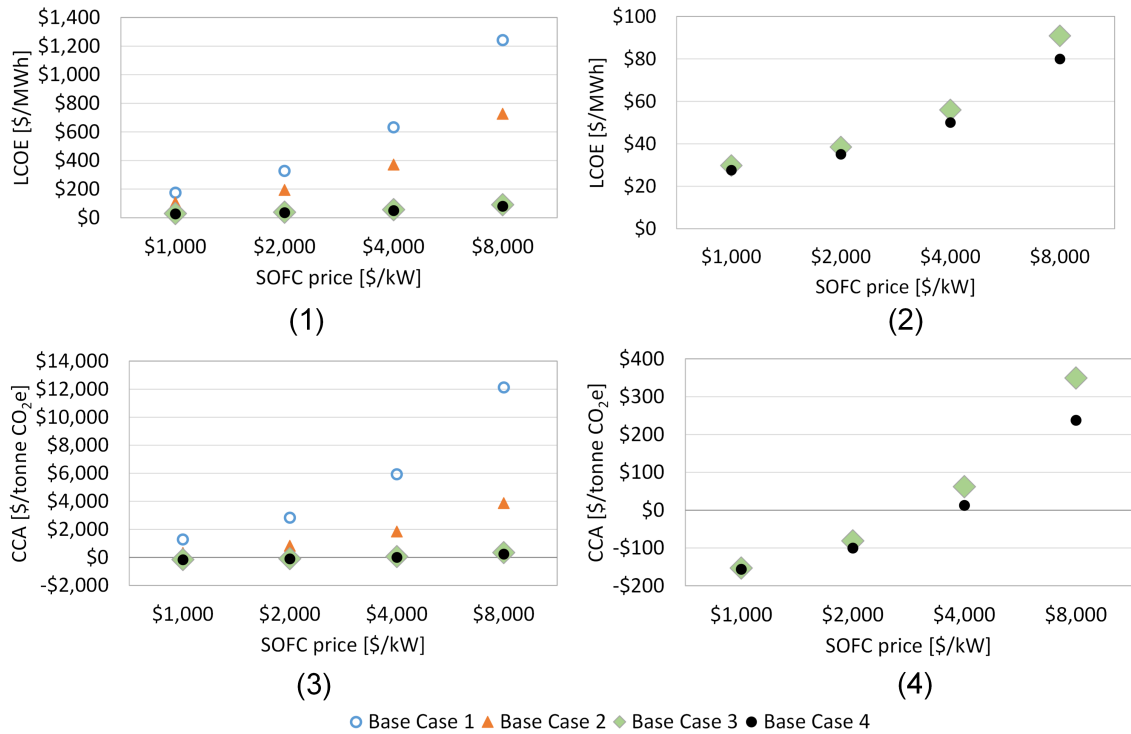
Figure 3.7: Sensitivity analysis of the four base cases with various SOFC prices. Subplots (2) and (4) are the same plots of (1) and (3), respectively, but showing only Base Case 3 and 4 for clarity.

the baseline NGCC plant was also recalculated for the range of NG prices, which were used to compute the CCA for the base cases. As can be seen in Figure 3.8, the CCA decreased as the NG price increased for all the base cases, mainly due to the higher net efficiency and lower CO_2 emissions of the base cases over the baseline NGCC plant. In other words, the higher the price of natural gas, the more advantageous it is using an SOFC-based system. However, the CCA of Base Case 1 and 2 were always very high, even when the NG price increased to 5 times of the base price. This implies that the SOFC replacement costs were still the most contribution of the total costs in Base Case 1 and 2. The CCAs of Base Case 3 and 4 were always negative; and as the NG price increased, these two cases were increasingly better from an eco-technoeconomic perspective. This is because Base Cases 3 and 4 have lower LCOEs and lower lifecycle

greenhouse gas emissions than NGCC.
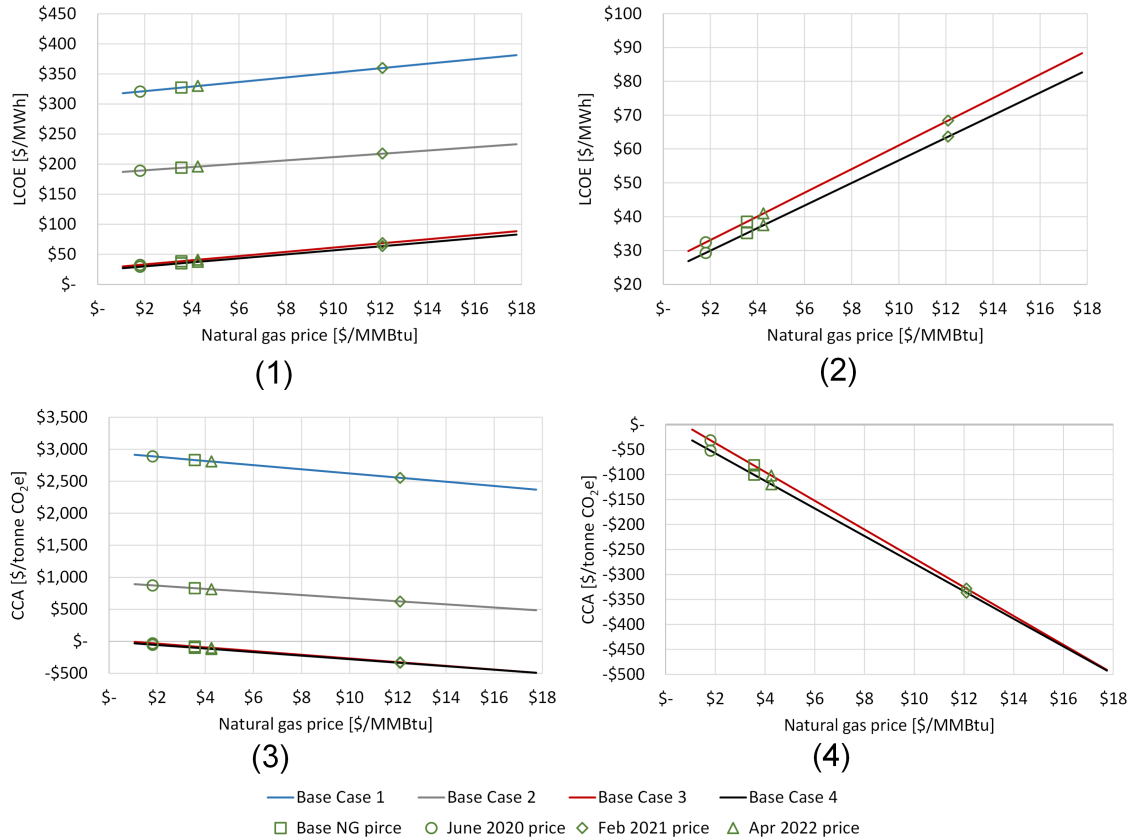
Figure 3.8: Sensitivity analysis of the four base cases with various natural gas prices. All the prices were converted to \$US2016. Subplots (2) and (4) are the same plots of (1) and (3), respectively, but showing only Base Case 3 and 4 for clarity.

Besides the NG prices (or fuel costs), the last sensitivity analysis was on the non-fuel costs. We varied the total non-fuel costs of the four base cases over the plant lifetime from 30% to 500% of their original non-fuel costs, while keeping the fuel price at the base level. The LCOE and CCA were re-computed and plotted against each other in Figure 3.9. The CCA of Base Case 1 and 2 were still positive even when the non-fuel costs were reduced to 30% of their original costs. When the non-fuel costs became double, Base Case 3 and 4 had higher LCOEs than the baseline NGCC

plant, with CCAs of \$133/tonneCO$_2$e and \$75.3/tonneCO$_2$e, respectively. Even with double-than-expected non-fuel costs, Base Case 3 and 4 have low enough CCA's to be commercially relevant CO$_2$-mitigation technology options, noting that the carbon tax floor in Canada will be 110 \$CA/tonneCO$_2$e (85 \$US/tonneCO$_2$e) in 2026 and 170 \$CA/tonneCO$_2$e (132 \$US/tonneCO$_2$e) in 2030 [56]. Note that the LCOE of the baseline NGCC plant remained the same for the CCA calculations throughout this sensitivity analysis.
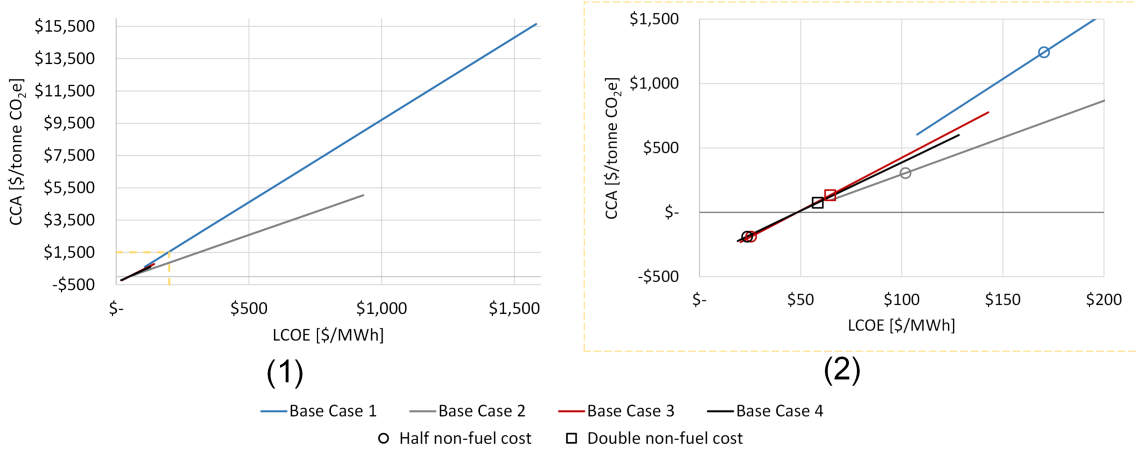
Figure 3.9: Sensitivity analysis of the four base cases with various non-fuel costs. Subplots (2) is a magnified window of the dashed box on subplot (1). The colors of the markers are associated with the colors of base cases.

3.5   Conclusion and Future Work

The simulation results showed that operating the SOFC stack in the SOFC/GT hybrid plants (Base Cases 3 and 4) at constant voltage greatly slowed degradation and increased the stack lifetime. As a result, the SOFC/GT hybrid plants had lower stack replacement costs over their 30-year lifetime compared to the standalone SOFC plants (Base Cases 1 and 2), wherein the SOFCs were operated in near-constant

power mode. The eTEA results further showed that the SOFC/GT hybrid plants (Base Cases 3 and 4) had much lower LCOEs and CCAs compared to the standalone SOFC plants (Base Cases 1 and 2), implying that the SOFC/GT hybrid design is preferrable to the standalone SOFC design from an eco-technoeconomic perspective. The addition of steam bottoming cycles in Base Cases 2 and 4 resulted in higher efficiency, lower LCOEs, and lower CCAs compared to Base Cases 1 and 3, respectively. Although the findings revealed that Base Case 2 (standalone SOFC plant with a steam bottoming cycle) had the highest overall plant efficiency ($65.0\%_{LHV)}$, the near-constant power mode of SOFC stack operation led to faster degradation and shorter SOFC stack lifetimes, resulting in high stack replacement costs over the 30-year plant lifetime. As a result, Base Case 2 is likely economically infeasible, as the high stack replacement costs contributed to an unacceptably high LCOE ($194/MWh) and CCA ($831/tonne CO_2e). In contrast, Base Case 4 had the lowest LCOE ($35.1/MWh) and CCA (-$99.9/tonne CO_2e) of the four base cases, which established it as the most economically and environmentally feasible design.

Sensitivity analyses were also conducted to examine how SOFC stack lifetime and SOFC cost in the SOFC/GT hybrid plants influenced the eTEA results. The findings of these analyses revealed that prolonging the lifetime of the SOFC stack (i.e., replacing it at lower FU) resulted in lower net efficiency due to the power load being gradually shifted to the less efficient GT; however, the results also indicated that prolonging the SOFC's lifetime led to a lower LCOE and CCA due to the reduced costs associated with SOFC replacement. By altering the SOFC stack's lifetime, the hybrid plants can be re-designed according to the required size of GT, though this may be limited by the existing commercial GT models in practice. The sensitivity analysis of SOFC price showed that the standalone SOFC plants (Base Cases 1 and 2) were

more sensitive to changes in SOFC price, mainly due to the need to replace the SOFC stack more frequently in these designs. Ultimately, the sensitivity analysis of SOFC price and NG price revealed that Base Case 4 remained a competitive alternative to the baseline NGCC plant when the SOFC price or the NG price was doubled from the price used in the base cases, respectively.

Besides the factors investigated in this work, the eTEA results of SOFC systems might also be strongly affected by long-term degradation. If the degradation occurred much slower in reality than predicted by the model, the standalone SOFC plants (Base 1 and 2) could be economically feasible. The degradation model used in this work was limited to one specific SOFC type (in terms of materials) and certain operating windows (where the cases in this work were designed). As such, different degradation models should be incorporated into future eTEA studies to cross-validate the proposed degradation model and to explore different SOFC operations.

In this work, we conducted an eTEA of four large-scale NG-powered baseload SOFC power plants that accounted for long-term degradation. Future research could examine SOFC/GT hybrid designs and standalone SOFC designs in peaking power or load-following applications at large or small scales. Such research could include household, building, and community power systems, and consider how these systems might be integrated with other applications such as combined heat and power (CHP), energy storage, and wind and solar systems.

Acknowledgement

Simulation Files

Models and codes related to this work have been released to the public in LAPSE (link: https://psecommunity.org/LAPSE:2022.0027)

Declaration of Competing Interest

The authors declare that they have no known competing financial interests or personal relationships that could have appeared to influence the work reported in this paper.

Nomenclature

AC   Alternating Current

CCA   Cost of CO_2 Avoided

DC   Direct Current

EOS   Equation Of State

eTEA   Eco-technoeconomic Analysis

FU   Fuel Utilization

GT   Gas Turbine

HHV   Higher Heating Value

LCOE   Levelized Cost of Electricity

LHV   Lower Heating Value

PID   Proportional Integral Derivative (Controller)

SOFC   Solid Oxide Fuel Cell

YSZ   Yttria-stabilized Zirconia

References

[1] Adams II, T. A., Nease, J., Tucker, D., and Barton, P. I., 2013, "Energy Conversion with Solid Oxide Fuel Cell Systems: A Review of Concepts and Outlooks for the Short-and Long-Term," Ind. Eng. Chem. Res., 52(9), pp. 3089–3111.

[2] Tucker, D., Abreu-Sepulveda, M., and Harun, N. F., 2014, "SOFC Lifetime Assessment in Gas Turbine Hybrid Power Systems," J. Fuel Cell Sci. Technol., 11(5).

[3] Hagen, A., Barfod, R., Hendriksen, P. V., Liu, Y.-L., and Ramousse, S., 2006, "Degradation of Anode Supported SOFCs as a Function of Temperature and Current Load," J. Electrochem. Soc., 153(6), pp. A1165–A1171.

[4] Da Silva, F. S., and de Souza, T. M., 2017, "Novel Materials for Solid Oxide Fuel Cell Technologies: A Literature Review," Int. J. Hydrog. Energy, 42(41), pp. 26020–26036.

[5] Tucker, D., VanOsdol, J., Liese, E., Lawson, L., Zitney, S., Gemmen, R., Ford, J. C., and Haynes, C., 2012, "Evaluation of Methods for Thermal Management in a Coal-Based SOFC Turbine Hybrid through Numerical Simulation," J. Fuel Cell Sci. Technol., 9(4).

[6] Lai, H., Harun, N. F., Tucker, D., and Adams II, T. A., 2021, "Design and Eco-Technoeconomic Analyses of SOFC/GT Hybrid Systems Accounting for Long-Term Degradation Effects," Int. J. Hydrog. Energy, 46(7), pp. 5612–5629.

[7] Kandepu, R., Imsland, L., Foss, B. A., Stiller, C., Thorud, B., and Bolland, O., 2007, "Modeling and Control of a SOFC-GT-Based Autonomous Power System," Energy, 32(4), pp. 406–417.

[8] Toonssen, R., Sollai, S., Aravind, P. V., Woudstra, N., and Verkooijen, A. H. M., 2011, "Alternative System Designs of Biomass Gasification SOFC/GT Hybrid Systems," Int. J. Hydrog. Energy, 36(16), pp. 10414–10425.

[9] Zhang, B., Maloney, D., Farida Harun, N., Zhou, N., Pezzini, P., Medam, A., Hovsapian, R., Bayham, S., and Tucker, D., 2022, "Rapid Load Transition for Integrated Solid Oxide Fuel Cell – Gas Turbine (SOFC-GT) Energy Systems: A Demonstration of the Potential for Grid Response," Energy Convers. Manag., 258, p. 115544.

[10] Calise, F., Palombo, A., and Vanoli, L., 2006, "Design and Partial Load Exergy Analysis of Hybrid SOFC–GT Power Plant," J. Power Sources, 158(1), pp. 225–244.

[11] Akkaya, A. V., Sahin, B., and Erdem, H. H., 2008, "An Analysis of SOFC/GT CHP System Based on Exergetic Performance Criteria," Int. J. Hydrog. Energy, 33(10), pp. 2566–2577.

[12] Huang, S., Yang, C., Chen, H., Zhou, N., and Tucker, D., 2022, "Coupling Impacts of SOFC Operating Temperature and Fuel Utilization on System Net Efficiency in Natural Gas Hybrid SOFC/GT System," Case Stud. Therm. Eng., 31, p. 101868.

[13] Behzadi, A., Habibollahzade, A., Zare, V., and Ashjaee, M., 2019, "Multi-Objective Optimization of a Hybrid Biomass-Based SOFC/GT/Double Effect Absorption Chiller/RO Desalination System with CO_2 Recycle," Energy Convers. Manag., 181, pp. 302–318.

[14] Calise, F., d'Accadia, M. D., Vanoli, L., and Von Spakovsky, M. R., 2006, "Single-Level Optimization of a Hybrid SOFC–GT Power Plant," J. Power Sources, 159(2), pp. 1169–1185.

[15] Calise, F., d'Accadia, M. D., Vanoli, L., and von Spakovsky, M. R., 2007, "Full Load Synthesis/Design Optimization of a Hybrid SOFC–GT Power Plant," Energy, 32(4), pp. 446–458.

[16] Fredriksson Möller, B., Arriagada, J., Assadi, M., and Potts, I., 2004, "Optimisation of an SOFC/GT System with CO_2-Capture," J. Power Sources, 131(1), pp. 320–326.

[17] Karimi, M. H., Chitgar, N., Emadi, M. A., Ahmadi, P., and Rosen, M. A., 2020, "Performance Assessment and Optimization of a Biomass-Based Solid Oxide Fuel Cell and Micro Gas Turbine System Integrated with an Organic Rankine Cycle," Int. J. Hydrog. Energy, 45(11), pp. 6262–6277.

[18] Chitgar, N., and Emadi, M. A., 2021, "Development and Exergoeconomic Evaluation of a SOFC-GT Driven Multi-Generation System to Supply Residential Demands: Electricity, Fresh Water and Hydrogen," Int. J. Hydrog. Energy, 46(34), pp. 17932–17954.

[19] Kumar, P., and Singh, O., 2019, "Thermoeconomic Analysis of SOFC-GT-VARS-ORC Combined Power and Cooling System," Int. J. Hydrog. Energy, 44(50), pp. 27575–27586.

[20] Santin, M., Traverso, A., Magistri, L., and Massardo, A., 2010, "Thermoeconomic Analysis of SOFC-GT Hybrid Systems Fed by Liquid Fuels," Energy, 35(2), pp. 1077–1083.

[21] Vojdani, M., Fakhari, I., and Ahmadi, P., 2021, "A Novel Triple Pressure HRSG Integrated with MED/SOFC/GT for Cogeneration of Electricity and Freshwater: Techno-Economic-Environmental Assessment, and Multi-Objective Optimization," Energy Convers. Manag., 233, p. 113876.

[22] Parhizkar, T., and Roshandel, R., 2017, "Long Term Performance Degradation Analysis and Optimization of Anode Supported Solid Oxide Fuel Cell Stacks," Energy Convers. Manag., 133, pp. 20–30.

[23] Nakajo, A., Mueller, F., Brouwer, J., and Favrat, D., 2012, "Progressive Activation of Degradation Processes in Solid Oxide Fuel Cell Stacks: Part II: Spatial Distribution of the Degradation," J. Power Sources, 216, pp. 434–448.

[24] Gao, S., Li, J., and Lin, Z., 2014, "Theoretical Model for Surface Diffusion Driven Ni-Particle Agglomeration in Anode of Solid Oxide Fuel Cell," J. Power Sources, 255, pp. 144–150.

[25] Neidhardt, J. P., Fronczek, D. N., Jahnke, T., Danner, T., Horstmann, B., and Bessler, W. G., 2012, "A Flexible Framework for Modeling Multiple Solid, Liquid and Gaseous Phases in Batteries and Fuel Cells," J. Electrochem. Soc., 159(9), p. A1528.

[26] Ryan, E. M., Xu, W., Sun, X., and Khaleel, M. A., 2012, "A Damage Model for Degradation in the Electrodes of Solid Oxide Fuel Cells: Modeling the Effects of Sulfur and Antimony in the Anode," J. Power Sources, 210, pp. 233–242.

[27] Hansen, J. B., 2008, "Correlating Sulfur Poisoning of SOFC Nickel Anodes by a Temkin Isotherm," Electrochem. Solid State Lett., 11(10), p. B178.

[28] Cayan, F. N., Pakalapati, S. R., Celik, I., Xu, C., and Zondlo, J., 2012, "A Degradation Model for Solid Oxide Fuel Cell Anodes Due to Impurities in Coal Syngas: Part i Theory and Validation," Fuel Cells, 12(3), pp. 464–473.

[29] Divisek, J., Wilkenhöner, R., and Volfkovich, Y., 1999, "Structure Investigations of SOFC Anode Cermets Part I: Porosity Investigations," J. Appl. Electrochem., 29(2), pp. 153–163.

[30] Hardjo, E., Monder, D. S., and Karan, K., 2011, "Numerical Modeling of Nickel-Impregnated Porous YSZ-Supported Anodes and Comparison to Conventional

Composite Ni-YSZ Electrodes," ECS Trans., 35(1), p. 1823.

[31] Gazzarri, J. I., and Kesler, O., 2008, "Short-Stack Modeling of Degradation in Solid Oxide Fuel Cells: Part I. Contact Degradation," J. Power Sources, 176(1), pp. 138–154.

[32] Yang, Z., Guo, M., Wang, N., Ma, C., Wang, J., and Han, M., 2017, "A Short Review of Cathode Poisoning and Corrosion in Solid Oxide Fuel Cell," Int. J. Hydrog. Energy, 42(39), pp. 24948–24959.

[33] Virkar, A. V., 2007, "A Model for Solid Oxide Fuel Cell (SOFC) Stack Degradation," J. Power Sources, 172(2), pp. 713–724.

[34] Coors, W., O'Brien, J., and White, J., 2009, "Conductivity Degradation of NiO-Containing 8YSZ and 10YSZ Electrolyte during Reduction," Solid State Ion., 180(2–3), pp. 246–251.

[35] Larrain, D., and Favrat, D., 2006, "Simulation of SOFC Stack and Repeat Elements Including Interconnect Degradation and Anode Reoxidation Risk," J. Power Sources, 161(1), pp. 392–403.

[36] Naeini, M., Lai, H., Cotton, J. S., and Adams II, T. A., 2021, "A Mathematical Model for Prediction of Long-Term Degradation Effects in Solid Oxide Fuel Cells," Ind. Eng. Chem. Res., 60(3), pp. 1326–1340.

[37] Abreu-Sepulveda, M. A., Harun, N. F., Hackett, G., Hagen, A., and Tucker, D., 2015, "Accelerated Degradation for Hardware in the Loop Simulation of Fuel Cell-Gas Turbine Hybrid System," J. Fuel Cell Sci. Technol., 12(2).

[38] Zaccaria, V., Tucker, D., and Traverso, A., 2016, "A Distributed Real-Time Model of Degradation in a Solid Oxide Fuel Cell, Part I: Model Characterization," J. Power Sources, 311, pp. 175–181.

[39] Wang, Z., Chen, H., Xia, R., Han, F., Ji, Y., and Cai, W., 2022, "Energy, Exergy and Economy (3E) Investigation of a SOFC-GT-ORC Waste Heat Recovery System for Green Power Ships," Therm. Sci. Eng. Prog., 32, p. 101342.

[40] Rosner, F., Rao, A., and Samuelsen, S., 2020, "Economics of Cell Design and Thermal Management in Solid Oxide Fuel Cells under SOFC-GT Hybrid Operating Conditions," Energy Convers. Manag., 220, p. 112952.

[41] Li, Z., Zhang, X., He, X., Wu, G., Tian, S., Zhang, D., Zhang, Q., and Liu, Y., 2022, "Comparative Analysis of Thermal Economy of Two SOFC-GT-ST Triple

Hybrid Power Systems with Carbon Capture and LNG Cold Energy Utilization," Energy Convers. Manag., 256, p. 115385.

[42] Eisavi, B., Chitsaz, A., Hosseinpour, J., and Ranjbar, F., 2018, "Thermo-Environmental and Economic Comparison of Three Different Arrangements of Solid Oxide Fuel Cell-Gas Turbine (SOFC-GT) Hybrid Systems," Energy Convers. Manag., 168, pp. 343–356.

[43] Peng, W., Chen, H., Liu, J., Zhao, X., and Xu, G., 2021, "Techno-Economic Assessment of a Conceptual Waste-to-Energy CHP System Combining Plasma Gasification, SOFC, Gas Turbine and Supercritical CO2 Cycle," Energy Convers. Manag., 245, p. 114622.

[44] James III PhD, R. E., Kearins, D., Turner, M., Woods, M., Kuehn, N., and Zoelle, A., 2019, Cost and Performance Baseline for Fossil Energy Plants Volume 1: Bituminous Coal and Natural Gas to Electricity, NETL-PUB-22638, NETL.

[45] Zaccaria, V., Tucker, D., and Traverso, A., 2016, "A Distributed Real-Time Model of Degradation in a Solid Oxide Fuel Cell, Part II: Analysis of Fuel Cell Performance and Potential Failures," J. Power Sources, 327, pp. 736–742.

[46] Zaccaria, V., Traverso, A., and Tucker, D., 2015, "A Real-Time Degradation Model for Hardware in the Loop Simulation of Fuel Cell Gas Turbine Hybrid Systems," American Society of Mechanical Engineers, p. V003T06A022.

[47] Rossi, I., Zaccaria, V., and Traverso, A., 2018, "Advanced Control for Clusters of SOFC/Gas Turbine Hybrid Systems," J. Eng. Gas Turbines Power, 140(5).

[48] Nease, J., and Adams II, T. A., 2013, "Systems for Peaking Power with 100% CO_2 Capture by Integration of Solid Oxide Fuel Cells with Compressed Air Energy Storage," J. Power Sources, 228, pp. 281–293.

[49] Adams II, T. A., and Barton, P. I., 2010, "High-Efficiency Power Production from Coal with Carbon Capture," AIChE J., 56(12), pp. 3120–3136.

[50] Adams II, T. A., Hoseinzade, L., Madabhushi, P. B., and Okeke, I. J., 2017, "Comparison of CO_2 Capture Approaches for Fossil-Based Power Generation: Review and Meta-Study," Processes, 5(3), p. 44.

[51] "SGT6-9000HL (405 MW) Heavy-Duty Gas Turbine," Siemenscom Glob. Website [Online]. Available: https://new.siemens.com/global/en/products/energy/power-generation/gas-turbines/sgt6-9000hl.html. [Accessed: 23-Feb-2020].

[52] "Siemens SGT5-2000/3000/4000 Series | PowerWeb" [Online]. Available: http://www.fi-powerweb.com/Engine/Industrial/Siemens-SGT5-2000-3000-4000.html. [Accessed: 23-Feb-2020].

[53] Rath, L. K., Chou, V. H., and Kuehn, N. J., 2011, Assessment of Hydrogen Production with CO_2 Capture Volume 1: Baseline State-of-the-Art Plants (Final Report), DOE/NETL-2011/1434-Rev.01, National Energy Technology Laboratory (NETL), Pittsburgh, PA, Morgantown, WV, and Albany, OR (United States); Booz Allen Hamilton, Inc., McLean, VA (United States).

[54] "U.S. Natural Gas Electric Power Price (Dollars per Thousand Cubic Feet)" [Online]. Available: https://www.eia.gov/dnav/ng/hist/n3045us3m.htm. [Accessed: 19-Jul-2022].

[55] U.S. Bureau of Labor Statistics, 1952, "Consumer Price Index for All Urban Consumers: Utility (Piped) Gas Service in U.S. City Average," FRED Fed. Reserve Bank St Louis [Online]. Available: https://fred.stlouisfed.org/series/CUSR0000SEHF02. [Accessed: 19-Jul-2022].

[56] Canada, E. and C. C., 2021, "Update to the Pan-Canadian Approach to Carbon Pollution Pricing 2023-2030" [Online]. Available: https://www.canada.ca/en/environment-climate-change/services/climate-change/pricing-pollution-how-it-will-work/carbon-pollution-pricing-federal-benchmark-information/federal-benchmark-2023-2030.html. [Accessed: 26-Jul-2022].

Supplemental Material

Appendix A

Appendix A: Model-based Controller for SOFC/GT Hybrid Plants

One of the functions of the control system design for the SOFC/GT plant was to maintain the total net system power at 550 MW. In order to achieve this, a cascade control system was used in which a supervisory controller manipulated the SOFC power setpoint. Because of long-term degradation and other challenges associated with the complex dynamics of the SOFC/GT hybrid system as well as power being produced and consumed in the balance-of-plant, traditional PID controllers were unable to maintain a net 550 MW power satisfactorily. Instead, a model-based controller was employed to manipulate the SOFC power setpoint more elegantly.

Specifically, a reduced model was created that helps us compute the total balance of plant power (P_{bal}), including parasitic loads as follows. The efficiency of the balance of plant (η_{bal}) is a function of (P_{bal}) as follows:

$$h_{bal} = f(P_{bal}) \qquad (A.1)$$

Where

$$h_{bal} = \frac{P_{bal}}{Fuel_{HHV}} \qquad (A.2)$$

And

$$P_{bal} = P_{GT} + P_{CC} + P_{turb} - P_{comps} - P_{pumps} \qquad (A.3)$$

Where Fuel_{HHV} is the higher heating value of the fuel fed to the gas turbine (fed to the balance-of-plant), P_{GT} is the electrical power produced by the gas turbine system, P_{CC} is the power produced by the combined cycle (steam cycle in Base Case 4 and some other cases in sensitivity analyses), P_{turb} is the power produced by the upstream expansion turbine, P_{comp} is the power consumed by the compressors, and P_{pumps} is the power consumed by the pumps.

The GT power P_{GT} can be estimated through a GT characteristic curve (or turbine map) which is the electrical efficiency of the gas turbine ($\eta_G T, HHV$) described explicitly as a function of its capacity factor (X_{GT}):

$$h_{GT,HHV} = f(X_{GT}) \qquad (A.4)$$

Where

$$h_{GT} = \frac{P_{GT}}{Fuel_{HHV}} \qquad (A.5)$$

And

$$X_{GT} = \frac{P_{GT}}{P_{GT,Max}} \qquad (A.6)$$

$\text{P}_{(GT,Max)}$ is the maximum power (or power capacity) of the turbine and $\text{P}_{GT} \leq \text{P}_{(GT,Max)}$. For Base Case 3, $\text{P}_{(GT,Max)}$=405 MW, and the turbine characteristic curve can then be written as follows:

$$h_{GT,HHV} = f(P_{GT}) \qquad (A.7)$$

Although the data cannot be released for intellectual property reasons, the characteristic curve was described as a polynomial of the following shape:

$$h_{GT} = a + bP_{GT} + cP_{GT}^2 + dP_{GT}^3 \qquad (A.8)$$

Since the GT contributed the most power production in the balance-of-plant (different at each time step), we described $f(P_{bal})$ firstly based on $f(P_{GT})$ as a polynomial of the same shape:

$$h_{GT} = a + bP_{bal} + cP_{bal}^2 + dP_{bal}^3 \qquad (A.9)$$

Then, the coefficients a through d were determined iteratively. As an initial guess, the coefficients were first set to the same coefficients as that used in Eq.A.8. Then, a full dynamic simulation was run. At each timestep t, the power setpoint of the SOFC at the current timestep ($P_{SOFC,SETPOINT}(t)$) was computed by inverting the reduced model to compute P_{bal} as a function of anode exhaust heating value $Fuel_{HHV}$, and then computing

$$P_{SOFC,SETPOINT}(t) = 550MW - P_{bal}(t) \qquad (A.10)$$

However, the quality of the controller outcomes depended on the quality of the coefficients, and the initial guesses were not satisfactory. Therefore, a guess-and-check approach was used to iteratively improve upon the coefficients a through d. This was done by examining the error in the new power output against the 550 MW setpoint, and adjusting the coefficients to achieve a more desirable curve. After several iterations, a suitable set of coefficients were found that resulted in an almost constant net 550 MW power output, and significantly outperforming a PID controller. Each case study required a different set of coefficients, with one example shown below (Base Case 3):
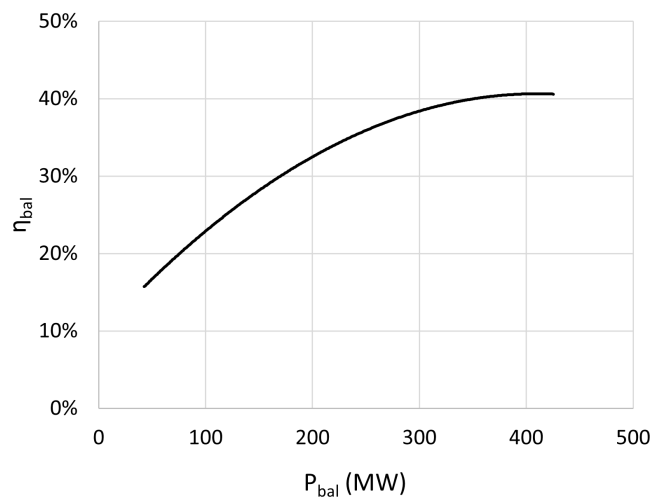
Figure 3.10: Reduced model polynomial for predicting the balance-of-plant power in Base Case 3

Appendix B

Appendix B: Selected Cost Estimations

In addition to those discussed in the main text, the following cost assumptions were used in the analysis. Capital costs were estimated via standard power law relationships as follows (with basis years noted): CEPCI values were used for scaling costs adjusted to the year 2016 (CEPCI for 2018=603.1, 2016=541.7, 2007=525.4, 1970=123). See main text for discussion and references.

- Gas turbine (including the turbine, compressor, and recuperator): exponent of 0.6 and basis of $73 million ($US 2016) for a 268 MW gas turbine.

- Steam turbine system (including turbines, boilers, and pump): exponent of 0.6, basis of $340/kW ($US 2018).

- Blower: 5120$US1970 for 30 kW system, 0.55 exponent

- Primary heat exchangers: 8000$US1970 for 100 m^2 surface area, 0.71 exponent

- NG upstream process (including reformer, water-gas shift reactor, and other accessories): approximately $103 million ($US 2007) for a feed rate of about 95 tonnes NG per hour, 0.6 exponent.

- Fixed operating costs (complete system): approximately $19.5 million ($US 2018) for a feed rate of about 93 tonnes NG per hour, 1.0 exponent; and 21% of about $22.7 million ($US 2007) for a feed rate of about 95 tonnes NG per hour, 1.0 exponent.

- Variable operating costs (complete system): about $9 million ($US 2018) for a feed rate of about 93 tonnes NG per hour, 1.0 exponent; and about $14 million ($US 2007) for a feed rate of about 95 tonnes NG per hour, 1.0 exponent.

Appendix C

Appendix C: Selected Stream Conditions

Sample stream conditions for Base Case 2 and Base Case 4 are given in Tables 3.C.1 and 3.C.2, respectively. The reader can find more detailed stream information for additional substreams and cases at the LAPSE link provided in the Simulation Files section.

Table 3.C.1. Sample stream conditions of Base Case 2 near the end of the cell life (about 25 weeks), with stream numbers corresponding to Figure 3.2

Stream	1	2	3	4	5	6	7	8
Temp (°C)	15.0	15.9	690.0	1271.5	631.4	161.1	994.9	800.0
P (bar)	1.0	1.0	1.0	1.0	1.0	1.0	11.5	1.0
F (kmol/s)	37.45	37.45	37.45	41.16	41.16	41.16	5.16	5.54
CH_4	-	-	-	-	-	-	0.00127	0.00182
C_2H_6	-	-	-	-	-	-	71 ppm	66 ppm
C_3H_8	-	-	-	-	-	-	15 ppm	14 ppm
C_4H_10	-	-	-	-	-	-	trace	trace
CO	-	-	-	-	-	-	0.17068	0.00942
CO_2	-	-	-	0.029	0.029	0.029	0.05619	0.20167
H_2	-	-	-	-	-	-	0.49978	0.61438
H_2O	-	-	-	0.105	0.105	0.105	0.26632	0.16800
N_2	0.790	0.790	0.790	0.720	0.720	0.720	0.00566	0.00527
O_2	0.210	0.210	0.210	0.147	0.147	0.147	-	-

Table 3.C.2. Sample stream conditions of Base Case 4 near the beginning of the cell life (about 2 weeks), with stream numbers corresponding to Figure 3.2

Stream	1	2	3	4	5	6	7	8	9	10
Temp (°C)	15.0	169.7	690.0	1006.5	261.3	220.0	994.7	800.0	918.7	707.4
P (bar)	1.0	4.1	4.1	4.1	1.0	1.0	11.5	4.1	4.1	1.0
F (kmol/s)	36.39	36.39	36.39	40.47	40.47	40.47	5.30	5.69	40.47	40.47
CH_4	-	-	-	-	-	-	0.00127	0.00118	-	-
C_2H_6	-	-	-	-	-	-	71 ppm	66 ppm	-	-
C_3H_8	-	-	-	-	-	-	15 ppm	14 ppm	-	-
C_4H_10	-	-	-	-	-	-	trace	trace	-	-
CO	-	-	-	-	-	-	0.17067	0.00942	-	-
CO_2	-	-	-	0.030	0.030	0.030	0.05620	0.20166	0.02979	0.02979
H_2	-	-	-	-	-	-	0.49978	0.61437	-	-
H_2O	-	-	-	0.109	0.109	0.109	0.26631	0.16800	0.10926	0.10926
N_2	0.790	0.790	0.790	0.715	0.715	0.715	0.00566	0.00527	0.71506	0.71506
O_2	0.210	0.210	0.210	0.146	0.146	0.146	-	-	0.14589	0.14589

Chapter 4

Life Cycle Analyses of SOFC/Gas Turbine Hybrid Power Plants Accounting for Long-term Degradation Effects

Life Cycle Analyses of SOFC/Gas Turbine Hybrid Power Plants Accounting for Long-term Degradation Effects

Haoxiang Lai[a] and Thomas A. Adams II[b*]

a McMaster University, Department of Chemical Engineering, Hamilton, ON, Canada

b Norwegian University of Science and Technology, Department of Energy and Process Engineering, Trondheim, Norway * Corresponding Author. thomas.a.adams@ntnu.no

Highlights

- Cradle-to-product life cycle analysis

- LCA for solid oxide fuel cell and gas turbine hybrid systems compared against standalone solid oxide fuel cell

- Considers long-term degradation effects

- Natural gas-based plants and coal-based plants

- Considers plant operation, SOFC manufacturing, balance-of-plant manufacturing, and plant maintenance as the LCA boundary

- Considers boundary expansion that includes cooling options and AC to DC conversion

Abstract

In this study, cradle-to-product life cycle analyses were conducted for a variety of natural-gas-based and coal-based SOFC power plant conceptual designs, while

also accounting for long-term SOFC degradation. For each type of plant, four base case designs were considered: a standalone SOFC plant, a standalone SOFC plant with a steam cycle, an SOFC/GT hybrid plant, and an SOFC/GT hybrid plant with a steam cycle. The boundary of each base case was subsequently expanded to include either wet cooling or dry cooling options and DC to AC conversion, and was subjected to additional cradle-to-product life cycle analyses. The environmental impact results were computed using ReCiPe 2016 (H) and TRACI 2.1 V1.05 in SimaPro. The main factors affecting the midpoint impacts between cases were the plant efficiency and total SOFC manufacturing required over the plant's lifetime, which were both strongly connected to long-term degradation effects. The findings also showed that the standalone SOFC plant with a steam cycle (which featured higher plant efficiency) had lower midpoint impacts with respect to global warming potential and fossil resource scarcity, which were largely the product of plant operation. The case with the longer SOFC stack lifetime (e.g., a SOFC/GT hybrid power plant with a steam cycle) had lower midpoint impacts with respect to fine particulate matter formation, terrestrial acidification, terrestrial ecotoxicity, and mineral resource scarcity due to the large proportion of midpoint contributed by SOFC manufacturing. Ultimately, the SOFC/GT hybrid plant with a steam cycle was found to be the best option, as it had the lowest ReCiPe endpoint impact (4.5% to 42% lower than the other cases) among both the natural gas-based and coal-based cases.

Keywords: life cycle analysis, SOFC, SOFC/GT hybrid, SOFC degradation, environmental impacts

4.1   Introduction

Increases in global energy demand and public awareness of global warming have amplified the importance of reliable and sustainable power production [1]. Although sustainable power production technologies such as solar and wind are rapidly developing, their implementation is challenging due to their intermittent nature. Successful integration of wind and solar power into a large-scale energy system depends heavily on other power-generation systems that can produce power when sunlight and wind are in insufficient supply [2]. For this reason, conventional baseload power production using fossil fuels such as natural gas (NG) or coal remains highly prominent, and is anticipated to continue to account for a major share of global power production (e.g., anticipated for a share of 40-50% in 2030 in the U.S.) [3,4]. As such, it is critical to improve existing NG-based and coal-based baseload power production methods, especially from an eco-technoeconomic perspective. Solid oxide fuel cells (SOFC) are a promising technology for reliable baseload power production, as their use of electrochemical reactions allows them to generate electricity more efficiently compared to conventional combustion-based power production technologies. From an emissions perspective, SOFCs not only produce lower CO_2 emissions due to their higher efficiency, but they also enable efficient CO_2 capture at a low cost [5,6]. However, the life cycle environmental impacts of SOFCs are uncertain, as their efficiency and lifetime are dynamically influenced by their degradation rate.

An SOFC's degradation rate is strongly affected by its operating conditions [7]. The most common operating strategy for baseload power production is to maintain a constant SOFC power output; this results in a higher degradation rate and, thus, a shorter SOFC lifetime. Changing the operating strategy to utilize constant

voltage instead of constant power output significantly slows the degradation rate and dramatically increases the SOFC's lifetime (up to more than 10 times). However, the trade-off with this approach is a decrease in power output over time. As the power output decreases in this constant voltage operating mode, the amount of unspent fuel in the SOFC exhaust increases, which can be used by a gas turbine (GT) for secondary power production to maintain a net baseload power production [7–10]. While an SOFC/GT hybrid plant that accounts for degradation effects has been shown to be technically and economically feasible in prior works, its life cycle environmental impacts are still unclear [10,11]. Given the huge difference (more than 10 times) in SOFC stack lifetime due to degradation effects under different operating conditions, it is possible that the environmental impacts of SOFC manufacturing might strongly affect the full LCA result from case to case.

A review of the literature shows that researchers have conducted life cycle analyses (LCA) focusing on various aspects of SOFCs. For instance, Strazza et al. conducted an LCA on a 230 kW SOFC system and compared its impact to a micro-gas turbine system that utilized NG and biogas as fuel sources [12]. To account for degradation effects, they assumed four SOFC stack replacements over a 10-year system lifetime for simplicity [12]. In a different study, Rillo et al. conducted an LCA for a 250 kW biogas-fed SOFC system, wherein they assumed a stack lifetime of six years and that 17% of the stack would be replaced each year over its lifetime [13]. Elsewhere, Bicer and Khalid performed an LCA comparison that assumed a 5-year lifetime for a 250 kW SOFC system fueled by various sources, including NG, hydrogen, ammonia, and methanol [14], while Al-Khori et al. conducted an LCA for the integration of an SOFC into an NG plant that assumed a 10-year SOFC lifetime [15]. In another work, Nease and Adams performed cradle-to-grave LCAs for bulk-scale SOFC plants

powered by NG and coal and compared their results to those obtained for conventional power plants such as natural gas combined cycle plants and supercritical pulverized coal power plants. In that study, Nease and Adams assumed that the SOFC could be operated at full capacity for 10 years [16,17]. Reenaas conducted an LCA for an SOFC/GT system and compared the results to those for a diesel auxiliary power production unit on a ship, assuming SOFC stack lifetimes of 40000 or 20000 hours depending on the case study [18].

Although the above studies assumed various SOFC stack lifetimes, their degradation effects were not considered in detail. In another work, Ghorbani et al. performed exergoeconomic and exergoenvironmental analyses of an SOFC-GT-ORC (Organic Rankine Cycle) hybrid system with an approximate power scale of 1.2 MW [19]. Although they included voltage loss calculations in their SOFC model, the life cycle environmental impacts remained unclear, as did the effect of degradation on the SOFC stack's lifetime. Naeini et al. conducted an LCA on an NG-based SOFC system that accounted for degradation effects and considered 5- and 10-year stack replacement plans [20]. To reduce the degradation rate, they allowed the operating conditions of the SOFC stack to change over time instead of maintaining constant power output, which resulted significantly improved stack lifetimes of up to 10 years [21,22]. Although they considered various operating conditions to counteract the degradation effects, they focused on a standalone SOFC system without considering power integration at the systems level—for example, they did not consider utilizing the waste heat from the SOFC exhaust stream for secondary power production.

To the best of our knowledge, the present study is the first detailed cradle-to-product LCA for large-scale NG-based and coal-based SOFC/GT hybrid plants (including

SOFC/GT hybrid plants with a steam cycle). This work both accounts for degradation effects and compares the results to those recorded for standalone SOFC plants (including standalone SOFC plants with a steam cycle). In our prior work, the SOFC stacks in SOFC/GT hybrid plants were found to have much longer lifetimes (more than 10 times) compared to those in standalone SOFC plants due to the much slower degradation in constant voltage operating mode [10,11]. Thus, SOFC/GT hybrid plants would potentially have a much lower environmental impact with respect to SOFC manufacturing than standalone SOFC plants. However, we also found that standalone SOFC plants with a steam cycle had higher net efficiency compared to SOFC/GT hybrid plants, which would potentially result in lower environmental impact from plant operation [10,11]. Therefore, it is vital to perform full LCAs to further compare the respective life cycle environmental impacts of SOFC/GT hybrid plants and standalone SOFC plants with a steam cycle.

This study provides LCA results of large-scale NG-based and coal-based SOFC/GT hybrid plants and standalone SOFC plants accounting for long-term degradation effects, which can be used to understand the life cycle environmental impacts for the application of SOFC in large-scale industrial power systems without requiring further improvements to new materials for making SOFC stacks. The LCA comparisons in this study can also help decision making on the adoption of technologies, designs, and operations as part of the energy shift towards sustainability.

4.2   Methodology

The cradle-to-product LCAs were performed for four base cases utilizing NG and four base cases utilizing coal as the fuel sources. The base cases were named based on their major components for power production as follows:

(1) Base Case 1 (BC1): standalone SOFC plant

(2) Base Case 2 (BC2): standalone SOFC plant with a steam cycle

(3) Base Case 3 (BC3): SOFC/GT hybrid plant

(4) Base Case 4 (BC4): SOFC/GT hybrid plant with a steam cycle

These base case designs applied to both NG-based cases and coal-based cases (as shown in Table 4.1), with the major differences being in the upstream treatment processes for fuel prior to entering the SOFC stack. The upstream treatment process in NG-based cases included major components such as the steam reforming of NG and a water-gas shift process, while the upstream process in coal-based cases mainly included coal gasification, scrubbing, water-gas shift, and Selexol processes. All the base cases were designed to have a power scale of 550 MW (mixed AC and DC electricity output) and a plant lifetime of 30 years. A basis of 1 MWh electricity product (mixed AC and DC) was chosen for the LCA.

These base cases were discussed in detail in a prior study by the authors, to which the reader is referred for detailed stream information, dynamic operating trajectories, and techno-economic analyses. [10,11]. The plant model of each base case consisted of a dynamic model (in Matlab Simulink) to account for the dynamic degradation behaviours of the SOFC stack with degradation considered and a pseudo-steady-state

model (in Aspen Plus) of the balance-of-plant which experiences insignificant degradation phenomena behaviours by comparison. The pseudo-steady-state approach was taken to integrate and simulate the dynamic model and the steady-state model. In this way, the overall system model considers both the specific degradation phenomena of the SOFC stacks and how the balance-of-plant slowly changes in response, over a period potentially lasting many years.

The degradation rate used in the dynamic model of the SOFC stacks was described as Eq (1), where r_d, FU, T, and i represent the degradation rate (%/(1000h)), fuel utilization (fraction), temperature (K), and current density (A/cm^2), respectively. For details of model descriptions, simulation methodologies, and derivation of Eq (1), the reader is referred to these prior studies [8-11].

$$r_d = \frac{0.59FU + 0.74}{1 + \exp\frac{T-1087}{22.92}}(e^{2.64i} - 1) \qquad (1)$$

The key mass and energy balance results of the model simulations with long-term degradation effects were taken from those prior studies and are summarized in Table 1, such as plant efficiency and stack lifetime [10,11]. These results were used in the inventory calculation in the LCAs for this work, which are described in greater details in the following sections.

Table 4.1: Basic data for the examined base cases [10,11]. ST = steam turbine system (a classic combined cycle using waste heat from the upstream units).

	NG-based Cases				Coal-based Cases			
	BC1	BC2	BC3	BC4	BC1	BC2	BC3	BC4
Overview								
Description	SOFC	SOFC +ST	SOFC/ GT	SOFC/ GT+ST	SOFC	SOFC +ST	SOFC/ GT	SOFC/ GT+ST
Net Power (MW)	550	550	550	550	550	550	550	550
Plant efficiency (LHV)	46.8%	65.0%	50.8%	53.0%	30.7%	48.7%	41.6%	44.6%
LCOE ($/MWh)	$327	$194	$38.5	$35.1	$430	$241	$82	$77
SOFC stack								
Stack size (cm^2 active membrane area)	1.26×10^9	9.18×10^8	1.04×10^9	1.03×10^9	1.4×10^9	9.04×10^8	9.8×10^8	9.14×10^8
Stack lifetime (year)	0.4	0.5	7.2	8.2	0.4	0.4	6.7	6.7
Total number of stacks	79	63	5	4	83	69	5	5
Components of BoP manufacturing								
SOFC sub-processes	Yes	Yes	Yes	Yes	Yes	Yes	Yes	Yes
Upstream treatment processes for fuel	Yes	Yes	Yes	Yes	Yes	Yes	Yes	Yes
Gas turbine	No	No	Yes	Yes	No	No	Yes	Yes
Steam cycle	No	Yes	No	Yes	No	Yes	No	Yes

4.2.1 Boundaries

The boundaries of the LCA for all base cases included gate-to-product plant operation, cradle-to-gate SOFC manufacturing, cradle-to-gate balance-of-plant (BoP) manufacturing, and cradle-to-gate plant maintenance, with a final product of 1 MWh mixed AC and DC electricity (Figure 4.1). For analysis purposes, the plant is in a non-specific United States location. For example, the fuel at plant data for the NG-based and coal-based plants were obtained from the SimaPro library as cradle-to-product high-pressure market NG in the U.S. and market hard coal in North America, respectively, with average transportation accounted being account for in both cases.

4.2.2 Plant Operation

The boundary for the plant operation includes all species that are transferred between the plant and the natural environment for the production of 1 MWh of net electricity (mixed AC and DC). Figure 4.1(b) shows a sample process flow diagram of the SOFC plant operation for NG-based BC4 and its additional cooling option included in boundary expanded cases (explained later in section 3.3). The data for plant operation of each case were obtained from our prior studies and are provided in the Supplemental Material [10,11].
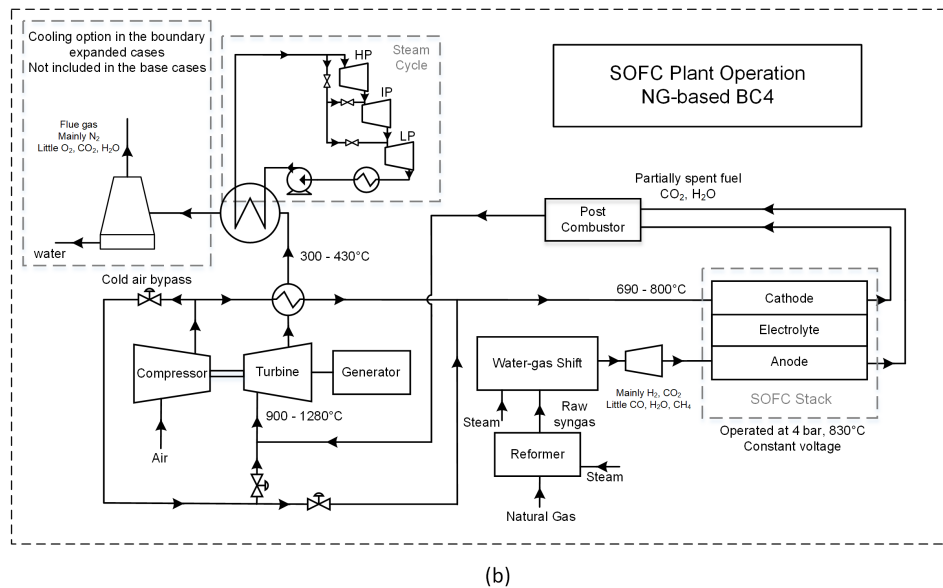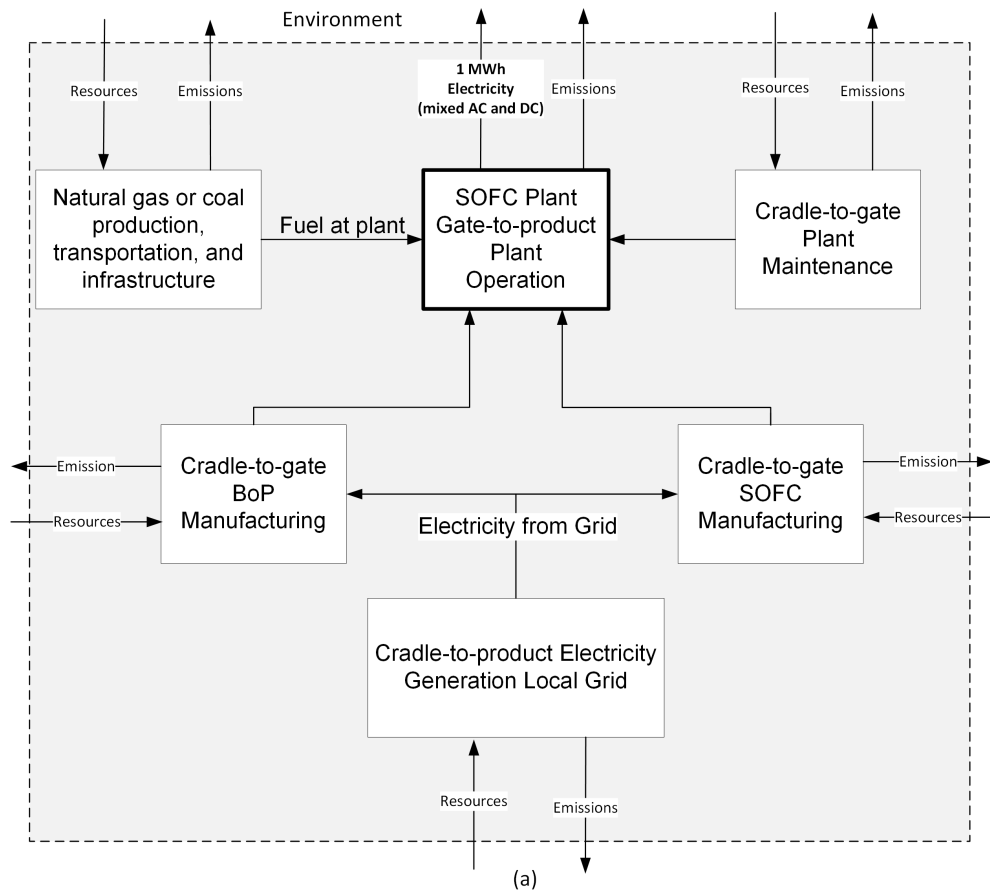
Figure 4.1: Life cycle boundary for SOFC plants and process flow diagram of the SOFC plant operation for NG-based BC4.

4.2.3   SOFC Manufacturing

A 1 cm^2 active membrane area was selected as the basis for the SOFC manufacturing inventory data. While a unit basis of 1 kW has been widely used in LCAs of SOFC manufacturing [13,14,23], this basis is specific only to situations in which SOFCs are operated under constant power production at nameplate capacity, and cannot be applied for SOFC stacks that are operated under different or transient conditions. Naeini et al. utilized Rillo et al.'s data and assumptions to construct an inventory basis of 1 cm^2 for SOFC manufacturing, which provides a more general reference point for use in LCAs of SOFCs with various operating conditions [13,20].

The SOFC stacks in the studied base cases varied in size due to the different system designs required to achieve a net power production of 550 MW. The SOFC model simulations considered long-term degradation, with the degradation rate changing according to the operating conditions in each case. Therefore, SOFC stack lifetime varied from case to case, as did the number of stacks used over the 30-year plant lifetime (Table 4.1). In this work, the SOFC manufacturing inventories were calculated based on the size and numbers of SOFC stacks in each case (Table 4.1) using the inventory basis per cm^2 presented by Naeini et al. [20]. The inventory accounts for the materials and energy used in SOFC manufacturing including, but not limited to, Nickel oxide (NiO), Yttrium stabilized zirconium (YSZ), Lanthanum strontium manganite (LSM), various solvents and binders, stainless steel, and electricity. The full inventory data and more detailed descriptions can be found in [14,20].

4.2.4   Balance-of-plant Manufacturing

The balance-of-plant (BoP) manufacturing includes SOFC accessories, upstream treatment processes for fuel (NG or coal), gas turbines (in BC3 and BC4), and steam cycles (in BC2 and BC4). The different sub-processes included in the BoP manufacturing for each case are summarized in Table 4.1 above. The SOFC sub-processes mainly included steel production, stainless steel production, and energy for fabricating auxiliary equipment and running the SOFC assembly process [14,20]. The inventories for the manufacturing of syngas upstream processes, gas turbines, and steam cycles were estimated based on data collected from the literature [18,24,25].

4.2.5   Plant Maintenance

The inventories for plant maintenance included the steel and stainless steel required for equipment maintenance, as well as the catalysts and chemicals consumed in the processes. The NG-based cases consumed Nickel-based and iron-based catalysts for reforming and water-gas-shift (WGS) processes. The coal-based cases consumed sulfur-impregnated activated carbon for Hg removal, iron-based catalyst for WGS reactions, Selexol for H_2S removal, and sodium hydroxide for HCl removal. All consumptions of catalysts and chemicals were estimated with their initial fills and daily makeups throughout the plant lifetime. For example, coal-based BC4 consumed an initial fill of 54.5×10^3 kg sulfur-impregnated activated carbon with a daily makeup of 74 kg/day, and the net consumption over the plant lifetime converted to the basis became 0.006 kg/MWh (Table 4.2). The inventories of these chemicals were estimated based on the following assumptions [26–30]:

- 1% of steel and stainless steel of the BoP would need to be replaced each year.

- Ni-honeycomb catalyst was used for the reforming process [26,28].

- Ferrite served as the iron-based catalyst for the water-gas-shift reactions [26,27,29].

- No initial fills of reforming catalyst for the NG-based cases and sodium hydroxide for the coal-based cases [26,27].

Table 4.2: Consumption of catalysts and chemicals in plant maintenance for NG-based and Coal-based BC4.

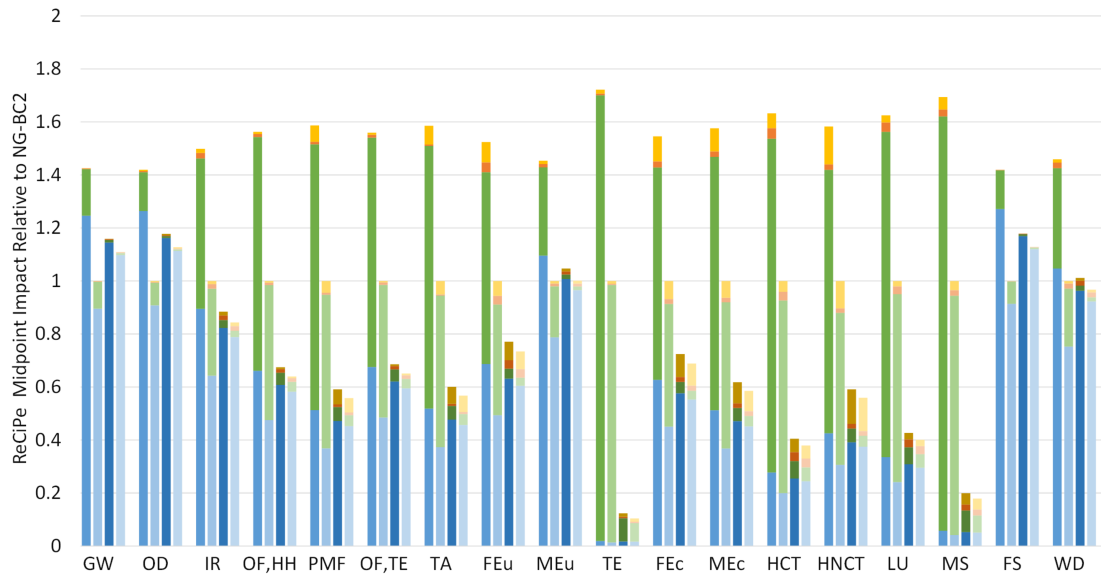|	Initial fill (10^3 kg)	Daily makeup (kg/day)	Net consumption (kg/MWh)
NG-based BC4			
Reforming catalyst	0	244	0.0185
WGS catalyst	73.8	235	0.0183
Coal-based BC4			
Sulfur-impregnated activated carbon	54.5	74	0.0060
WGS catalyst	258.5	177	0.0152
Selexol	1673.7	166	0.0242
Sodium hydroxide	0	7194	0.5450

4.2.6   Data Transparency

The original SimaPro files used in the analysis have been released to the public (See link at end of manuscript). The files contain the detailed gate-to-gate life cycle inventories used for all steps.
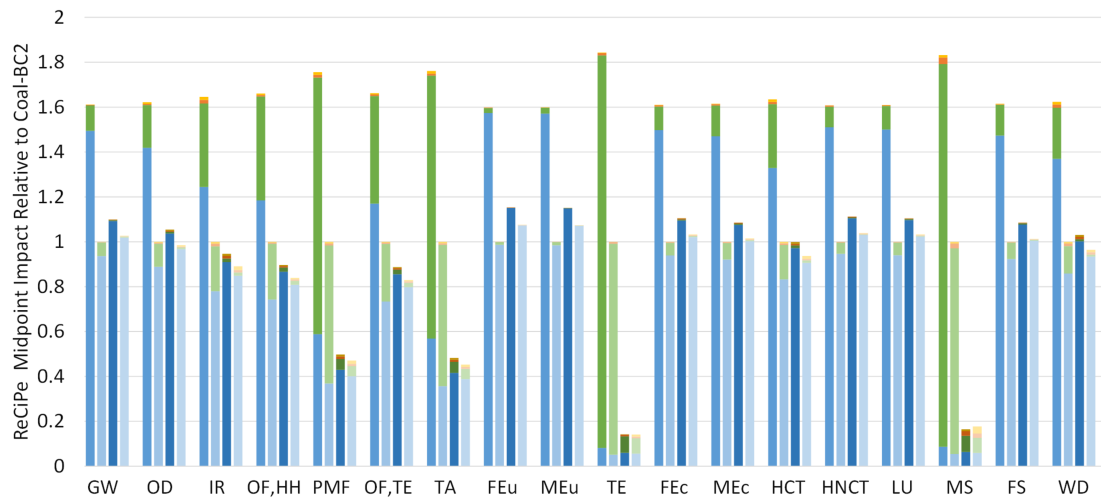
4.3   Results and Discussion

4.3.1   Base Cases

Figure 4.2 shows the midpoint characterization results of the base cases, which were obtained using ReCiPe 2016 (H). The results of the NG- and coal-based cases were normalized to the total midpoints of NG-based BC2 and coal-based BC2, respectively, in each category. For each case in each category, the contributions of plant operation (also including fuel production, transportation, and infrastructure, SOFC manufacturing, BoP manufacturing, and plant maintenance to the midpoint impact are shown as stack columns, with the legend shown in the figure. A more detailed overview of the results and data can be found in the Supplemental Material.

For the NG-based cases, plant operation made the largest contribution to the total midpoint impacts in categories such as global warming, stratospheric ozone depletion, ionizing radiation, marine eutrophication, fossil resource scarcity, and water consumption. Since BC2 had the highest plant efficiency, it had the lowest midpoint impacts from plant operation among the four NG-based cases in every category. As the plant efficiency decreases from BC2 → BC4 → BC3 → BC1 (Table 4.1), the midpoint impacts from plant operation in each category increased correspondingly. With regards to SOFC manufacturing, BC1 required the largest total active membrane area (around 24 times larger than BC4), followed by BC2 (around 14 times larger than BC4), BC3 (around 1.3 times larger than BC4), and BC4. Consequently, the midpoint impacts contributed by SOFC manufacturing decreased from BC1 to BC4. The midpoint impacts relating to terrestrial ecotoxicity and mineral resource scarcity were mostly from SOFC manufacturing. For BC1 and BC2, SOFC manufacturing

Figure 4.2: Normalized ReCiPe midpoint impact results (ReCiPe 2016 H) for the base cases. Subplots (a) and (b) show the four NG-based cases and four coal-based cases, respectively. The components' contributions to each impact category are shown as stacked columns.

also contributed a large amount of midpoint impacts in categories such as ozone formation, fine particulate matter formation, terrestrial acidification, freshwater ecotoxicity, marine ecotoxicity, human toxicity, land use, and mineral resource scarcity. The impacts from BoP manufacturing and plant maintenance were relatively small compared to plant operation and SOFC manufacturing in most categories. However, plant maintenance had noticeable impacts with respect to human toxicity, freshwater ecotoxicity, marine ecotoxicity, freshwater eutrophication, terrestrial acidification, and fine particulate matter formation, mainly due to the consumption of catalysts.

The comparison of BC2 (standalone SOFC with steam cycle) and BC4 (SOFC/GT with steam cycle) showed that BC2 had lower midpoint impacts in categories dominated by plant operation, such as global warming, stratospheric ozone depletion, and fossil resource scarcity, mainly due to its higher plant efficiency. However, the short SOFC stack lifetime (high degradation rate) in BC2 results in large impacts from SOFC manufacturing, which results in higher total midpoint impacts in almost all other categories compared to BC4. Similar results were observed in the comparison of BC2 and BC3, with one performing better in some categories and worse in other categories. BC4 had a lower impact than BC3 in all categories due to its higher plant efficiency and lower SOFC manufacturing.

For the coal-based cases, plant operation also contributed the highest midpoint impacts in the same categories as the NG-based cases, namely, in global warming, stratospheric ozone depletion, ionizing radiation, marine eutrophication, fossil resource scarcity, and water consumption. Besides these categories, plant operation in the coal-based cases also dominated the midpoint impacts in freshwater eutrophication, freshwater ecotoxicity, marine ecotoxicity, human toxicity, and land use. These results

indicate that, in the coal-based case, plant operation contributed higher midpoint impacts in these categories compared to the NG-based cases. This includes higher direct emissions during plant operation and higher emissions during upstream fuel processes. In addition, due to the higher midpoint impacts from plant operation in the coal-based cases, the relative total impacts for BC2 compared to BC4 with respect to freshwater eutrophication, freshwater ecotoxicity, marine ecotoxicity, human toxicity, and land use were much smaller than in NG-based cases. This implies that, in these categories, NG-BC2 is worse than NG-BC4, but coal-BC2 is about the same or even marginally better than coal-BC4. In the NG-based cases, SOFC manufacturing consistently contributed the greatest impacts in terrestrial ecotoxicity and mineral resource scarcity, while BoP manufacturing and plant maintenance had insignificant impacts in all categories.

4.3.2 Monte Carlo Sensitivity Analysis

A Monte Carlo sensitivity analysis was conducted to investigate how uncertainties in plant operation and SOFC manufacturing processes affected the ReCiPe midpoint impacts. Plant efficiency was assumed to fluctuate within $\pm 2\%$ (two percentage points) to account for uncertainties in plant operation. The inventories for SOFC manufacturing were assumed to fluctuate within $\pm 5\%$ to account for uncertainties during the manufacturing process. Using SimaPro, we conducted Monte Carlo sampling with 1000 runs that followed two normal distributions, with the two uncertainty ranges of plant operation and SOFC manufacturing as the 95% confidence intervals simultaneously. The ReCiPe midpoint impact results are shown in Figure 4.3. The average total midpoint impact of the Monte Carlo runs for each case in each

category was approximately the same as the corresponding base case. The standard deviation (represented as error bars in the figure) in each Monte Carlo case indicates that the uncertainties in plant operation and SOFC manufacturing did not have a large impact on the ReCiPe midpoint impact results.
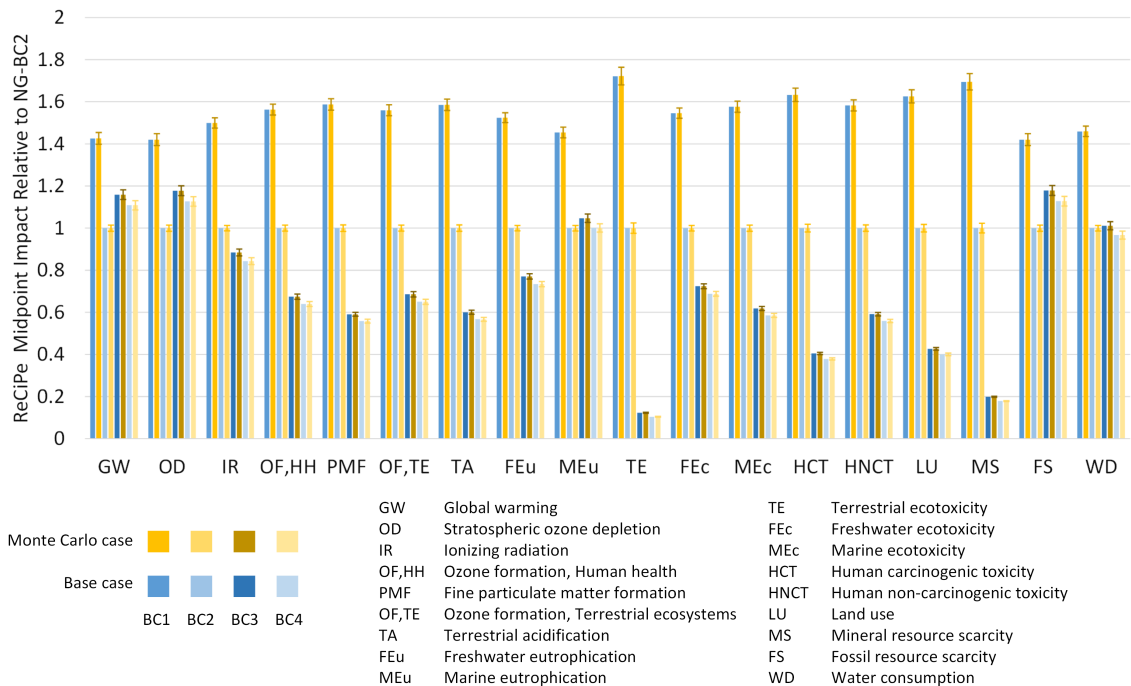
Figure 4.3: Normalized ReCiPe midpoint impact results (ReCiPe 2016 H) for the comparisons of the base cases and base cases with Monte Carlo sensitivity analyses.

4.3.3 Boundary Expansion

The plant operation boundaries used in the previous section for the four NG-based cases and four coal-based cases were based on previous works, which did not include cooling towers for cooling the flue gas stream at the end of the processes; this deficiency could be addressed by including either wet cooling towers or dry cooling towers (air cooled). Furthermore, these base cases utilized mixed AC and DC electricity production, which

could be converted to only AC grid-quality electricity with an inverter [10]. As such, we expanded the boundaries of the base cases to include two more cases for each category: (1) an expanded base case with wet cooling towers and AC grid-quality electricity as the output (e.g., BC1Wc), and (2) an expanded base case with dry cooling towers and AC grid-quality electricity as the output (e.g., BC1Dc). The boundary expansion was conducted using the following assumptions:

- A DC to AC conversion efficiency of 96% [31].

- The wet cooling towers consumed 0.42 L of water per MJ of electricity production and had 1% electricity penalty (of the gross power) compared to the base case [31–33].

- The dry cooling towers consumed no water for cooling purposes and had 7% electricity penalty (of the gross power) compared to the base case [31,32].

Figure 4.4(a) shows the ReCiPe midpoint impact results for the expanded NG-based cases compared to those of the corresponding base cases. With regards to water consumption, the expanded NG-based cases with wet cooling towers and AC grid-quality electricity output (BC1Wc to BC4Wc) more than doubled the water consumption of the corresponding base cases, whereas water consumption was greatly reduced in the expanded NG-based cases with dry cooling towers and AC grid-quality electricity output (BC1Dc to BC4Dc). Not only did the dry cooling towers consume no water for cooling purposes, they also enabled the recovery of water from the cooled flue gas stream. Indeed, more water was produced than consumed during plant operation in these cases. Since the water was recovered from the flue gas stream, the plant operation in the NG-based cases resulted in negative water consumption, which is consistent with previous work on SOFC flue gas water recovery by Adams and Barton [31]. Nonetheless, the other LCA boundary components (mainly the SOFC

manufacturing) did consume water, with consumption increasing from BC4 to BC1 in proportion to SOFC manufacturing. Therefore, BC1Dc and BC2Dc had positive net water consumption (combining negative water consumption from plant operation and positive water consumption from other components), while BC3Dc and BC4Dc had negative water consumption. In all other categories, the midpoint impacts of the expanded wet cooling cases were higher than the corresponding base cases due to the 1% electricity penalty; moreover, the midpoint impacts of the expanded dry cooling cases were even higher due to the higher electricity penalty (7%). As mentioned in the previous section, BC4 had lower midpoint impacts compared to BC2 in some categories and higher midpoint impacts in others. To further compare the two cases, ReCiPe endpoint impacts (ReCiPe 2016 H) were computed using SimaPro. The NG-based endpoint results are shown as the last category in Figure 4.4(a). As can be seen, the endpoint impacts of BC4, BC4Wc, and BC4Dc were lower (around 4.5% lower) than those of BC2, BC2Wc, and BC2Dc, respectively. Although BC4 had lower plant efficiency than BC2, its environmental impacts were lower overall. It is also interesting that the endpoint impact of BC3 (or BC3Wc or BC3Dc) was slightly lower than that of BC2 (or BC2Wc or BC2Dc). This result indicates that the SOFC/GT hybrid plants (BC3 and BC4) are better alternatives to the standalone SOFC plants (BC1 and BC2), and that the SOFC/GT hybrid plant with a steam cycle (BC4) is the best option among the four.

  Similarly, the midpoint impacts in water consumption were higher in coal-based BC1Wc to BC4Wc and significantly lower in coal-based BC1Dc to BC4Dc compared to the corresponding base cases. Due to the water recovery from the flue gas stream and the lack of water consumption in the dry cooling method, the plant operation in the Dc cases had negative water consumption. However, the other components, especially SOFC manufacturing, still consumed water, resulting in positive net water

Figure 4.4: Normalized ReCiPe midpoint impact results (ReCiPe 2016 H) for the comparisons between base cases and base cases with the two boundary expansions. Nc: No cooling. Wc: Wet cooling. Dc: Dry cooling.

consumption for the four coal-based Dc cases. Water consumption aside, the midpoint impact for BC1 to BC4 increased in other categories in the order of Nc, Wc, and Dc as the electricity penalty increased, respectively. The endpoint results for the coal-based

cases also showed that BC4, which is a SOFC/GT system with steam cycle, had lower environmental impacts (around 6.5% lower) than BC2 (standalone SOFC with a steam cycle).

In addition to the ReCiPe method, TRACI 2.1 V1.05 was also applied to compute the LCA results of all cases (Figure 4.5). In every category for both the NG- and coal-based plants, BC1Dc had the highest midpoint impact, followed by BC1Wc and BC1(Nc) due to the above-noted electricity penalties. The same trend can be seen for BC1 through BC4. Since the TRACI midpoint method did not include water consumption—to the advantage of the Dc cases—the results do not reflect the reduction of water consumption. Similar to the ReCiPe midpoint results, BC2 had the lowest impact among all the cases for some TRACI categories, while BC4 had the lowest impact for others. Specifically, NG-BC2 outperformed NG-BC4 with respect to global warming, ozone depletion, and fossil fuel depletion, mainly due to its higher plant efficiency. In contrast, it was outperformed by NG-BC4 in all other categories, mainly due to the need for much more SOFC manufacturing. Coal-BC2 outperformed Coal-BC4 with respect to global warming and eutrophication, but was outperformed by Coal-BC4 in all other categories. These TRACI midpoint results are generally consistent with the ReCiPe midpoint results, with the exception of fossil fuel depletion for the coal-based cases. The TRACI midpoint in fossil fuel depletion decreased from Coal-BC1 to BC4 (Figure 4.5), while the ReCiPe midpoint in the same category showed that Coal-BC4 had slightly higher impact than Coal-BC2, and Coal-BC3 had higher impact than Coal-BC2 and BC4 (Figure 4.4). This inconsistency was due to the fact that TRACI method computed lower impact in plant operation and higher impact in SOFC manufacturing compared to ReCiPe method. For example, the midpoint impact ratio of plant operation and SOFC manufacturing in Coal-BC2 was 4:1 when computed using TRACI, and 12:1 when computed using ReCiPe.
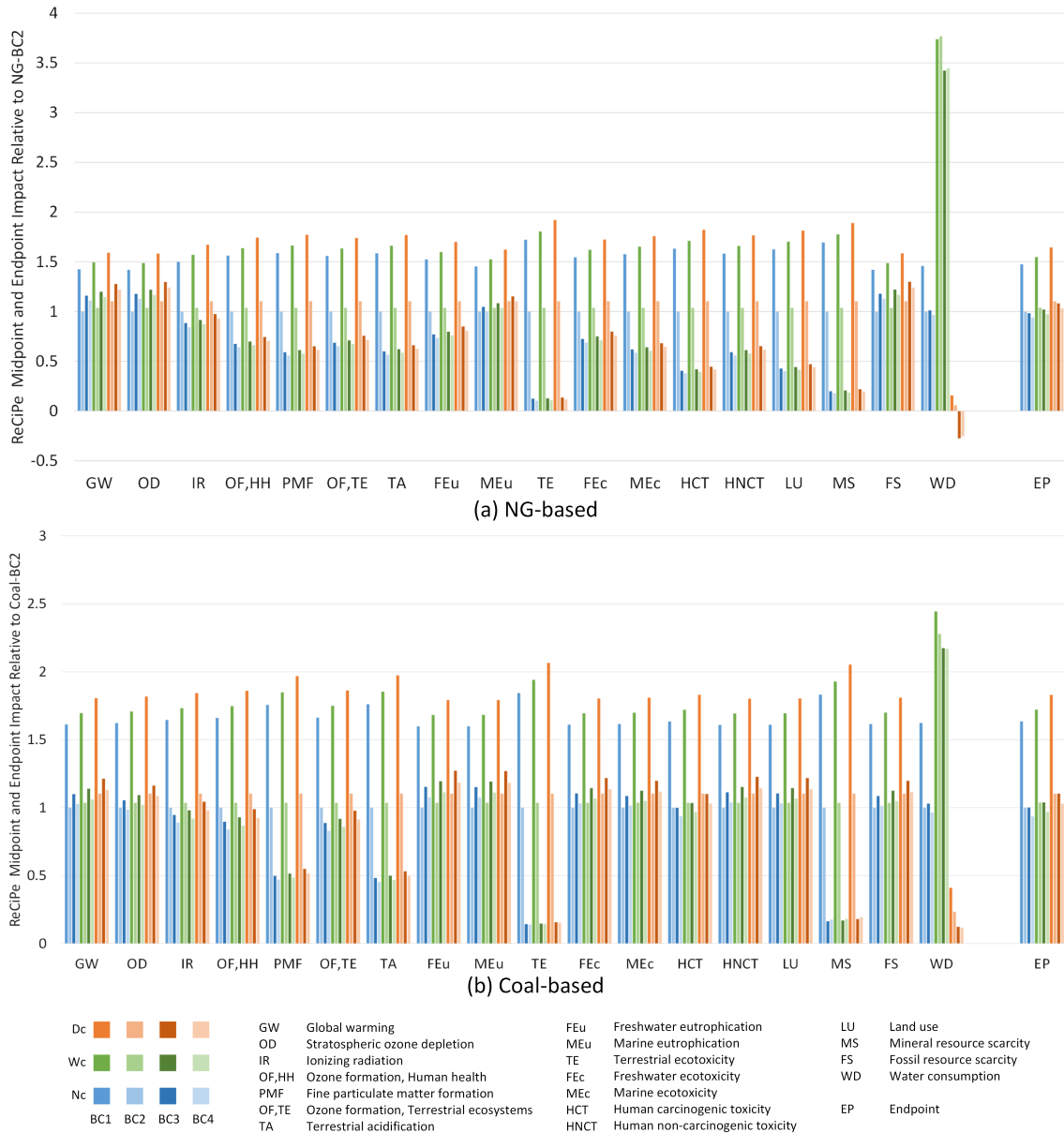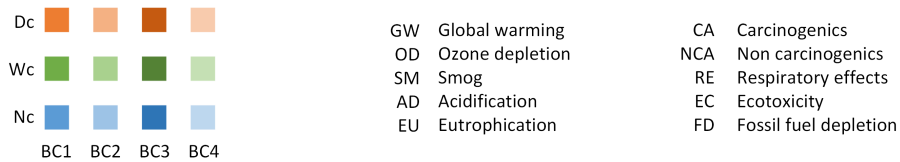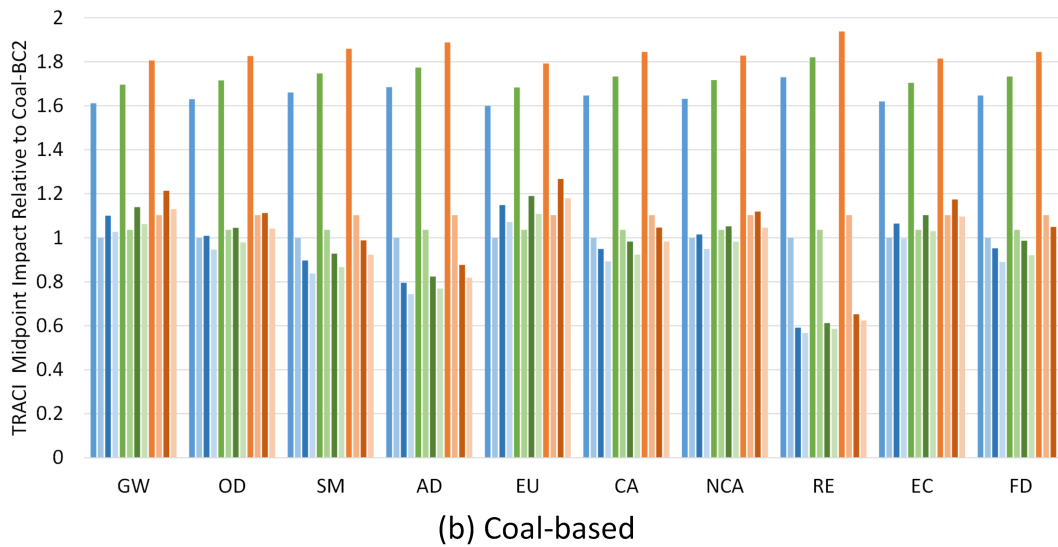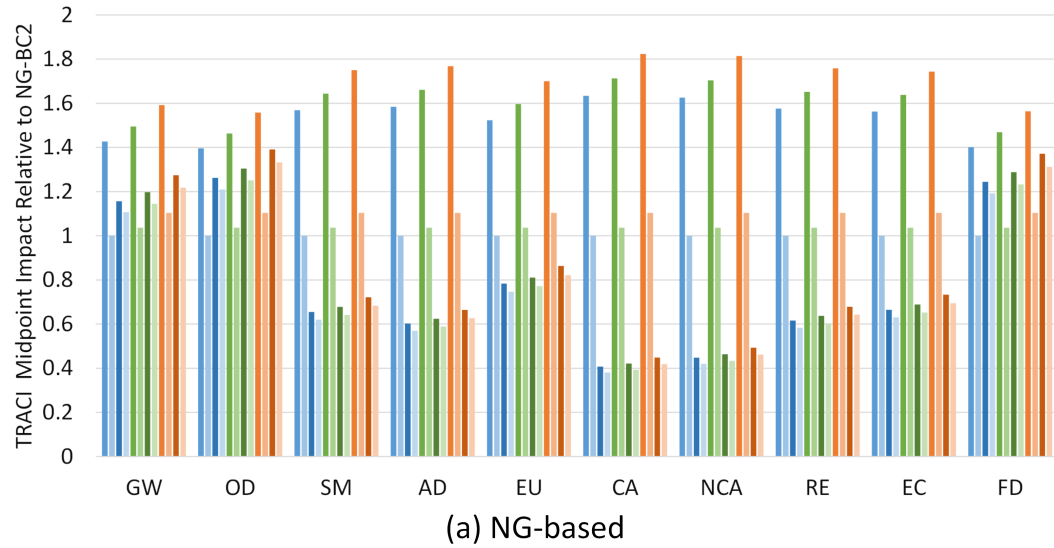
Figure 4.5: Normalized TRACI midpoint impact results for the comparisons between base cases and base cases with the two boundary expansions. Nc: No cooling. Wc: Wet cooling. Dc: Dry cooling.

4.3.4   Comparison with other SOFC Systems in the Literature

In addition to analyzing all the base cases and the expanded cases, we also compared the obtained LCA results with those of other SOFC systems in the literature. Compared to Nease and Adams' NG-based SOFC plant, (their case without considering carbon capture and transmission loss) which has a similar power scale as our cases, our NG-BC2 and NG-BC4 base cases had 20% and 33% higher ReCiPe midpoint impacts in global warming, respectively [16]. With regards to fossil resource scarcity, NG-BC2 and NG-BC4 had higher impacts of 9% and 23%, respectively, compared to Nease and Adams' NG-based SOFC plant [16]. The main reason for the higher midpoint impacts of our cases is that we used SOFC models that accounted for degradation effects, which not only reduced plant efficiency, but also the lifetime of SOFC stack. As a result, the midpoint impacts contributed by plant operation and SOFC manufacturing increased. Note that ReCiPe 2016 was used in this work, and ReCiPe 2008 was used in Nease and Adams. [16]. Overall these differences are reasonable, expected, and thus in good agreement with the literature.

We also compared our LCA results to Naeini et al.'s NG-based SOFC system, which featured the same power scale as ours, while also accounting for degradation effects (but with a different degradation model) [20]. The SOFC models used in our cases considered the overall degradation of the SOFC stack in relation to operating conditions, such as current density, fuel utilization, and temperature, based on experimental data. Unlike our SOFC model, Naeini et al. used an SOFC model that accounted for various degradation mechanisms in different components of the SOFC. At the system level, Naeini et al. focused more on the SOFC itself and did not

combine it with other power systems, such as gas turbines or steam cycles. Instead, they designed an SOFC stack replacement schedule of every 5 years or 10 years for a 20-year plant lifetime by changing the operating conditions [20]. These SOFC replacement schedules are comparable to the ones we used for NG-BC3 and NG-BC4, wherein the SOFC stacks were replaced every 7.2 years and 8.2 years, respectively. The operating strategy in Naeini et al.'s 5- or 10-year plan was to allow the current density or power output decrease over time, which was similar to the approach used in BC3 and BC4, wherein the voltage was kept constant and the current density or power was allowed to drop as the SOFC degraded. Since they did not harness the waste heat from the SOFC stack for additional power generation, the overall electrical efficiency was lower compared to NG-BC2, NG-BC3, and NG-BC4 in our study [20], as expected.

Figure 4.6 shows the ReCiPe midpoint impact comparison for selected categories, with all midpoints being normalized relative to Naeini et al.'s SOFC case with a 10-year replacement schedule [20]. As can be seen, with the exception of BC1 (including BC1Wc and BC1Dc), all our NG-based cases had lower midpoint impacts with respect to global warming, mainly due to their higher plant efficiency. SOFC manufacturing contributed a large portion of midpoint impacts in the categories of fine particle matter formation and terrestrial acidification, therefore, BC3 and BC4 (including the Wc and Dc cases) had impacts close to those reported for Naeini et al.'s SOFC-5yr and SOFC-10yr cases [20]. Since BC1 and BC2 (including the Wc and Dc cases) required considerably more SOFC manufacturing due to frequent SOFC replacement, they had much higher impacts in these two categories. The comparison results showed good agreement between our findings and those for SOFC systems in literature that account for long-term degradation effects.
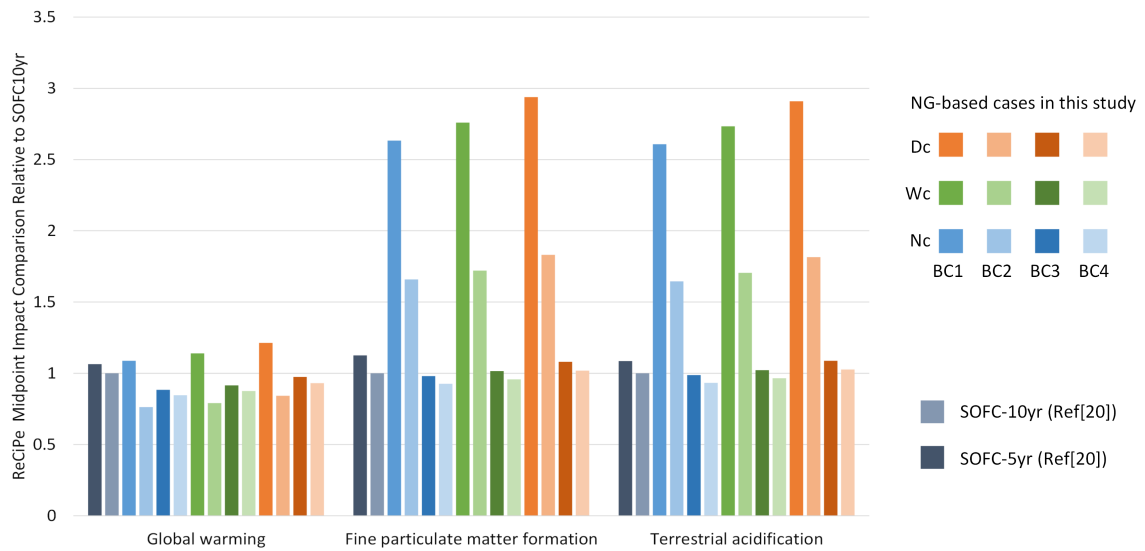
Figure 4.6: Normalized ReCiPe midpoint impact comparison (ReCiPe 2016 H) with other NG-based SOFC systems from [20].

4.4   Conclusion

In this study, we performed cradle-to-product life cycle analyses for four NG-based SOFC plant base cases and four coal-based SOFC plant base cases, as well as for two additional expanded boundary cases for each base case. The LCA results obtained via ReCiPe 2016 (H) in SimaPro showed that the standalone SOFC plants (NG-BC1 or Coal-BC1) had highest midpoint impacts in every category due to having the lowest plant efficiency (unused waste heat) and largest SOFC-stack manufacturing requirements (i.e., the shortest SOFC stack lifetime). The standalone SOFC plants with a steam cycle (NG-BC2 or Coal-BC2) outperformed the SOFC/GT hybrid plants with a steam cycle (NG-BC4 or Coal-BC4) in some midpoint categories (e.g., global warming) due to their higher plant efficiency, but had worse (higher) environmental impacts in other categories (e.g., terrestrial ecotoxicity) due to the need

for more SOFC manufacturing. Similar results can be seen between BC3 and BC2, while BC4 always had better (lower) environmental impacts than BC3 in either the NG-based or coal-based cases. The ReCiPe endpoint results indicated that NG-BC4 and Coal-BC4 had the lowest environmental impacts in their respective classes (i.e., natural-gas-based and coal-based designs). The design and operation of SOFC/GT hybrid with a steam cycle (BC4) strongly extended the stack lifetime (due to much slower degradation) compared to BC1 and BC2, and provided higher plant efficiency than BC3, resulting in the least SOFC manufacturing (smallest stack size and least numbers of stack during the plant's lifetime) among all the base cases and lower emissions in plant operation than BC3.

For all NG-based cases, plant operation accounted for the largest ReCiPe midpoint contributions to global warming, stratospheric ozone depletion, fossil resource scarcity, and water consumption, while SOFC manufacturing contributed the most to terrestrial ecotoxicity and mineral resource scarcity. The midpoint impacts contributed by plant operation decreased as plant efficiency increased (i.e., BC1 → BC3 → BC4 → BC2) for all categories, while the midpoint impacts contributed by SOFC manufacturing similarly decreased alongside the corresponding total number of SOFCs required over the 30-years plant lifetime (i.e., BC1 → BC2 → BC3 → BC4). While balance-of-plant manufacturing and plant maintenance generally accounted for lower midpoint impacts than the other two components, plant maintenance had noticeable impacts in some categories, such as human toxicity and freshwater and marine ecotoxicity, mainly due to the use of catalysts.

The sensitivity analyses with Monte Carlo sampling showed that the ReCiPe midpoint impacts of the base cases were not sensitive to uncertainties in plant operation

and SOFC manufacturing. The expanded boundary cases with wet cooling towers had higher ReCiPe midpoint impacts compared to the corresponding base cases in all categories, while the cases with dry cooling towers significantly reduced water consumption, but had higher overall impacts compared to the corresponding cases with wet cooling towers. The midpoint impacts results obtained using TRACI 2.1 were similar to the ReCiPe results. Finally, a comparison with other SOFC systems revealed that our findings agreed well with the those reported in the literature, and that including SOFC degradation in the model resulted in higher environmental impacts in relation to plant operation and SOFC manufacturing, thus increasing the midpoint impacts in every category.

Acknowledgement

Simulation Files

Models and codes related to this work have been released to the public in LAPSE (link: https://psecommunity.org/LAPSE:2023.0002).

Nomenclature

AC   Alternating Current

AD   Acidification

BoP   Balance-of-plant

CA   Carcinogenics

DC   Direct Current

EC   Ecotoxicity

eTEA   Eco-technoeconomic Analysis

EU   Eutrophication

FD   Fossil fuel Depletion

FEc   Freshwater Ecotoxicity

FEu   Freshwater Eutrophication

FS   Fossil resource Scarcity

FU   Fuel Utilization

GT   Gas Turbine

GW   Global Warming

HCT   Human Carcinogenic Toxicity

HNCT   Human Non-carcinogenic Toxicity

IR   Ionizing Radiation

LCOE   Levelized Cost of Electricity

LHV   Lower Heating Value

L LSM   Lanthanum Strontium Manganite

LU   Land Use

MEc   Marine Ecotoxicity

MEu	Marine Eutrophication
MS	Mineral resource Scarcity
NCA	Non carcinogenics
NG	Natural Gas
OD	Stratospheric Ozone Depletion
OF, HH	Ozone Formation, Human Health
OF, TE	Ozone Formation, Terrestrial Ecosystems
PMF	Fine Particulate Matter Formation
RE	Respiratory Effects
SOFC	Solid Oxide Fuel Cell
SM	Smog
ST	Steam cycle (steam turbine)
TA	Terrestrial Acidification
TE	Terrestrial Ecotoxicity
WD	Water consumption (depletion)
WGS	Water-gas-shift reaction
YSZ	Yttria-stabilized Zirconia

References

[1] Kang, J.-N., Wei, Y.-M., Liu, L.-C., Han, R., Yu, B.-Y., and Wang, J.-W., 2020, "Energy Systems for Climate Change Mitigation: A Systematic Review," Appl. Energy, 263, p. 114602.

[2] Tahir, M. F., Haoyong, C., and Guangze, H., 2021, "A Comprehensive Review of 4E Analysis of Thermal Power Plants, Intermittent Renewable Energy and Integrated Energy Systems," Energy Rep., 7, pp. 3517–3534.

[3] Jackson, R. B., Friedlingstein, P., Andrew, R. M., Canadell, J. G., Quéré, C. L., and Peters, G. P., 2019, "Persistent Fossil Fuel Growth Threatens the Paris Agreement and Planetary Health," Environ. Res. Lett., 14(12), p. 121001.

[4] "World Energy Outlook 2022 – Analysis," IEA [Online]. Available: https://www.iea.org/reports/world-energy-outlook-2022. [Accessed: 08-Dec-2022].

[5] Adams II, T. A., Nease, J., Tucker, D., and Barton, P. I., 2013, "Energy Conversion with Solid Oxide Fuel Cell Systems: A Review of Concepts and Outlooks for the Short-and Long-Term," Ind. Eng. Chem. Res., 52(9), pp. 3089–3111.

[6] Nease, J., and Adams II, T. A., 2014, "Coal-Fuelled Systems for Peaking Power with 100% CO_2 Capture through Integration of Solid Oxide Fuel Cells with Compressed Air Energy Storage," J. Power Sources, 251, pp. 92–107.

[7] Tucker, D., Abreu-Sepulveda, M., and Harun, N. F., 2014, "SOFC Lifetime Assessment in Gas Turbine Hybrid Power Systems," J. Fuel Cell Sci. Technol., 11(5).

[8] Abreu-Sepulveda, M. A., Harun, N. F., Hackett, G., Hagen, A., and Tucker, D., 2015, "Accelerated Degradation for Hardware in the Loop Simulation of Fuel Cell-Gas Turbine Hybrid System," J. Fuel Cell Sci. Technol., 12(2).

[9] Zaccaria, V., Traverso, A., and Tucker, D., 2015, "A Real-Time Degradation Model for Hardware in the Loop Simulation of Fuel Cell Gas Turbine Hybrid Systems," American Society of Mechanical Engineers, p. V003T06A022.

[10] Lai, H., Harun, N. F., Tucker, D., and Adams II, T. A., 2021, "Design and Eco-Technoeconomic Analyses of SOFC/GT Hybrid Systems Accounting for Long-Term Degradation Effects," Int. J. Hydrog. Energy, 46(7), pp. 5612–5629.

[11] Lai, H., and Adams II, T. A., 2022, "Eco-Technoeconomic Analyses of NG-Powered SOFC/GT Hybrid Plants Accouting for Long-Term Degradation Effects via Pseudo-Steady-State Model Simulations," J. Electrochem. Energy Convers. Storage. (In review, JEECS-22-1137)

[12] Strazza, C., Del Borghi, A., Costamagna, P., Gallo, M., Brignole, E., and Girdinio, P., 2015, "Life Cycle Assessment and Life Cycle Costing of a SOFC System for Distributed Power Generation," Energy Convers. Manag., 100, pp. 64–77.

[13] Rillo, E., Gandiglio, M., Lanzini, A., Bobba, S., Santarelli, M., and Blengini, G., 2017, "Life Cycle Assessment (LCA) of Biogas-Fed Solid Oxide Fuel Cell (SOFC) Plant," Energy, 126, pp. 585–602.

[14] Bicer, Y., and Khalid, F., 2020, "Life Cycle Environmental Impact Comparison of Solid Oxide Fuel Cells Fueled by Natural Gas, Hydrogen, Ammonia and Methanol for Combined Heat and Power Generation," Int. J. Hydrog. Energy, 45(5), pp. 3670–3685.

[15] Al-Khori, K., Al-Ghamdi, S. G., Boulfrad, S., and Koç, M., 2021, "Life Cycle Assessment for Integration of Solid Oxide Fuel Cells into Gas Processing Operations," Energies, 14(15), p. 4668.

[16] Nease, J., and Adams, T. A., 2015, "Life Cycle Analyses of Bulk-scale Solid Oxide Fuel Cell Power Plants and Comparisons to the Natural Gas Combined Cycle," Can. J. Chem. Eng., 93(8), pp. 1349–1363.

[17] Nease, J., and Adams II, T. A., 2015, "Comparative Life Cycle Analyses of Bulk-Scale Coal-Fueled Solid Oxide Fuel Cell Power Plants," Appl. Energy, 150, pp. 161–175.

[18] Reenaas, M., 2005, "Solid Oxide Fuel Cell Combined with Gas Turbine versus Diesel Engine as Auxiliary Power Producing Unit Onboard a Passenger Ferry: A Comparative Life Cycle Assessment and Life Cycle Cost Assessment."

[19] Ghorbani, S., Khoshgoftar-Manesh, M. H., Nourpour, M., and Blanco-Marigorta, A. M., 2020, "Exergoeconomic and Exergoenvironmental Analyses of an Integrated SOFC-GT-ORC Hybrid System," Energy, 206, p. 118151.

[20] Naeini, M., Cotton, J. S., and Adams II, T. A., 2022, "Dynamic Life Cycle Assessment of Solid Oxide Fuel Cell System Considering Long-Term Degradation Effects," Energy Convers. Manag., 255, p. 115336.

[21] Naeini, M., Cotton, J. S., and Adams II, T. A., 2021, "Economically Optimal

Sizing and Operation Strategy for Solid Oxide Fuel Cells to Effectively Manage Long-Term Degradation," Ind. Eng. Chem. Res., 60(47), pp. 17128–17142.

[22] Naeini, M., Lai, H., Cotton, J. S., and Adams II, T. A., 2021, "A Mathematical Model for Prediction of Long-Term Degradation Effects in Solid Oxide Fuel Cells," Ind. Eng. Chem. Res., 60(3), pp. 1326–1340.

[23] Staffell, I., Ingram, A., and Kendall, K., 2012, "Energy and Carbon Payback Times for Solid Oxide Fuel Cell Based Domestic CHP," Int. J. Hydrog. Energy, 37(3), pp. 2509–2523.

[24] Spath, P. L., and Mann, M. K., 2000, Life Cycle Assessment of Hydrogen Production via Natural Gas Steam Reforming, NREL/TP-570-27637, National Renewable Energy Lab. (NREL), Golden, CO (United States).

[25] Kannan, R., Tso, C. P., Osman, R., and Ho, H. K., 2004, "LCA–LCCA of Oil Fired Steam Turbine Power Plant in Singapore," Energy Convers. Manag., 45(18), pp. 3093–3107.

[26] Rath, L. K., Chou, V. H., and Kuehn, N. J., 2011, Assessment of Hydrogen Production with CO2 Capture Volume 1: Baseline State-of-the-Art Plants (Final Report), DOE/NETL-2011/1434-Rev.01, National Energy Technology Laboratory (NETL), Pittsburgh, PA, Morgantown, WV, and Albany, OR (United States); Booz Allen Hamilton, Inc., McLean, VA (United States).

[27] James III PhD, R. E., Kearins, D., Turner, M., Woods, M., Kuehn, N., and Zoelle, A., 2019, Cost and Performance Baseline for Fossil Energy Plants Volume 1: Bituminous Coal and Natural Gas to Electricity, NETL-PUB-22638, NETL.

[28] Xu, Y., Harimoto, T., Hirano, T., Ohata, H., Kunieda, H., Hara, Y., and Miyata, Y., 2018, "Catalytic Performance of a High-Cell-Density Ni Honeycomb Catalyst for Methane Steam Reforming," Int. J. Hydrog. Energy, 43(33), pp. 15975–15984.

[29] Li, Y., Li, X., Chang, L., Wu, D., Fang, Z., and Shi, Y., 1999, "Understandings on the Scattering Property of the Mechanical Strength Data of Solid Catalysts: A Statistical Analysis of Iron-Based High-Temperature Water-Gas Shift Catalysts," Catal. Today, 51(1), pp. 73–84.

[30] "SELEXOLTM Solvent" [Online]. Available: https://www.dow.com/en-us/pdp.selexol-solvent.85633z.html. [Accessed: 31-Oct-2022].

[31] Adams, T. A., and Barton, P. I., 2010, "High-efficiency Power Production from

Coal with Carbon Capture," AIChE J., 56(12), pp. 3120–3136.

[32] Veil, J. A., Littleton, D. J., Gross, R. W., Smith, D. N., Parsons Jr, E. L., Shelton, W. W., Feeley, T. J., and McGurl, G. V., 2006, Energy Penalty Analysis of Possible Cooling Water Intake Structurerequirements on Existing Coal-Fired Power Plants., Argonne National Lab.(ANL), Argonne, IL (United States).

[33] Baum, E., Chaisson, J., Evans, L., Lewis, J., Marshall, D., and Thompson, J., 2003, "The Last Straw: Water Use by Power Plants in the Arid West," Clean Air Task Force Land Water Fund Rock. Energy Found. Hewlett Found.

Chapter 5

Conclusions and Recommendations

5.1   Conclusions

Through this thesis, eco-technoeconomic performances and life cycle environmental impacts of standalone SOFC plants and SOFC/GT hybrid plants accounting for long-term degradation effects were assessed, which potentially contributed to the large-scale industrialization of SOFC/GT hybrid power production from fossil fuels.

The eTEA results for both coal-based and NG-based cases showed that the addition of a steam bottoming cycle improved the overall plant efficiency and reduce the LCOE, meaning that BC2 was better than BC1 and BC4 was better than BC3. Thus, the eco-technoeconomic comparison was narrowed down to only between standalone SOFC plant with a steam cycle (BC2) and SOFC/GT hybrid plant with a steam cycle (BC4) for both coal-based and NG-based cases. The results showed that coal-BC2 and NG-BC2 had 4.1 and 12 percentage points higher net efficiencies than coal-BC4 and NG-BC4, respectively. Due to the higher efficiencies, coal-BC2 and NG-BC2 had lower operating costs than coal-BC4 and NG-BC4. However, the SOFC stack lifetime in BC4 was much longer than in BC2 (more than 10 times) due to the constant voltage operating strategy which significantly slowed the degradation. This strongly reduced the SOFC replacement costs of coal-BC4 and NG-BC4 such that their LCOEs were 68% and 82% lower than those of coal-BC2 and NG-BC2, respectively. The SOFC/GT hybrid plant with a steam cycle was found to be the best case as it has the lowest LCOE of \$77/MWh among the coal-based cases and the lowest LCOE of \$35/MWh among the NG-based cases.

The cradle-to-product LCA results revealed that BC1 had the highest (worst) environmental impacts in every midpoint category due to its lowest net efficiency and

shortest SOFC stack lifetime, among both coal-based and NG-based cases. When comparing between BC2 and BC4 or between BC2 and BC3, one case was better than the other in some midpoint categories but worse in some other categories. Generally, BC2 had the lowest impacts in global warming potential and fossil fuel depletion due to its highest plant efficiency (true for both coal-based and NG-based cases). BC4 which had the least SOFC manufacturing requirements had the lowest impacts in ionizing radiation, ozone formation, fine particulate matter formation, terrestrial acidification, and terrestrial ecotoxicity. The ReCiPe endpoint concluded the final comparison, which showed that BC2 and BC3 had close endpoints and BC4 had the lowest among all the base cases, for both coal-based and NG-based cases.

The eTEA and LCA results were found to be mainly affected by the plant efficiency and the total SOFC manufacturing over the plant's lifetime, and the latter was the major factor. This confirmed the importance of considering long-term degradation effects in model simulations and these analyses. It also revealed that changing the operating strategy of the SOFC stack from constant power to constant voltage and integrating with a GT in a SOFC/GT hybrid system greatly increased the stack lifetime (slowed degradation) and had better economic performances and environmental impacts. The SOFC/GT hybrid plant with a steam cycle was found to have the best economic performances and life cycle environmental impacts among the base cases, and could be a strong competitive alternative to conventional power production from fossil fuels considering the global power reshaping. Therefore, the SOFC/GT hybrid plant with a steam cycle (BC4) is recommended as the best alternative (accounting for long-term degradation effects) to conventional power production from fossil fuels in the near to medium future.

The followings summarize the contributions of this thesis to the field:

- Designs and model simulations of standalone SOFC plants and SOFC/GT hybrid plants accounting for long-term degradation effects that utilize fossil fuels for power production

    - Designed and developed models for four SOFC plants utilizing coal as the fuel source

        * Standalone SOFC plant

        * Standalone SOFC plant with a steam cycle

        * SOFC/GT hybrid plant

        * SOFC/GT hybrid plant with a steam cycle

    - Designed and developed models for four SOFC plants utilizing NG as the fuel source (four plant designs similar to the previous bullet point)

    - Allowed eTEA, LCA, and any other analyses or process optimization in future work

    - Models are available to the public (see links in the corresponding chapters)

- Model integration and simulation by taking a pseudo-steady-state approach to integrate dynamic models and steady-state models

    - Provided a useful method and example to integrate dynamic models and steady-state models

    - Allowed eTEA, LCA, and any other analyses on dynamic and steady-state combined systems, especially when the dynamic behaviours of the systems affected equipment sizes and lifetimes

– Developed a model-based controller embedded in the pseudo-steady-state model simulation, which can be used in systems that were changing power load and efficiency with multiple power generation units and parasitic loads

– Models and codes are available to the public (see links in the corresponding chapters)

- Eco-technoeconomic analyses (eTEA) of standalone SOFC plants and SOFC/GT hybrid plants accounting for long-term degradation effects

    – Economic performance comparisons between SOFC plants and SOFC/GT hybrid plants accounting for long-term degradation effects

    – Examined the long-term degradation effects on economic performances of SOFC plants: operating SOFC stack with constant voltage instead of constant power could significantly reduce the degradation rate, increase stack lifetime, and thus reduce costs associated with stack replacements

    – Revealed that the standalone SOFC plants with a steam cycle had the highest efficiency among the base cases, but had high cost of SOFC stack replacements due to short lifetimes of the stacks

        * Coal-based standalone SOFC plant with a steam cycle (BC2) - Plant efficiency: $48.7\%_{LHV}$

        * NG-based standalone SOFC plant with a steam cycle (BC2) - Plant efficiency: $65.0\%_{LHV}$

    – Revealed that although the SOFC/GT hybrid plant with a steam cycle was not the most efficient case among the base cases, but had the best eco-technoeconomic performances with the lowest LCOE

* Coal-based SOFC/GT plant with a steam cycle (BC4) - Plant efficiency: $44.6\%_{LHV}$, LCOE: \$77/MWh

  * NG-based SOFC/GT plant with a steam cycle (BC4) - Plant efficiency: $53.0\%_{LHV}$, LCOE: \$35.1/MWh

- Contributed to the potential large-scale industrial adoption of SOFC/GT hybrid plants from an eco-technoeconomic perspective with lower LCOEs (LCOEs for the baseline IGCC and NGCC plant: \$97.5/MWh and \$48.4/MWh, respectively)

- Codes and sample calculations for eTEA are available to the public (see links in the corresponding chapters)

* Cradle-to-product life cycle analyses (LCA) for standalone SOFC plants and SOFC/GT hybrid plants accounting for long-term degradation effects.

  - Performed full life cycle cradle-to-product LCAs for all the base cases listed in the first bullet point using SimaPro

  - Divided LCAs into components such as plant operation, SOFC manufacturing, BoP manufacturing, and plant maintenance which might be used as parts in other LCAs

  - Examined LCAs for cases with boundary expansions to include wet cooling or dry cooling method as well as DC to AC conversion

  - Revealed that higher (better) plant efficiency was associated with lower (better) environmental impacts in global warming potential and fossil fuel depletion

  - Revealed that operating the SOFC stack in constant voltage mode rather than constant power mode, which reduced the degradation rate and extended

the stack lifetime, had lower environmental impacts in ionizing radiation, ozone formation, fine particulate matter formation, terrestrial acidification, and terrestrial ecotoxicity

– Identified that the conclusion of comparison cannot be made between BC2 and BC4 through midpoint method since one is better than the other in some categories and vice verses

– Revealed that the SOFC/GT hybrid plants with a steam cycle (both coal-base and NG-based) had the lowest (best) ReCiPe endpoints

– Contributed to the potential large-scale industrial adoption of SOFC/GT hybrid plants by providing a point of view from a life cycle environmental aspect

– Models are available to the public (see links in the corresponding chapters)

5.2 Recommended Future Work

The degradation model used in this thesis project was an empirical model based on experimental data, which was limited to the SOFC type (materials) and the range of operating conditions in the experiments. To further explore the system dynamics and eTEA of SOFC systems in different operating conditions, a different degradation model might be desired. As mentioned in the preliminary, the author also contributed to a project which is not included in this thesis [1]. Unlike the model in this thesis which correlates the degradation rate with various operating conditions, the side-project focuses on the most significant degradation mechanisms and integrates them into one model. Although it might neglect a small degree of degradation effects due to some minor mechanisms, it allows eTEA

and LCA for SOFC/GT hybrid systems to cross-validate the results in this thesis and explore different SOFC operating conditions (especially different fuel compositions).

Looking at the long-term future, as the global electricity supply is shifting to renewables, global electricity supply by fossil fuels might be reshaped to provide more load-following or peaking power supply rather than baseload to accommodate the intermittent nature of renewables. This thesis examines the eTEA and LCA of standalone SOFC plants and SOFC/GT hybrid plants accounting for the slow dynamics of degradation in baseload power production. It would be interesting to study the fast dynamics due to degradation and the corresponding eTEA and LCA, when these plants were operated for load-following or peaking power production. The analyses could be further extended to applications at smaller scales including household, building, and community power and heating systems or integrations with other systems such as renewable power, energy storage, and combined heat and power systems.

Reference

[1] M. Naeini, H. Lai, J. S. Cotton, and T. A. Adams II, "A Mathematical Model for Prediction of Long-Term Degradation Effects in Solid Oxide Fuel Cells," Ind. Eng. Chem. Res., vol. 60, no. 3, pp. 1326–1340, Jan. 2021, doi: 10.1021/acs.iecr.0c05302.

Appendix: Additional Model Descriptions

All models and codes used in this thesis project can be found and downloaded in LAPSE through the following links:

https://psecommunity.org/LAPSE:2020.0904

https://psecommunity.org/LAPSE:2022.0027

https://psecommunity.org/LAPSE:2023.0002

SOFC model

The SOFC model used in this thesis project is a 1D real-time model of a planar anode-supported SOFC consisting of a Nickel – Yttria-stabilized Zirconia (Ni-YSZ) anode, a YSZ – Lanthanum Strontium Magnetite (LSM) cathode, and YSZ electrolyte. The voltage, resistance, and degradation rate that are associated with SOFC degradation are calculated through Eq (1) – (11). The SOFC degradation is described as a function with respect to operating conditions such as current density, fuel utilization, and temperature (as Eq (10), or Eq (1) in Chapter 2, 3, and 4) based on experimental data. This equation calculates the overall degradation without considering detailed degradation mechanisms taking place in different parts of the SOFC stack. The degradation rate was incorporated into the SOFC model as the increase in the ohmic loss (in terms of ohmic resistance and irreversible contribution of degradation) as Eq (8) – (11). Finally, the resistances are used to calculate the voltage of the SOFC through Eq (1) – (7). The SOFC model also includes a large number of equations for mass balances, energy balances, mass transfer, and heat transfer. More details of the model can be found in prior works [1-5] and in the model file through the links above.

$$V_{NERNST} = -\frac{\Delta G^0_{H_2O}}{nF} + \frac{R_g T}{nF} \ln \left(\frac{pH_2 \sqrt{pO_2}}{pH_2O} \right) \tag{1}$$

$$V_{cell} = V_{NERNST} - \eta_{dif} - \eta_{act} - \eta_{ohm} \tag{2}$$

$$\eta_{dif} = \frac{R_g T}{2F} \left(\ln \left(\frac{x_{H_2,bulk} \cdot x_{H_2O,TPB}}{x_{H_2O,bulk} \cdot x_{H_2,TPB}} \right) + \frac{1}{2} \ln \left(\frac{x_{O_2,bulk}}{x_{O_2,TPB}} \right) \right) \tag{3}$$

$$\eta_{act} = \frac{R_g T}{\alpha n F} \sinh^{-1} \left(\frac{i}{2 i_0} \right) \tag{4}$$

$$\eta_{ohm} = R \cdot i \tag{5}$$

$$i_{0,an} = 5.5 \cdot 10^8 \frac{pH_2}{p_{amb}} \frac{pH_2O}{p_{amb}} \exp \left(-\frac{50 \cdot 10^3}{R_g T} \right) \tag{6}$$

$$i_{0,ca} = 7 \cdot 10^8 \left(\frac{pO_2}{p_{amb}} \right)^{0.25} \exp \left(-\frac{100 \cdot 10^3}{R_g T} \right) \tag{7}$$

$$R = (R_{ohm} + R_{irr}) \cdot \left(1 + r_d \cdot \frac{t}{1000} \right) \tag{8}$$

$$R_{ohm} = R_{PEN} + R''_{oxide} = \rho_{an} th_{an} + \rho_{el} th_{el} + \rho_{ca} th_{ca} + R''_{oxide} \tag{9}$$

$$r_d = \frac{0.59 FU + 0.74}{1 + \exp \left(\frac{T - 1087}{22.92} \right)} \left(e^{2.64i} - 1 \right) \tag{10}$$

$$R_{irr} = \sum_{time} \left(R_{PEN} + R''_{oxide} \right) \cdot \frac{r_d}{1000} \tag{11}$$

Where

F   Faraday's constant [C/mol]

i   current density [A/cm^2]

i_0 exchange current density [A/cm^2]

n   number of electrons transfer per reaction

p   partial pressure [Pa]

R   area specific resistance [Ω*m^2]

r_d degradation rate [%*k/h]

R_g ideal gas constant [J/(mol*K)]

T   temperature [K]

t   time [h]

V   voltage [V]

x   mole fraction

α charge transfer coefficient

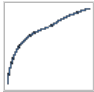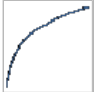η electrochemical loss [V]

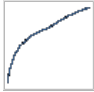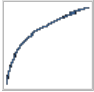ρ resistance [Ω*m]

Steam cycle

The steam cycle in BC2 was designed to generate steam at 550°C and 100 bar after the steam generator. The outlet pressure and hot bypass ratio of each stage in the multi-stage turbine were determined using the optimization tool in Aspen Plus in an attempt to maximize power production while still achieving 100% vapor fraction between the stages and at least 95% vapor fraction in the outlet stream. The optimal outlet pressures of the three stages were determined to be 24.7 bar, 4.7 bar, and 1.1 bar, with bypass ratios of 8% and 2% of the total steam to the medium- and low-pressure turbines, respectively. More details of the steam cycle can be found in the main text of the thesis and the Aspen model in LAPSE.

Compressed air impacts

As mentioned in the plant description in the main text in Chapter 2 and 3, the air bypass streams in BC3 and BC4 were designed to control the temperature of the stream entering the GT and the stream entering the cathode of the SOFC. As the

bypass ratio changed with time, the total amount of air being compressed changed and consequently the power consumed by the compressor also changed. The following table summarizes the changes associated with the compressed air stream throughout the SOFC stack lifetime in BC3 and BC4. Please refer to the model files for more details.

	BC3		BC4	
	Trend	Percentage	Trend	Percentage
Air bypass ratio		98%		95%
Compressor consumed power		12%		10%

Reference

[1] Abreu-Sepulveda, M. A., Harun, N. F., Hackett, G., Hagen, A., and Tucker, D., 2015, "Accelerated Degradation for Hardware in the Loop Simulation of Fuel Cell-Gas Turbine Hybrid System," J. Fuel Cell Sci. Technol., 12(2).

[2] Zaccaria, V., Tucker, D., and Traverso, A., 2016, "A Distributed Real-Time Model of Degradation in a Solid Oxide Fuel Cell, Part I: Model Characterization," J. Power Sources, 311, pp. 175–181.

[3] Zaccaria, V., Tucker, D., and Traverso, A., 2016, "A Distributed Real-Time Model of Degradation in a Solid Oxide Fuel Cell, Part II: Analysis of Fuel Cell Performance and Potential Failures," J. Power Sources, 327, pp. 736–742.

[4] Zaccaria, V., Traverso, A., and Tucker, D., 2015, "A Real-Time Degradation Model for Hardware in the Loop Simulation of Fuel Cell Gas Turbine Hybrid Systems," American Society of Mechanical Engineers, p. V003T06A022.

[5] Rossi, I., Zaccaria, V., and Traverso, A., 2018, "Advanced Control for Clusters of SOFC/Gas Turbine Hybrid Systems," J. Eng. Gas Turbines Power, 140(5).